**Supporting Information**

# Selective access to either a doubly boron-doped tetrabenzopentacene or an oxadiborepin from the same precursor

Julian Radtke, Kai Schickedanz, Marcel Bamberg, Luigi Menduti, Dieter Schollmeyer, Michael Bolte, Hans-Wolfram Lerner and Matthias Wagner

## 1. General experimental remarks

If not stated otherwise, all reactions and manipulations were carried out under an inert atmosphere using Schlenk techniques or a glovebox and carefully degassed and dried solvents.

*n*-Hexane was distilled from Na; $C_6H_6$, PhMe, $Et_2O$, and THF were distilled from Na/benzophenone prior to use. $CDCl_3$ and $CH_2Cl_2$ were distilled from $CaH_2$ and stored over 3 Å molecular sieves.

$B(OMe)_3$ was distilled from Na and stored over 3 Å molecular sieves. 1,8-Diaminonaphthalene, bis(1,5-cyclooctadiene)nickel ($Ni(COD)_2$; stored in an argon-filled glovebox at –30 °C), and $BBr_3$ (stored over Hg) were purchased from *Sigma-Aldrich*. Dry pyridine (already stored over molecular sieves) was purchased from *Acros Organics*. *n*-BuLi (ca. 1.56 M in hexanes) and *t*-BuLi (ca. 2.0 M in pentane) were donated by *Albemarle Lithium*.

9,10-Dibromo-9,10-dihydro-9,10-diboraanthracence,[S1] 1,5-dibromo-9,10-dihydroxy-9,10-dihydro-9,10-diboraanthracene, 1,5-dichloro-9,10-dihydroxy-9,10-dihydro-9,10-dibora-anthracene, and 1,5-difluoro-9,10-dihydroxy-9,10-dihydro-9,10-diboraanthracene were prepared according to literature procedures.[S2]

NMR spectra were recorded at 298 K using the following spectrometers: *Bruker* Avance-300, Avance-400, Avance-500, or drx-600. Chemical shift values are referenced to (residual) solvent signals ($^1H/^{13}C\{^1H\}$; $CHCl_3$: $\delta$ = 7.26/77.2 ppm, $C_6HD_5$: $\delta$ = 7.16/128.1 ppm) or external $BF_3 \cdot Et_2O$ ($^{11}B\{^1H\}$: 0.00 ppm). Abbreviations: s = singlet, d = doublet, dd = doublet of doublets, t = triplet, vt = virtual triplet, q = quartet, m = multiplet, br = broad, n.r. = not resolved. Resonances of carbon atoms attached to boron atoms were typically broadened and sometimes not observed due to the quadrupolar relaxation of boron. Resonance assignments were aided by $^{H,H}$COSY, $^{H,C}$HSQC, and, if necessary, also $^{H,C}$HMBC spectra.

Column chromatography was performed using silica gel 60 (*Macherey–Nagel*). Flash chromatography was performed on a *Biotage* ISOLERA ONE with *Biotage* "SNAP-Ultra" or *Interchim* puriFlash cartridges.

UV-vis absorption spectra were recorded at room temperature using a *Varian* Cary 60 Scan UV-vis spectrophotometer. Photoluminescence (PL) spectra were recorded at room temperature using a *Jasco* FP-8300 spectrofluorometer equipped with a calibrated *Jasco* ILF-835 100 mm diameter integrating sphere and analyzed using the *Jasco* FWQE-880 software. For PL quantum yield ($\phi_{PL}$) measurements, each sample was carefully degassed with argon

for at least 3 min using an injection needle and a septum-capped cuvette. Under these conditions, $\phi_{PL}$ of the fluorescence standard 9,10-diphenylanthracene was determined as 97% (lit.: 97%[S3]). For all measurements of $\phi_{PL}$, at least three samples of different concentrations were used (range between $10^{-5}$ and $10^{-7}$ mol $L^{-1}$). Due to self-absorption, slightly lower $\phi_{PL}$ values were observed at higher concentrations. This effect was corrected by applying a method reported by Bardeen *et al.*,[S4] which slightly improved the $\phi_{PL}$ values.

Cyclic voltammetry (CV) measurements were performed in an inert-atmosphere glovebox at room temperature using a one-chamber, three-electrode cell and an *EG&G* Princeton Applied Research 263A potentiostat. A platinum disk electrode (2.00 mm diameter) was used as the working electrode with a platinum wire counter electrode and a silver wire reference electrode, which was coated with AgCl by immersion into $HCl/HNO_3$ (3:1). Prior to measurements, the solvents THF (dried over Na/K alloy) and $CH_2Cl_2$ (dried over $CaH_2$) were condensed into a J-Young flask, and subsequently degassed with argon. [*n*-$Bu_4N$][$PF_6$] was employed as the supporting electrolyte (0.1 mol $L^{-1}$). All potential values were referenced against the $FcH/FcH^+$ redox couple (FcH = ferrocene; $E_{½}$ = 0 V). Scan rates were varied between 50 and 400 mV $s^{-1}$.

High resolution mass spectra were measured in positive mode using a *Thermo Fischer Scientific* MALDI LTQ Orbitrap XL and 2,5-dihydroxybenzoic acid or α-cyano-4-hydroxycinnamic acid as the matrix. Exact masses were calculated based on the predominant combination of natural isotopes.

DFT and TD-DFT calculations were performed using the Gaussian 09 suite of programs.[S5] Starting geometries were built using the program Avogadro[S6] and optimized at the B3LYP/6-31G(d)[S7–S9] level of theory, with the resulting structures confirmed as stationary points through vibrational frequency analysis. The graphics were produced with Avogadro[S6] and POV-Ray.[S10] TD-DFT vertical excitations were calculated using the same parameters. The data used in creating the predicted UV-vis spectra was generated by the program GaussSum V2.2.[S11] Relative energies discussed in the text refer to Gibbs free energies at 298.15 K, which were obtained at the B3LYP/6-31G(d)[S7–S9] level of theory.

## 2. Synthetic details

**1,8-Diiodonaphthalene:**

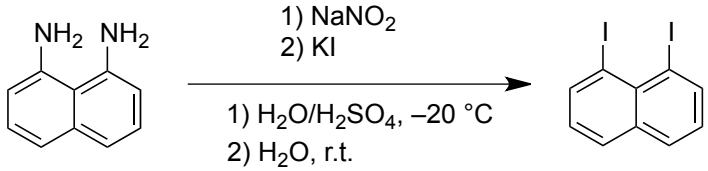


1,8-Diaminonaphthalene (99%, black platelets) and Zn-dust (20wt%) were stirred at 80 °C for 3 h (caution: depending on the impurities, vigorous frothing might occur). After cooling to ambient temperature, pure 1,8-diaminonaphthalene was isolated via distillation ($10^{-3}$ mbar, 150 °C) as an off-white solid (typical yield: 80% on a 100 mmol scale), which can be used without further purification. *Note*: The Zn-dust distillation is crucial for the success of the subsequent Sandmeyer reaction.

1,8-Diaminonaphthalene (10.0 g, 63.2 mmol) was suspended in a mixture of $H_2O/H_2SO_4$ (2:1, 120 mL) and cooled to −20 °C. A solution of $NaNO_2$ (10.9 g, 158 mmol) in $H_2O$ (50 mL) was added dropwise with vigorous stirring. After complete addition, the slurry was stirred for further 30 min and then cautiously (evolution of $N_2$ causes rigorous frothing) poured portion-wise into a vigorously stirred solution of KI (63.0 g, 379 mmol) in $H_2O$ (50 mL). *Note:* To prevent decomposition of the diazonium salt-containing slurry, it was immediately placed back in the −20 °C bath, each time after a portion of it had been poured into the KI solution.

After complete addition, the mixture was heated to 80 °C for 1 h, cooled to ambient temperature, neutralized with NaOH (5 M in $H_2O$) and $NaHSO_3$ (sat. aqueous solution), and vacuum-filtered. After drying with suction, the dark residue was extracted using a Soxhlet extractor (300 mL $Et_2O$, 14 h). The solvent was evaporated from the extract, and the residue was subjected to column chromatography (*c*-hexane) to afford 1,8-diiodonaphthalene as a yellow solid. Yield: 14.4 g (37.9 mmol, 60%).

$^1$H and $^{13}$C{$^1$H} NMR data were in accord with published values.[S12]

**1,8-Dibromonaphthalene:**

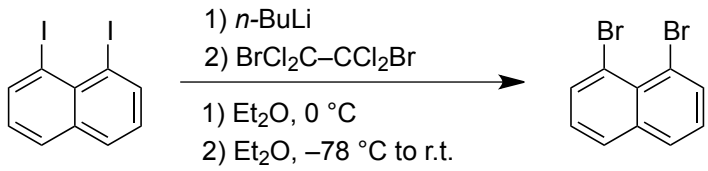


A 500 mL flame-dried Schlenk flask was charged with 1,8-diiodonaphthalene (6.00 g, 15.8 mmol) and $Et_2O$ (200 mL). The solution was cooled to 0 °C over 30 min. *n*-BuLi (25.3 mL, 1.56 M, 39.5 mmol) was added dropwise, and the yellow solution was stirred at 0 °C for 1 h. The reaction mixture was cooled to –78 °C over 30 min and a suspension of $BrCl_2C–CCl_2Br$ (12.9 g, 39.5 mmol) in $Et_2O$ (60 mL) was added dropwise. The resulting mixture was slowly warmed to room temperature and stirred overnight. After the addition of $Na_2SO_3$ (100 mL, sat. aqueous solution), the organic layer was separated, and the aqueous layer extracted with $Et_2O$ (2 × 15 mL). The combined organic layers were washed with water (2 × 15 mL) and brine (2 × 15 mL), dried over anhydrous $MgSO_4$, and filtered. All volatiles were removed from the filtrate under reduced pressure and the crude product was purified by column chromatography (*c*-hexane) to furnish 1,8-dibromonaphthalene as a yellow solid. Yield: 4.25 g (14.9 mmol, 94%).

$^1$H and $^{13}$C{$^1$H} NMR data were in accord with published values.[S13]

**1,5-Difluoro-9,10-dibromo-9,10-dihydro-9,10-diboraanthracene ($1^F$):**

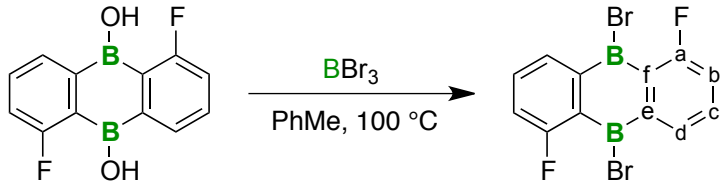


1,5-Difluoro-9,10-dihydroxy-9,10-dihydro-9,10-diboraanthracene (0.77 g, 3.16 mmol) was dried under vacuum for 1 h in a J-Young flask and afterwards suspended in PhMe (20 mL). Upon dropwise addition of $BBr_3$ (4.75 g, 18.95 mmol) at room temperature, the suspension turned into a clear solution, which was stirred for 16 h at 100 °C, whereupon the solution gradually became turbid. After removal of insolubles by syringe filtration in a glovebox, all volatiles were removed from the filtrate under reduced pressure. The obtained solid was washed with ice-cold *n*-pentane (2 × 5 mL) to give **$1^F$** as an off-white solid. Yield: 1.12 g (3.03 mmol, 96%).

$^1$H NMR (500.18 MHz, $CDCl_3$): $\delta$ = 8.32 (d, $^3J_{H\text{-}H}$ = 7.5 Hz, 2H; H-d), 7.78-7.72 (m, 2H; H-c), 7.37-7.33 (m, 2H; H-b)

$^{13}$C{$^1$H} NMR (125.77 MHz, $CDCl_3$): $\delta$ = 167.7 (d, $^1J_{C\text{-}F}$ = 257.6 Hz; C-a), 144.7* (br; C-e), 136.5 (d, $^3J_{C\text{-}F}$ = 10.0 Hz; C-c), 134.7 (d, $^4J_{C\text{-}F}$ = 2.5 Hz; C-d), 128.4* (br, C-f), 122.3 (d, $^2J_{C\text{-}F}$ = 25.8 Hz; C-b)

$^{11}$B{$^1$H} NMR (160.48 MHz, $CDCl_3$): $\delta$ = 61.2 ($h_{1/2}$ ≈ 550 Hz)

$^{19}$F NMR (470.64 MHz, $CDCl_3$): $\delta$ = –95.2 (dd, $^3J_{H\text{-}F}$ = 10.3 Hz, $^4J_{H\text{-}F}$ = 5.1 Hz)

$^{19}$F{$^1$H} NMR (282.29 MHz, $CDCl_3$): $\delta$ = –95.1 (s)

*These signals were only detectable in the $^{H,C}$HMBC-spectrum.

**1,5,9,10-Tetrabromo-9,10-dihydro-9,10-diboraanthracene ($1^{Br}$):**

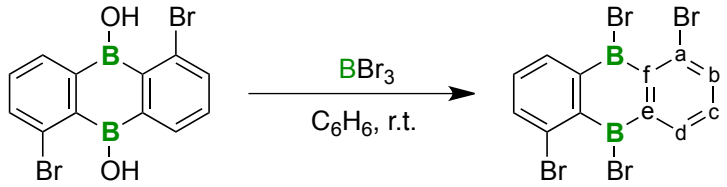


1,5-Dibromo-9,10-dihydroxy-9,10-dihydro-9,10-diboraanthracene (1.02 g, 2.79 mmol) was dried in vacuo for 1 h in a J-Young flask and afterwards suspended in $C_6H_6$ (20 mL). Upon dropwise addition of $BBr_3$ (4.19 g, 16.7 mmol) at room temperature, the suspension turned into a clear solution, which was stirred for 2 h at room temperature, whereupon the solution gradually became turbid. After removal of insolubles by syringe filtration in a glovebox, all volatiles were removed from the filtrate under reduced pressure. The obtained solid was washed with ice-cold *n*-pentane (2 × 5 mL) to give $\mathbf{1^{Br}}$ as a pale yellow solid. Yield: 1.33 g (2.71 mmol, 97%).

$^1$H NMR (400.13 MHz, $CDCl_3$): $\delta$ = 8.23 (d, $^3J_{H\text{-}H}$ = 7.8 Hz, 2H; H-d), 7.84 (d, $^3J_{H\text{-}H}$ = 7.9 Hz, 2H; H-b), 7.46 (vt, 2H; H-c)

$^{13}$C{$^1$H} NMR (100.61 MHz, $CDCl_3$): $\delta$ = 145.4* (br; C-e), 141.5* (br,; C-f), 139.1 (C-b), 135.6 (C-d), 133.7 (C-c), 130.7 (C-a)

$^{11}$B{$^1$H} NMR (128.38 MHz, $CDCl_3$): $\delta$ = 63.8 ($h_{1/2} \approx$ 450 Hz)

*These signals were only detectable in the $^{H,C}$HMBC-spectrum.

**General protocol for the preparation of 9,10-dinaphth-1-yl-functionalized 9,10-dihydro-9,10-diboraanthracenes ($2^{X,Y}$):**

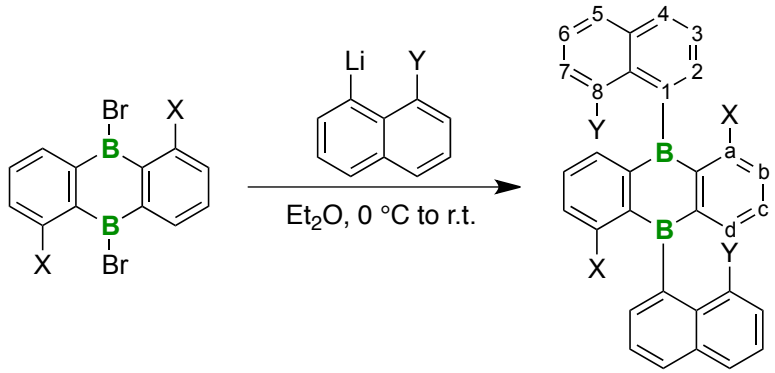


A 100 mL flame-dried Schlenk flask was charged with the corresponding 1,8-dihalogenated naphthalene (2.1 mmol) and $Et_2O$ (60 mL). The solution was cooled to 0 °C over 15 min. *n*-BuLi (1.56 M, 2.1 mmol) was added dropwise with stirring. The ice bath was removed after 15 min, and the bright-yellow solution stirred at room temperature for 30 min. The respective 9,10-dihydro-9,10-diboraanthracene (1.0 mmol) was added as a neat solid in one portion and the mixture stirred overnight. After neutralization with MeOH (10 mL), all volatiles were removed under vacuum and the crude product was purified by flash chromatography.

*Note*: Analytically pure and even single-crystalline samples of all 9,10-dinaphth-1-yl-functionalized 9,10-dihydro-9,10-diboraanthracenes gave rise to two sets of resonances with similar chemical shift values in their $^{1}H$ and $^{13}C\{^{1}H\}$ NMR spectra. This finding is explained by the formation of two conformers with *syn*- and *anti*-positioned halogen atoms.

**9,10-Bis(8-bromonaphth-1-yl)-9,10-dihydro-9,10-diboraanthracene ($2^{H,Br}$):**

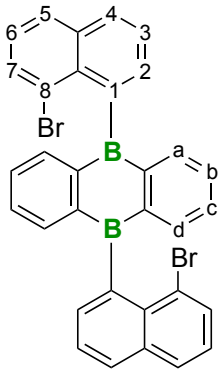


Following the general procedure, 1,8-dibromonaphthalene (600 mg, 2.10 mmol), *n*-BuLi (1.34 mL, 1.56 M, 2.10 mmol), and 9,10-dibromo-9,10-dihydro-9,10-diboraanthracene (333 mg, 1.00 mmol) were used to obtain $\mathbf{2^{H,Br}}$ after purification by flash chromatography (*c*-hexane:$CH_2Cl_2$ = 5:1) as a yellow solid. Yield: 503 mg (0.86 mmol, 86%). Single crystals of $\mathbf{2^{H,Br}}$ were grown by slow gas-phase diffusion of *n*-hexane into a saturated solution of $\mathbf{2^{H,Br}}$ in $C_6H_6$ at room temperature. Conformer ratio A:B ≈ 1.3:1 (determined by $^1$H NMR spectroscopy).

***A*:**

$^1$H NMR (500.18 MHz, $CDCl_3$): $\delta$ = 7.99 (d, $^3J_{H\text{-}H}$ = 8.2 Hz, 2H; H-5), 7.93 (dd, $^3J_{H\text{-}H}$ = 8.1 Hz, $^4J_{H\text{-}H}$ = 0.9 Hz, 2H; H-4), 7.69 (dd, $^3J_{H\text{-}H}$ = 7.4, $^4J_{H\text{-}H}$ = 1.0 Hz, 2H; H-7), 7.64 (dd, $^3J_{H\text{-}H}$ = 8.1 Hz, $^3J_{H\text{-}H}$ = 7.0 Hz, 2H; H-3), 7.53 (dd, $^3J_{H\text{-}H}$ = 7.0 Hz, $^4J_{H\text{-}H}$ = 0.9 Hz, 2H; H-2), 7.43–7.40 (m, 2H; H-6), 7.35 (m, 4H; H-a,d), 7.31–7.28 (m, 4H; H-b,c)

$^{13}$C{$^1$H} NMR (125.77 MHz, $CDCl_3$): $\delta$ = 148.1 (br; C-e,f), 145.8 (br; C-1), 137.9 (C-a,d), 137.0 (C-8a), 135.4 (C-4a), 131.5 (C-b,c), 129.1 (C-2), 128.7 (C-7), 128.6 (C-5), 127.3 (C-4), 126.5 (C-6), 126.2 (C-3), 125.4 (C-8)

$^{11}$B{$^1$H} NMR (160.48 MHz, $CDCl_3$): $\delta$ = 58.5

***B*:**

$^1$H NMR (500.18 MHz, $CDCl_3$): $\delta$ = 7.99 (d, $^3J_{H\text{-}H}$ = 8.2 Hz, 2H; H-5), 7.92 (dd, $^3J_{H\text{-}H}$ = 8.1 Hz, $^4J_{H\text{-}H}$ = 0.8 Hz, 2H; H-4), 7.74 (dd, $^3J_{H\text{-}H}$ = 7.4 Hz, $^4J_{H\text{-}H}$ = 0.9 Hz, 2H; H-7), 7.60 (dd, $^3J_{H\text{-}H}$ = 8.1 Hz, $^3J_{H\text{-}H}$ = 7.0 Hz, 2H; H-3), 7.43 (m, 2H; H-2), 7.43–7.40 (m, 2H; H-6), 7.41–7.38 (m, 4H; H-a,d), 7.31–7.28 (m, 4H; H-b,c)

$^{13}$C{$^1$H} NMR (125.77 MHz, $CDCl_3$): $\delta$ = 147.8 (br; C-e,f), 146.4 (br; C-1), 138.1 (C-a,d), 136.8 (C-8a), 135.3 (C-4a), 131.5 (C-b,c), 128.8 (C-7), 128.6 (C-2), 128.6 (C-5), 127.4 (C-4), 126.5 (C-6), 126.3 (C-3), 125.4 (C-8)

$^{11}$B{$^1$H} NMR (160.48 MHz, $CDCl_3$): $\delta$ = 58.5

HRMS: Calculated m/z for $C_{32}H_{20}B_2Br_2$ [$M^+$]: 584.01124, found: 584.01199

**9,10-Bis(8-iodonaphth-1-yl)-9,10-dihydro-9,10-diboraanthracene ($2^{H,I}$):**

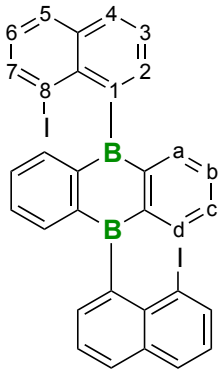


Following the general procedure, 1,8-diiodonaphthalene (800 mg, 2.11 mmol), *n*-BuLi (1.35 mL, 1.56 M, 2.11 mmol), and 9,10-dibromo-9,10-dihydro-9,10-diboraanthracene (335 mg, 1.00 mmol) were used to obtain $\mathbf{2^{H,I}}$ after purification by flash chromatography (*c*-hexane:$CH_2Cl_2$ = 5:1) as a yellow solid. Yield: 572 mg (0.84 mmol, 84%). Conformer ratio A:B ≈ 1.4:1 (determined by $^1$H NMR spectroscopy).

***A*:**

$^1$H NMR (500.18 MHz, $CDCl_3$): $\delta$ = 8.06–8.02 (m, 4H; H-5,7), 7.83 (dd, $^3J_{H\text{-}H}$ = 8.1 Hz, $^4J_{H\text{-}H}$ = 1.0 Hz, 2H; H-4), 7.53 (dd, $^3J_{H\text{-}H}$ = 8.1 Hz, $^3J_{H\text{-}H}$ = 7.0 Hz, 2H; H-3), 7.45–7.42 (m, 4H; H-a,d), 7.35–7.33 (m, 2H; H-2), 7.33–7.29 (m, 2H; H-6), 7.27–7.24 (m, 4H; H-b,c)

$^{13}$C{$^1$H} NMR (125.77 MHz, $CDCl_3$): $\delta$ = 150.6 (C-1), 149.3 (C-e,f), 140.6 (C-8a), 138.3 (C-a,d), 136.3 (C-7), 135.6 (C-4a), 131.1 (C-b,c), 129.6 (C-2), 129.4 (C-5), 127.9 (C-4), 127.1 (C-6), 126.2 (C-3), 103.8 (C-8)

$^{11}$B{$^1$H} NMR (160.48 MHz, $CDCl_3$): $\delta$ = 56.4

***B*:**

$^1$H NMR (500.18 MHz, $CDCl_3$): $\delta$ = 8.06–8.03 (m, 2H; H-5), 7.99 (dd, $^3J_{H\text{-}H}$ = 7.2 Hz, $^4J_{H\text{-}H}$ = 1.1 Hz, 2H; H-7), 7.86 (dd, $^3J_{H\text{-}H}$ = 8.0 Hz, $^4J_{H\text{-}H}$ = 1.1 Hz, 2H; H-4), 7.58 (dd, $^3J_{H\text{-}H}$ = 8.0 Hz, $^3J_{H\text{-}H}$ = 7.0 Hz, 2H; H-3), 7.48 (dd, $^3J_{H\text{-}H}$ = 7.0 Hz, $^4J_{H\text{-}H}$ = 1.1 Hz, 2H; H-2), 7.37–7.35 (m, 2H; H-a,d), 7.33–7.29 (m, 2H; H-6), 7.27–7.24 (m, 2H; H-b,c)

$^{13}$C{$^1$H} NMR (125.77 MHz, $CDCl_3$): $\delta$ = 150.6 (C-1), 148.8 (C-e,f), 141.0 (C-8a), 137.8 (C-a,d), 136.0 (C-7), 135.7 (C-4a), 131.1 (C-b,c), 130.3 (C-2), 129.6 (C-5), 127.8 (C-4), 127.1 (C-6), 126.2 (C-3), 103.9 (C-8)

$^{11}$B{$^1$H} NMR (160.48 MHz, $CDCl_3$): $\delta$ = 56.4

HRMS: Calculated m/z for $C_{32}H_{21}B_2I_2$ [$MH^+$]: 680.99132, found: 680.99208

**1,5-Difluoro-9,10-bis(8-bromonaphth-1-yl)-9,10-dihydro-9,10-diboraanthracene ($2^{F,Br}$):**

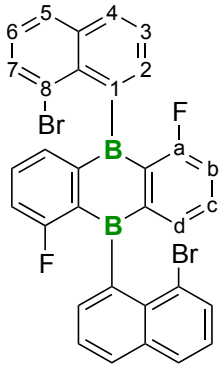


Following the general procedure, 1,8-dibromonaphthalene (600 mg, 2.11 mmol), *n*-BuLi (1.34 mL, 1.56 M, 2.11 mmol), and 1,5-difluoro-9,10-dibromo-9,10-dihydro-9,10-diboraanthracene (370 mg, 1.00 mmol) were used to obtain $\mathbf{2^{F,Br}}$ after purification by flash chromatography (*c*-hexane:$CH_2Cl_2$ = 5:1) as a yellow solid. Yield: 372 mg (0.60 mmol, 60%). Conformer ratio A:B ≈ 1.3:1 (determined by $^1$H NMR spectroscopy).

***A*:**

$^1$H NMR (500.18 MHz, $CDCl_3$): $\delta$ = 7.98 (dd, $^3J_{H\text{-}H}$ = 8.2 Hz, $^4J_{H\text{-}H}$ = 1.0 Hz, 2H; H-5), 7.87 (dd, $^3J_{H\text{-}H}$ = 8.1 Hz, $^4J_{H\text{-}H}$ = 0.8 Hz, 2H; H-4), 7.74 (dd, $^3J_{H\text{-}H}$ = 7.3 Hz, $^4J_{H\text{-}H}$ = 1.0 Hz, 2H; H-7), 7.58 (dd, $^3J_{H\text{-}H}$ = 8.1 Hz, $^3J_{H\text{-}H}$ = 7.0 Hz, 2H; H-3), 7.44–7.40 (m, 2H; H-6), 7.40 (dd, $^3J_{H\text{-}H}$ = 7.0 Hz, $^4J_{H\text{-}H}$ = 0.8 Hz, 2H; H-2), 7.33–7.29 (m, 2H; H-c), 7.13 (d, $^3J_{H\text{-}H}$ = 7.3 Hz, 2H; H-d), 6.94–6.90 (m, 2H; H-b)

$^{13}$C{$^1$H} NMR (125.77 MHz, $CDCl_3$): $\delta$ = 168.2 (d, $^1J_{C\text{-}F}$ = 256.1 Hz; C-a), 150.0 (br; C-e), 148.2 (br; C-1), 136.4 (C-8a), 135.4 (C-4a), 134.6 (d, $^4J_{C\text{-}F}$ = 2.5 Hz; C-d), 134.0 (d, $^3J_{C\text{-}F}$ = 9.2 Hz; C-c), 132.6* (very br; C-f), 128.6 (C-5), 127.9 (C-7), 126.8 (C-4), 126.6 (C-2), 126.5 (C-3), 126.3 (C-6), 125.7 (C-8), 119.1 (d, $^2J_{C\text{-}F}$ = 25.6 Hz; C-b)

$^{11}$B{$^1$H} NMR (160.48 MHz, $CDCl_3$): $\delta$ = 54.4

$^{19}$F NMR (470.64 MHz, $CDCl_3$): $\delta$ = –95.9 (dd, $^3J_{H\text{-}F}$ = 9.7 Hz, $^4J_{H\text{-}F}$ = 5.4 Hz)

$^{19}$F{$^1$H} NMR (282.29 MHz, $CDCl_3$): $\delta$ = –95.9 (s)

***B*:**

$^1$H NMR (500.18 MHz, $CDCl_3$): $\delta$ = 7.98 (dd, $^3J_{H\text{-}H}$ = 8.2 Hz, $^4J_{H\text{-}H}$ = 1.0 Hz, 2H; H-5), 7.86 (dd, $^3J_{H\text{-}H}$ = 8.0 Hz, $^4J_{H\text{-}H}$ = 0.8 Hz, 2H; H-4), 7.76 (dd, $^3J_{H\text{-}H}$ = 7.3 Hz, $^4J_{H\text{-}H}$ = 1.0 Hz, 2H; H-7), 7.55 (dd, $^3J_{H\text{-}H}$ = 8.0 Hz, $^3J_{H\text{-}H}$ = 7.0 Hz, 2H; H-3), 7.46–7.41 (m, 2H; H-6), 7.31–7.28 (m, 2H; H-c), 7.30–7.28 (m, 2H; H-2), 7.16 (d, $^3J_{H\text{-}H}$ = 7.3 Hz, 2H; H-d), 6.93–6.89 (m, 2H; H-b)

$^{13}C\{^1H\}$ NMR (125.77 MHz, $CDCl_3$): $\delta$ = 168.1 (d, $^1J_{C\text{-}F}$ = 256.1 Hz; C-a), 149.6 (br; C-e), 148.1 (br; C-1), 136.3 (C-8a), 135.3 (C-4a), 134.8 (d, $^4J_{C\text{-}F}$ = 2.6 Hz; C-d), 134.0 (d, $^3J_{C\text{-}F}$ = 9.1 Hz; C-c), 132.4* (br; C-f), 128.6 (C-5), 127.9 (C-7), 126.8 (C-4), 126.6 (C-2), 126.5 (C-3), 126.3 (C-6), 125.9 (C-8), 118.9 (d, $^2J_{C\text{-}F}$ = 25.6 Hz; C-b)

$^{11}B\{^1H\}$ NMR (160.48 MHz, $CDCl_3$): $\delta$ = 54.4

$^{19}F$ NMR (470.64 MHz, $CDCl_3$): $\delta$ = –96.0 (dd, $^3J_{H\text{-}F}$ = 9.8 Hz, $^4J_{H\text{-}F}$ = 5.4 Hz)

$^{19}F\{^1H\}$ NMR (282.29 MHz, $CDCl_3$): $\delta$ = –96.0 (s)

*These signals were only detectable in the $^{H,C}$HMBC-spectrum.

HRMS: Calculated m/z for $C_{32}H_{18}B_2Br_2F_2$ [$M^+$]: 619.99239, found: 619.99293

**1,5-Difluoro-9,10-bis(8-iodonaphth-1-yl)-9,10-dihydro-9,10-diboraanthracene ($2^{F,I}$):**

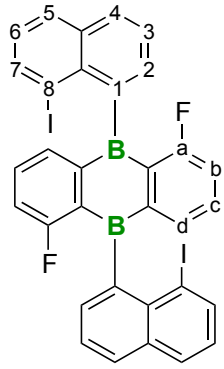


Following the general procedure, 1,8-diiodonaphthalene (800 mg, 2.11 mmol), *n*-BuLi (1.34 mL, 1.56 M, 2.11 mmol), and 1,5-difluoro-9,10-dibromo-9,10-dihydro-9,10-diboraanthracene (371 mg, 1.00 mmol) were used to obtain $\mathbf{2^{F,I}}$ after purification by flash chromatography (*c*-hexane:$CH_2Cl_2$ = 5:1) as a yellow solid. Yield: 474 mg (0.66 mmol, 66%). Conformer ratio A:B ≈ 1.1:1 (determined by $^1$H NMR spectroscopy).

***A*:**

$^1$H NMR (500.18 MHz, $CDCl_3$): $\delta$ = 8.06–7.98 (m, 4H, H-5,7), 7.77 (d, $^3J_{H\text{-}H}$ = 8.0 Hz, 2H; H-4), 7.48 (vt, $^3J_{H\text{-}H}$ = 7.9 Hz, $^3J_{H\text{-}H}$ = 7.2 Hz, 2H; H-3), 7.37–7.31 (m, 2H; H-6), 7.31–7.23 (m, 2H; H-c), 7.19 (d, $^3J_{H\text{-}H}$ = 7.3 Hz, 2H; H-d), 7.17 (d, $^3J_{H\text{-}H}$ = 7.0 Hz, 2H; H-2), 6.92–6.86 (m, 2H; H-b)

$^{13}$C{$^1$H} NMR (125.77 MHz, $CDCl_3$): $\delta$ = 167.9 (d, $^1J_{C\text{-}F}$ = 256.8 Hz; C-a), 152.3* (br; C-1), 150.9* (br; C-e), 140.3 (C-8a), 135.7 (C-4a), 135.1 (C-7), 134.5 (C-d), 133.9* (br; C-f), 133.4 (C-c), 129.6 (C-5), 127.3 (C-2), 127.2 (C-4), 126.9 (C-6), 126.4 (C-3), 118.5 (C-b), 104.9 (C-8)

$^{11}$B{$^1$H} NMR (160.48 MHz, $CDCl_3$): $\delta$ = 52.1

$^{19}$F NMR (470.64 MHz, $CDCl_3$): $\delta$ = –95.6 (m)

$^{19}$F{$^1$H} NMR (282.29 MHz, $CDCl_3$): $\delta$ = –95.5 (s)

***B*:**

$^1$H NMR (500.18 MHz, $CDCl_3$): $\delta$ = 8.06–7.98 (m, 4H; H-5,7), 7.79 (d, $^3J_{H\text{-}H}$ = 7.9 Hz, 2H; H-4), 7.53 (vt, $^3J_{H\text{-}H}$ = 7.8 Hz, $^3J_{H\text{-}H}$ = 7.5 Hz, 2H; H-3), 7.36 (d, $^3J_{H\text{-}H}$ = 7.0 Hz, 2H; H-2), 7.37–7.31 (m, 2H; H-6), 7.31–7.23 (m, 2H; H-c), 7.11 (d, $^3J_{H\text{-}H}$ = 7.4 Hz, 2H; H-d), 6.92–6.86 (m, 2H; H-b)

$^{13}$C{$^1$H} NMR (125.77 MHz, $CDCl_3$): $\delta$ = 167.6 (d, $^1J_{C\text{-}F}$ = 256.8 Hz; C-a), 152.8* (br; C-1), 150.9* (br; C-e), 140.4 (C-8a), 135.7 (C-4a), 135.1 (C-7), 134.5 (C-d), 133.9* (br; C-f), 133.3

(C-c), 129.6 (C-5), 127.8 (C-2), 127.2 (C-4), 126.9 (C-6), 126.5 (C-3), 118.2 (C-b), 104.6 (C-8)

$^{11}B\{^{1}H\}$ NMR (160.48 MHz, $CDCl_3$): $\delta$ = 52.1

$^{19}F$ NMR (470.64 MHz, $CDCl_3$): $\delta$ = –95.6 (m)

$^{19}F\{^{1}H\}$ NMR (282.29 MHz, $CDCl_3$): $\delta$ = –95.5 (s)

HRMS: Calculated m/z for $C_{32}H_{18}B_2F_2I_2$ [$M^+$]: 715.96466, found: 715.96560

**1,5-Dibromo-9,10-bis(8-bromonaphth-1-yl)-9,10-dihydro-9,10-diboraanthracene ($2^{Br,Br}$):**

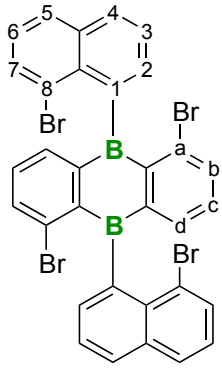


Following the general procedure, 1,8-dibromonaphthalene (600 mg, 2.11 mmol), *n*-BuLi (1.34 mL, 1.56 M, 2.11 mmol), and 1,5,9,10-tetrabromo-9,10-dihydro-9,10-diboraanthracene (491 mg, 1.00 mmol) were used to obtain $\mathbf{2^{Br,Br}}$ after purification by flash chromatography (*c*-hexane:$CH_2Cl_2$ = 5:1) as a yellow solid. Yield: 549 mg (0.74 mmol, 74%). Conformer ratio A:B ≈ 2.2:1 (determined by $^1$H NMR spectroscopy).

***A*:**

$^1$H NMR (500.18 MHz, $CDCl_3$): $\delta$ = 7.97 (d, $^3J_{H\text{-}H}$ = 8.1 Hz, 2H; H-5), 7.85 (d, $^3J_{H\text{-}H}$ = 7.2 Hz, 2H; H-4), 7.81 (dd, $^3J_{H\text{-}H}$ = 7.7 Hz, $^4J_{H\text{-}H}$ = 0.8 Hz, 2H; H-7), 7.55 (dd, $^3J_{H\text{-}H}$ = 7.7 Hz, $^4J_{H\text{-}H}$ = 1.1 Hz, 2H; H-b), 7.53–7.49 (m, 2H; H-3), 7.45 (vt, $^3J_{H\text{-}H}$ = 8.1 Hz, $^3J_{H\text{-}H}$ = 7.7 Hz, 2H; H-6), 7.22 (dd, $^3J_{H\text{-}H}$ = 7.6 Hz, $^4J_{H\text{-}H}$ = 1.1 Hz, 2H; H-d), 7.20 (m, 2H; H-2), 7.04 (vt, 2H; H-c)

$^{13}$C{$^1$H} NMR (125.77 MHz, $CDCl_3$): $\delta$ = 153.8* (br; C-e), 148.9* (br; C-1), 143.9* (br; C-f), 138.4 (C-d), 137.4 (C-8a), 137.3 (C-b), 135.4 (C-4a), 135.2 (C-a), 132.5 (C-c), 128.6 (C-5), 128.0 (C-7), 127.0 (C-3), 126.8 (C-8), 126.7 (C-4), 126.3 (C-6), 126.3 (C-2)

$^{11}$B{$^1$H} NMR (160.48 MHz, $CDCl_3$): $\delta$ = 53.5

***B*:**

$^1$H NMR (500.18 MHz, $CDCl_3$): $\delta$ = 7.97 (d, $^3J_{H\text{-}H}$ = 8.1 Hz, 2H; H-5), 7.88–7.85 (m, 2H; H-4), 7.80–7.78 (m, 2H; H-7), 7.58–7.55 (m, 2H; H-b), 7.53–7.49 (m, 2H; H-3), 7.44 (vt, 2H; H-6), 7.26–7.25 (m, 2H; H-2), 7.19–7.17 (m, 2H; H-d), 7.05 (vt, 2H; H-c)

$^{13}$C{$^1$H} NMR (125.77 MHz, $CDCl_3$): $\delta$ = 152.7* (br; C-e), 148.8* (br; C-1), 143.5* (br; C-f), 138.0 (C-d), 137.7 (C-8a), 137.3 (C-b), 135.4 (C-4a), 135.2 (C-a), 132.6 (C-c), 128.6 (C-5), 128.0 (C-7), 126.9 (C-3), 126.8 (C-8), 126.7 (C-4), 126.3 (C-6), 126.1 (C-2)

$^{11}$B{$^1$H} NMR (160.48 MHz, $CDCl_3$): $\delta$ = 53.5

HRMS: Calculated m/z for $C_{32}H_{18}B_2Br_4$ [$M^+$]: 739.83226, found: 739.83431

**1,5-Dibromo-9,10-bis(8-iodonaphth-1-yl)-9,10-dihydro-9,10-diboraanthracene ($2^{Br,I}$):**

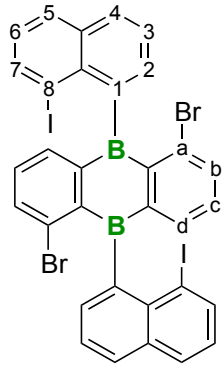


Following the general procedure, 1,8-diiodonaphthalene (800 mg, 2.11 mmol), *n*-BuLi (1.34 mL, 1.56 M, 2.11 mmol), and 1,5,9,10-tetrabromo-9,10-dihydro-9,10-diboraanthracene (493 mg, 1.00 mmol) were used to obtain $\mathbf{2^{Br,I}}$ after purification by flash chromatography (*c*-hexane:$CH_2Cl_2$ = 5:1) as a yellow solid. Yield: 668 mg (0.89 mmol, 89%). Single crystals of $\mathbf{2^{Br,I}}$ were grown by slow evaporation of a saturated solution of $\mathbf{2^{Br,I}}$ in $CH_2Cl_2$ at room temperature. Conformer ratio A:B ≈ 10:1 (determined by $^1$H NMR spectroscopy).

***A*:**

$^1$H NMR (500.18 MHz, $CDCl_3$): $\delta$ = 8.04–8.00 (m, 4H; H-5,7), 7.79 (dd, $^3J_{H\text{-}H}$ = 8.1 Hz, $^4J_{H\text{-}H}$ = 0.9 Hz, 2H; H-4), 7.55 (dd, $^3J_{H\text{-}H}$ = 7.8 Hz, $^4J_{H\text{-}H}$ = 1.2 Hz, 2H; H-b), 7.49 (dd, $^3J_{H\text{-}H}$ = 8.1 Hz, $^3J_{H\text{-}H}$ = 7.1 Hz, 2H; H-3), 7.33 (dd, $^3J_{H\text{-}H}$ = 8.1 Hz, $^3J_{H\text{-}H}$ = 7.3 Hz, 2H; H-6), 7.22 (dd, $^3J_{H\text{-}H}$ = 7.1 Hz, $^4J_{H\text{-}H}$ = 0.9 Hz, 2H; H-2), 7.11 (dd, $^3J_{H\text{-}H}$ = 7.6 Hz, $^4J_{H\text{-}H}$ = 1.2 Hz, 2H; H-d), 7.01 (vt, 2H; H-c)

$^{13}$C{$^1$H} NMR (125.77 MHz, $CDCl_3$): $\delta$ = 154.3 (br; C-e), 153.0 (br; C-1), 144.8 (br; C-f), 141.4 (C-8a), 138.1 (C-d), 136.9 (C-b), 136.0 (C-4a), 135.3 (C-a), 135.0 (C-7), 132.1 (C-c), 129.6 (C-5), 127.3 (C-2), 127.1 (C-4), 127.0 (C-3), 126.8 (C-6), 106.3 (C-8)

$^{11}$B{$^1$H} NMR (160.48 MHz, $CDCl_3$): $\delta$ = 49.7

***B*:**

$^1$H NMR (500.18 MHz, $CDCl_3$): $\delta$ = 8.07 (dd, $^3J_{H\text{-}H}$ = 7.3 Hz, $^4J_{H\text{-}H}$ = 1.0 Hz, 2H; H-7), 8.02–8.00 (m, 2H; H-5), 7.76 (dd, $^3J_{H\text{-}H}$ = 8.1 Hz, $^4J_{H\text{-}H}$ = 0.9 Hz, 2H; H-4), 7.55–7.52 (m, 2H; H-b), 7.47–7.43 (m, 2H; H-3), 7.37–7.32 (m, 2H; H-6), 7.25–7.22 (m, 2H; H-2), 7.11–7.08 (m, 2H; H-d), 7.03–7.00 (m, 2H; H-c)

$^{13}$C{$^1$H} NMR (125.77 MHz, $CDCl_3$): n.o.

$^{11}$B{$^1$H} NMR (160.48 MHz, $CDCl_3$): $\delta$ = 49.7

HRMS: Calculated m/z for $C_{32}H_{18}B_2Br_2I_2$ [$M^+$]: 835.80452, found: 835.80676

**Reaction of 1,5-difluoro-9,10-bis(8-iodonaphth-1-yl)-9,10-dihydro-9,10-diboraanthracene with selected organometallic reagents**

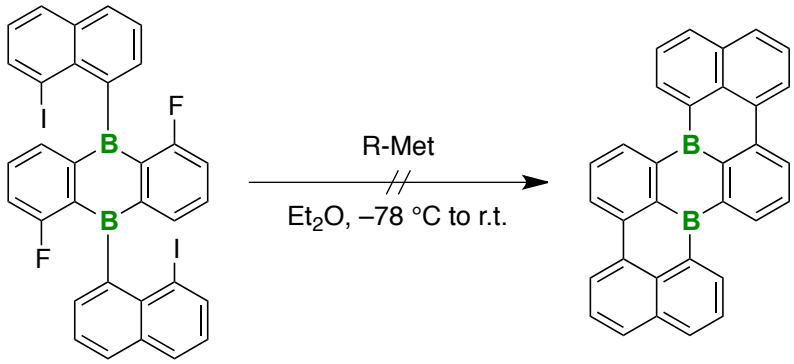


An $Et_2O$ solution of 1,5-difluoro-9,10-bis(8-iodonaphth-1-yl)-9,10-dihydro-9,10-diboraanthracene was treated at –78 °C with selected organometallic reagents (*n*-BuLi, *t*-BuLi, or *i*PrMgBr•LiCl). In none of these cases, the intended cyclization to give **$B_2$-TBPA** was observed. We rather isolated either unconsumed starting material 1,5-difluoro-9,10-bis(8-iodonaphth-1-yl)-9,10-dihydro-9,10-diboraanthracene (no reaction) or naphthalene (indicating decomposition).

**Table S2-1:** Reactivity of 1,5-difluoro-9,10-bis(8-iodonaphthalen-1-yl)-9,10-dihydro-9,10-diboraanthracene toward selected organometallic reagents (R-Met).

| R-Met | amount | result |
|---|---|---|
| *n*-BuLi | 2 equiv | no reaction |
| *n*-BuLi | excess | decomposition |
| *t*-BuLi | 2 equiv | no reaction |
| *t*-BuLi | excess | decomposition |
| *i*PrMgBr•LiCl | 2 equiv | no reaction |
| *i*PrMgBr•LiCl | excess | no reaction |

**Reaction of 1,5-difluoro-9,10-dibromo-9,10-dihydro-9,10-diboraanthracene with 1,8-dilithionaphthalene**

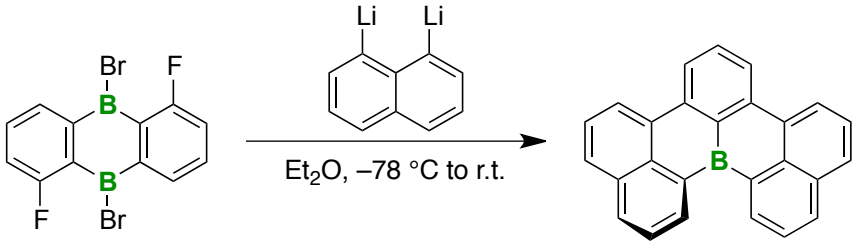


A 100 mL flame-dried Schlenk flask was charged with 1,8-diiodonaphthalene (617 mg, 1.62 mmol) and $Et_2O$ (30 mL). The solution was cooled to 0 °C over 15 min and *n*-BuLi (2.60 mL, 1.56 M, 4.06 mmol) was added dropwise with stirring. The ice bath was removed after 15 min, and the bright orange solution stirred at room temperature for 30 min. The solution was cooled to –78 °C over 30 min and 1,5-difluoro-9,10-dibromo-9,10-dihydro-9,10-diboraanthracene (300 mg, 0.81 mmol) was added in one portion. The reaction mixture was stirred overnight and subsequently quenched with MeOH (10 mL). All volatiles were removed under vacuum and the crude product was purified by flash chromatography (*c*-hexane:$CH_2Cl_2$ = 5:1) to furnish the [4]helicene **IV** as an orange solid. Yield: 29 mg (0.09 mmol, 11%). $^1$H and $^{13}$C{$^1$H} NMR data were in accord with published values.[S14]

**Reactions of 1,5-dibromo-9,10-bis(8-bromonaphth-1-yl)-9,10-dihydro-9,10-dibora-anthracene ($2^{Br,Br}$) with $Ni(COD)_2$ under Yamamoto conditions:**

**Reaction in pyridine leading to $B_2$-TBPA**

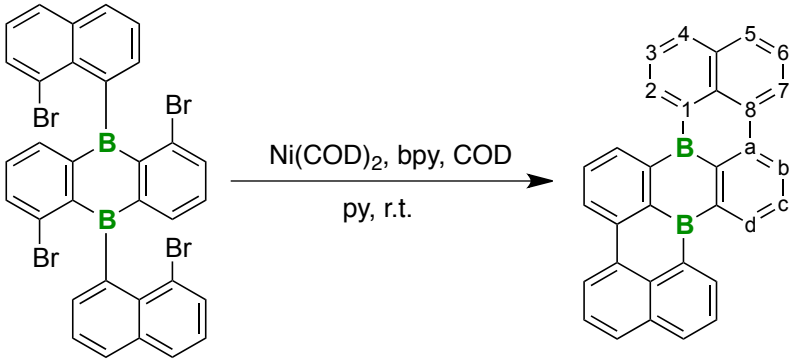


2,2'-Bipyridyl (37 mg, 0.24 mmol; bpy) was dissolved in pyridine (20 mL; py), neat 1,5-cyclooctadiene (24 mg, 0.21 mmol; COD) and $Ni(COD)_2$ (65 mg, 0.24 mmol) were added, and the mixture was stirred at room temperature for 1 h. The resulting dark-colored mixture was slowly added (over 4 h using a syringe pump) at room temperature to a pale yellow solution of $\mathbf{2^{Br,Br}}$ (40 mg, 54 µmol) in pyridine (60 mL). After complete addition, stirring was continued for 24 h at room temperature, the mixture was placed in an ice bath and quenched by bubbling air through it. A beige solution containing an off-white precipitate was obtained. All volatiles were removed under vacuum and the brownish solid residue was subjected to flash-column chromatography (*c*-hexane → *c*-hexane:$CH_2Cl_2$ = 1:1). The fraction containing the luminescent **$B_2$-TBPA** was evaporated to dryness under reduced pressure and the residue washed with ice-cold *n*-pentane (2 × 1 mL). **$B_2$-TBPA** was obtained as a yellow solid. Yield: 18 mg (42 µmol, 79%). Single crystals of **$B_2$-TBPA** were grown by slow evaporation of a saturated solution in $CHCl_3$ at room temperature.

*Note:* The cyclization experiment was also performed with 1,5-dibromo-9,10-bis(8-iodonaphthalen-1-yl)-9,10-dihydro-9,10-diboraanthracene $\mathbf{2^{Br,I}}$ (40 mg, 48 µmol) and furnished **$B_2$-TBPA** in a comparable yield of 70% (14 mg, 33 µmol).

$^1$H NMR (500.18 MHz, $CDCl_3$): $\delta$ = 8.80 (d, $^3J_{H\text{-}H}$ = 7.0 Hz, 2H; H-2), 8.77 (d, $^3J_{H\text{-}H}$ = 7.7 Hz, 2H; H-7), 8.71 (d, $^3J_{H\text{-}H}$ = 8.1 Hz, 2H; H-b), 8.33 (d, $^3J_{H\text{-}H}$ = 8.0 Hz, 2H; H-4), 8.26 (d, $^3J_{H\text{-}H}$ = 7.1 Hz, 2H; H-d), 8.12 (d, $^3J_{H\text{-}H}$ = 8.0 Hz, 2H; H-5), 7.87 (2 × vt, 4H; H-3,c), 7.80 (vt, $^3J_{H\text{-}H}$ = 8.0 Hz, $^3J_{H\text{-}H}$ = 7.7 Hz, 2H; H-6)

$^{13}C\{^1H\}$ NMR (125.77 MHz, $CDCl_3$): $\delta$ = 145.1* (br; C-e), 143.4* (br; C-f), 141.0 (C-2), 140.5 (C-a), 137.7 (C-d), 135.3 (C-4), 133.3 (C-4a), 132.7 (C-8), 132.2 (C-8a), 131.5 (C-c), 130.8 (C-5), 126.5 (C-b), 126.1 (C-6), 126.0 (C-3), 125.1 (C-7), n.o. (C-1)

$^{11}B\{^1H\}$ NMR (160.48 MHz, $CDCl_3$): $\delta$ = 56.0

*These signals were only detectable in the $^{H,C}$HMBC-spectrum.

HRMS: Calculated m/z for $C_{32}H_{18}B_2$ [$M^+$]: 424.15891, found: 424.15938

UV-vis (*c*-hexane): $\lambda_{max}$ (ε) = 456 nm (14600 $M^{-1}cm^{-1}$)

Fluorescence (*c*-hexane, $\lambda_{ex}$ = 340 nm): $\lambda_{max}$ = 472 nm; $\Phi_{PL}$ = 69%

Cyclic voltammetry ($CH_2Cl_2$, [*n*-$Bu_4N$][$PF_6$], 0.1 M, 200 mV $s^{-1}$, vs. FcH/$FcH^+$): $E_{1/2}$ = –1.65 V, $E_{pc}$ = –2.22, –2.45, –2.65 V

Cyclic voltammetry (THF, [*n*-$Bu_4N$][$PF_6$], 0.1 M, 200 mV $s^{-1}$, vs. FcH/$FcH^+$): $E_{1/2}$ = –1.73 V, $E_{pc}$ = –2.30 V

Cyclic voltammetry (pyridine, [*n*-$Bu_4N$][$PF_6$], 0.1 M, 200 mV $s^{-1}$, vs. FcH/$FcH^+$): $E_{1/2}$ = –2.16 V

**Reaction in pyridine leading to 4**

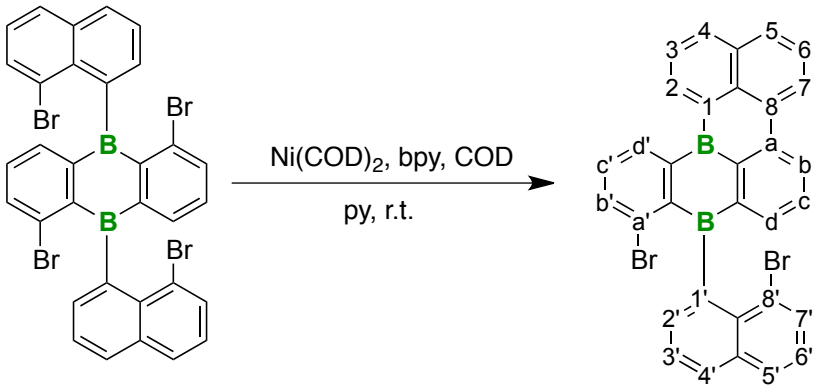


2,2'-Bipyridyl (18 mg, 113 µmol; bpy) was dissolved in pyridine (20 mL; py), neat 1,5-cyclooctadiene (13 mg, 113 µmol; COD) and $Ni(COD)_2$ (31 mg, 113 µmol) were added, and the mixture was stirred at room temperature for 1 h. The resulting dark-colored mixture was slowly added (over 4 h using a syringe pump) at room temperature to a pale yellow solution of $\mathbf{2^{Br,Br}}$ (40 mg, 54 µmol) in pyridine (60 mL). After complete addition, stirring was continued for 24 h at room temperature, the mixture was placed in an ice bath and quenched by bubbling air through it. A beige solution containing an off-white precipitate was obtained. All volatiles were removed under vacuum and the brownish solid residue was subjected to flash-column chromatography (*c*-hexane → *c*-hexane:$CH_2Cl_2$ = 1:1). The fraction containing

**4** was evaporated to dryness under reduced pressure and the residue washed with ice-cold *n*-pentane (2 × 1 mL). **4** was obtained as an orange solid. Yield: 24 mg, (41 µmol, 77%).

$^{1}$H NMR (500.18 MHz, $CDCl_3$): $\delta$ = 8.71 (d, $^{3}J_{H-H}$ = 7.2 Hz, 1H; H-2), 8.67 (d, $^{3}J_{H-H}$ = 7.5 Hz, 1H; H-7), 8.44 (d, $^{3}J_{H-H}$ = 8.1 Hz, 1H; H-b), 8.34 (d, $^{3}J_{H-H}$ = 8.2 Hz, 1H; H-4), 8.19 (d, $^{3}J_{H-H}$ = 7.3 Hz, 1H; H-d'), 8.10 (d, $^{3}J_{H-H}$ = 8.0 Hz, 1H; H-5), 7.97 (d, $^{3}J_{H-H}$ = 8.4 Hz, 1H; H-5'), 7.87 (dd, $^{3}J_{H-H}$ = 8.2 Hz, $^{3}J_{H-H}$ = 7.2 Hz, 1H; H-3), 7.86–7.84 (m, 1H; H-4'), 7.80–7.75 (m, 3H; H-6,7',b'), 7.52 (vt, 1H; H-3'), 7.50 (vt, 1H; H-c), 7.46 (vt, 1H; H-c'), 7.43 (vt, 1H; H-6'), 7.27 (d, $^{3}J_{H-H}$ = 7.4 Hz, 1H; H-2'), 7.20 (d, $^{3}J_{H-H}$ = 7.0 Hz, 1H; H-d)

$^{13}$C{$^{1}$H} NMR (125.77 MHz, $CDCl_3$): $\delta$ = 151.6 (br; C-e'), 148.9 (br; C-1'), 148.2 (br; C-e), 146.6 (br; C-f'), 141.5 (br; C-f), 141.3 (C-2), 139.6 (C-a), 137.9 (C-d'), 137.8 (C-d), 137.5 (C-b'), 137.5 (C-8a'), 136.4 (C-a'), 135.6 (C-4), 135.4 (C-4a'), 132.6 (C-8), 132.5 (C-c), 131.9 (C-4a), 131.5 (C-8a), 131.5 (C-c'), 130.8 (C-5), 128.5 (C-5'), 127.8 (C-7'), 126.9 (C-3'), 126.9 (C-8'), 126.6 (C-b), 126.5 (C-2'), 126.2 (C-4'), 126.2 (C-6), 126.2 (C-6'), 125.9 (C-3), 125.3 (C-7), n.o. (C-1)

$^{11}$B{$^{1}$H} NMR (160.48 MHz, $CDCl_3$): $\delta$ = 55.3

HRMS: Calculated m/z for $C_{32}H_{18}B_2Br_2$ [$M^+$]: 581.99559, found: 581.99832

*Note:* Besides the major set of resonances compiled above, samples of compound **4** also gave rise to a minor set of resonances with similar chemical shift values in the $^{1}$H as well as $^{13}$C{$^{1}$H} NMR spectra. Given that the samples had been purified by column chromatography and show only one peak in the HRMS mass spectrum, the minor resonances are probably not due to impurities but most likely originate from a second diastereomer. Listed below are those signals of the minor component, which do not overlap with resonances of the major species.

$^{1}$H NMR (500.18 MHz, $CDCl_3$): $\delta$ = 8.25 (d), 7.84–7.80 (m), 7.63–7.57 (m), 7.35–7.30 (m)

$^{13}$C{$^{1}$H} NMR (125.77 MHz, $CDCl_3$): $\delta$ = 133.1, 130.1, 128.1, 127.5, 127.3, 126.9, 126.8, 126.3

**Reaction in THF leading to the B–O–B species ODBE**

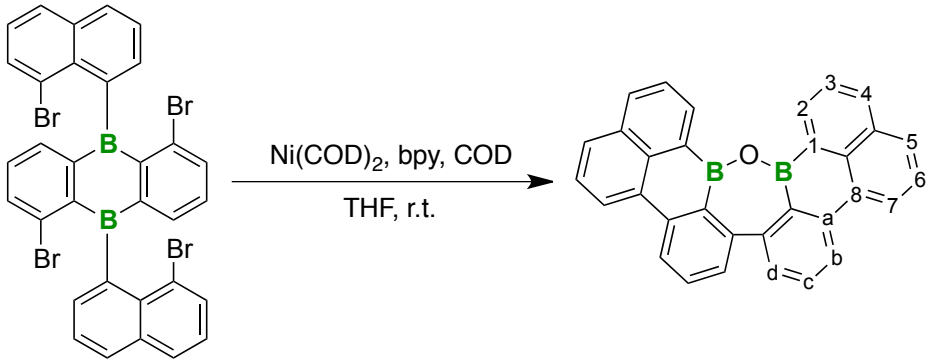


2,2'-Bipyridyl (37 mg, 0.24 mmol; bpy) was dissolved in THF (20 mL), neat 1,5-cyclooctadiene (24 mg, 0.21 mmol; COD) and $Ni(COD)_2$ (65 mg, 0.24 mmol) were added, and the mixture was stirred at room temperature for 1 h. The resulting deeply purple-colored mixture was slowly added (over 4 h using a syringe pump) at room temperature to a solution of $\mathbf{2^{Br,Br}}$ (40 mg, 54 µmol) in THF (60 mL). The initial pale yellow solution turned dark during the process. After complete addition, stirring was continued for 24 h at room temperature, the mixture was placed in an ice bath and quenched by bubbling air through it. A yellow solution containing an off-white precipitate was obtained. All volatiles were removed under vacuum and the brownish solid residue was subjected to flash-column chromatography (*c*-hexane → *c*-hexane:$CH_2Cl_2$ = 1:1). The fraction containing the luminescent **ODBE** was evaporated to dryness under reduced pressure and the residue washed with ice-cold *n*-pentane (3 × 2 mL). **ODBE** was obtained as a bright yellow solid. Yield: 19 mg (43 µmol, 81%). Single crystals of **ODBE** were grown by slow gas-phase diffusion of *n*-hexane into a saturated solution of **ODBE** in $CHCl_3$ at room temperature.

*Note*: Despite numerous attempts, we did not succeed in avoiding the $O_2/H_2O$ quenching step during workup of the reaction product(s) obtained in THF, because residual nickel species could not be removed quantitatively under inert conditions. These attempts included filtering through Celite, manual chromatography, and flash-column chromatography; both silica- and alumina-based stationary phases have been employed, as well as THF, $CHCl_3$, and $C_6H_6$ as mobile phases. We also tried to use $S_8$ as a quenching reagent, but again without success. The product(s) obtained always had a greyish tint and produced NMR spectra with extremely broadened resonances, indicative of the presence of paramagnetic Ni(II) impurities. Importantly, the majority of the few available protocols on intramolecular Yamamoto-type coupling reactions contain an aqueous workup step, in some cases even with addition of HCl or $NH_4Cl$.[S15–S22]

$^{1}$H NMR (500.18 MHz, $CDCl_3$): $\delta$ = 8.79 (d, $^{3}J_{H-H}$ = 6.8 Hz, 2H; H-2), 8.57 (d, $^{3}J_{H-H}$ = 7.7 Hz, 2H; H-7), 8.54 (d, $^{3}J_{H-H}$ = 7.9 Hz, 2H; H-b), 8.21 (d, $^{3}J_{H-H}$ = 8.0 Hz, 2H; H-4), 8.03 (d, $^{3}J_{H-H}$ = 8.1 Hz, 2H; H-5), 7.80 (vt, 2H; H-3), 7.79 (vt, 2H; H-c), 7.71 (vt, $^{3}J_{H-H}$ = 8.1 Hz, $^{3}J_{H-H}$ = 7.7 Hz, 2H; H-6), 7.68 (d, $^{3}J_{H-H}$ = 7.7 Hz, 2H; H-d)

$^{13}$C{$^{1}$H} NMR (125.77 MHz, $CDCl_3$): $\delta$ = 149.8 (C-e), 144.5 (C-a), 134.6 (C-2), 133.8 (C-4), 133.5 (C-8a), 132.9 (C-4a), 132.6 (C-8), 132.1 (C-c), 131.4 (C-d), 130.0 (C-5), 126.3 (C-3), 126.1 (C-6), 125.1 (C-7), 123.9 (C-b), n.o. (C-1,f)

$^{11}$B{$^{1}$H} NMR (160.48 MHz, $CDCl_3$): $\delta$ = 42.7

$^{1}$H NMR (500.18 MHz, $C_6D_6$): $\delta$ = 8.85 (dd, $^{3}J_{H-H}$ = 6.8 Hz, $^{4}J_{H-H}$ = 1.1 Hz, 2H; H-2), 8.30 (d, $^{3}J_{H-H}$ = 7.5 Hz, 2H; H-7), 8.25 (d, $^{3}J_{H-H}$ = 7.9 Hz, 2H; H-b), 7.92 (dd, $^{3}J_{H-H}$ = 8.0 Hz, $^{4}J_{H-H}$ = 1.1 Hz, 2H; H-4), 7.76 (d, $^{3}J_{H-H}$ = 8.0 Hz, 2H; H-5), 7.54 (dd, $^{3}J_{H-H}$ = 8.0 Hz, $^{3}J_{H-H}$ = 6.8 Hz, 2H; H-3), 7.51 (dd, $^{3}J_{H-H}$ = 7.8 Hz, $^{4}J_{H-H}$ = 0.9 Hz, 2H; H-d), 7.46 (vt, 2H; H-c), 7.44 (vt, 2H; H-6)

$^{13}$C{$^{1}$H} NMR (125.77 MHz, $C_6D_6$): $\delta$ = 150.2 (C-e), 144.9 (C-a), 135.0 (C-2), 134.0 (C-8a), 133.8 (C-4), 133.3 (C-4a), 133.1 (C-8), 132.1 (C-c), 131.6 (C-d), 130.1 (C-5), 126.4 (C-3), 126.2 (C-6), 125.3 (C-7), 124.1 (C-b), n.o. (C-1,f)

$^{11}$B{$^{1}$H} NMR (160.48 MHz, $C_6D_6$): $\delta$ = 44.4

HRMS: Calculated m/z for $C_{32}H_{18}B_2O$ [$M^+$]: 440.15381, found: 440.15383

UV-vis (*c*-hexane): $\lambda_{max}$ ($\varepsilon$) = 392 nm (17200 $M^{-1}cm^{-1}$)

Fluorescence (*c*-hexane, $\lambda_{ex}$ = 300 nm): $\lambda_{max}$ = 411 nm; $\Phi_{PL}$ = 45%

Cyclic voltammetry ($CH_2Cl_2$, [*n*-$Bu_4N$][$PF_6$], 0.1 M, 200 mV $s^{-1}$, vs. FcH/$FcH^+$): $E_{pc}$ = –2.19 V

**Lewis-base adducts of the B-O-B species ODBE**:

**ODBE·DMAP**

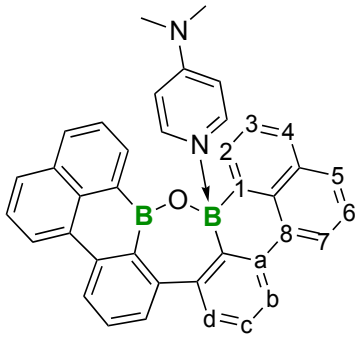


4-Dimethylaminopyridine (6 mg, 45.4 µmol; DMAP) was added to a solution of **ODBE** (10 mg, 22.7 µmol) in $C_6D_6$ (0.5 mL), whereupon a color change of the solution from yellow to colorless was observed.

$^1$H NMR (500.18 MHz, $C_6D_6$): $\delta$ = 8.56 (d, $^3J_{H\text{-}H}$ = 7.3 Hz, 2H; H-7), 8.48 (dd, $^3J_{H\text{-}H}$ = 6.8 Hz, $^4J_{H\text{-}H}$ = 1.2 Hz, 2H; H-2), 8.38 (dd, $^3J_{H\text{-}H}$ = 7.9 Hz, $^4J_{H\text{-}H}$ = 1.1 Hz, 2H; H-b), 8.31 (br; DMAP-$H_{Ar}$), 7.93 (d, $^3J_{H\text{-}H}$ = 8.0 Hz, 2H; H-5), 7.87 (dd, $^3J_{H\text{-}H}$ = 7.9 Hz, $^4J_{H\text{-}H}$ = 1.2 Hz, 2H; H-4), 7.70 (dd, $^3J_{H\text{-}H}$ = 7.9 Hz, $^3J_{H\text{-}H}$ = 6.8 Hz, 2H; H-3), 7.63 (vt, $^3J_{H\text{-}H}$ = 8.0 Hz, $^3J_{H\text{-}H}$ = 7.3 Hz, 2H; H6), 7.26 (vt, 2H; H-c), 7.23 (dd, $^3J_{H\text{-}H}$ = 7.5 Hz, $^4J_{H\text{-}H}$ = 1.1 Hz, 2H; H-d), 5.67 (br; DMAP-$H_{Ar}$), 1.98 (s; DMAP-$CH_3$)

$^{13}$C{$^1$H} NMR (125.77 MHz, $C_6D_6$): $\delta$ = 152.6* (br; C-1), 150.5 (C-e), 148.6* (br; C-f), 139.5 (C-a), 136.3 (C-8), 134.3 (C-4a), 133.4 (C-8a), 131.1 (C-2), 129.3 (C-d), 128.5 (C-5), 127.2 (C-3), 127.2 (C-c), 126.2 (C-4), 125.2 (C-6), 122.3 (C-b), 121.2 (C-7), 38.1 (DMAP-$CH_3$), n.o. (DMAP-$C_{Ar}$)

$^{11}$B{$^1$H} NMR (160.48 MHz, $C_6D_6$): $\delta$ = 3.2

*These signals were only detectable in the $^{H,C}$HMBC-spectrum.

NMR spectroscopy indicated an adduct formation of **ODBE** also with other nitrogen-donor bases [pyridine, pyridazine, phthalazine (pthz)]. Single crystals of **ODBE·pthz** were obtained by slow gas-phase diffusion of *n*-hexane into a solution of **ODBE** and phthalazine (1:1) in $C_6D_6$ at room temperature.

**Treatment of the B–O–B species ODBE with $BBr_3$ to furnish 3**:

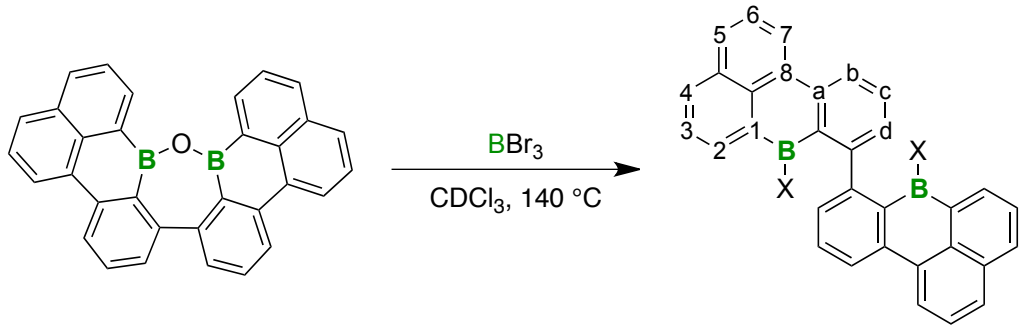


**3** X = Br, Cl

$BBr_3$ (0.1 mL, 0.57 M in $CDCl_3$, 57 µmol) was added to a solution of **ODBE** (5 mg, 11 µmol) in $CDCl_3$ (0.35 mL) in a sealable NMR tube. The tube was flame-sealed under vacuum and heated to 140 °C for 2 d; the reaction progress was monitored by NMR spectroscopy. After the conversion was complete, the pale yellow solution was transferred to a Schlenk flask, and all volatiles were removed under vacuum at 60 °C to afford **3** as an orange solid. Yield: 6 mg (10 µmol, 91%).

$^1$H NMR (500.18 MHz, $CDCl_3$): $\delta$ = 8.98 (dd, $^3J_{H\text{-}H}$ = 7.2 Hz, $^4J_{H\text{-}H}$ = 1.2 Hz, 2H; H-2), 8.90 (d, $^3J_{H\text{-}H}$ = 7.6 Hz, 2H; H-7), 8.90–8.85 (m, 2H; H-b), 8.78 (d, $^3J_{H\text{-}H}$ = 7.9 Hz, 2H; H-d), 8.38 (d, $^3J_{H\text{-}H}$ = 8.0 Hz, 2H; H-4), 8.12 (d, $^3J_{H\text{-}H}$ = 7.8 Hz, 2H; H-5), 7.99–7.94 (m, 2H; H-c), 7.85 (vt, 2H; H-3), 7.80 (vt, 2H; H-6)

$^{13}$C{$^1$H} NMR (125.77 MHz, $CDCl_3$): $\delta$ = 146.6 (C-e), 142.6 (C-a), 142.2 (C-2), 139.1 (C-d), 137.5 (C-4), 134.4* (C-f), 133.0 (C-4a), 131.7 (C-8a), 131.5 (C-5), 131.4 (C-8), 126.7 (C-7), 126.7 (C-c), 126.6 (C-3), 126.5 (C-6), 123.0 (C-b), n.o. (C-1)

$^{11}$B{$^1$H} NMR (160.48 MHz, $CDCl_3$): n.o.

*These signals were only detectable in the $^{H,C}$HMBC-spectrum.

**Experiments related to mechanistic investigations**

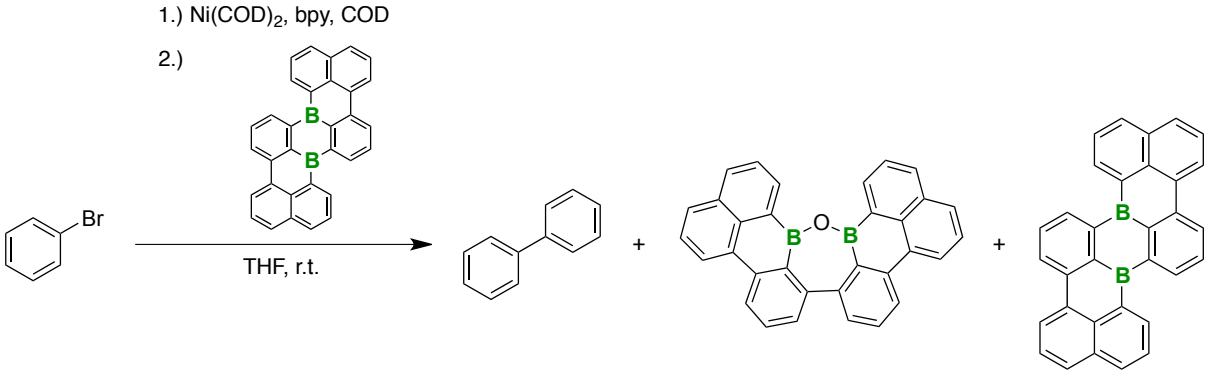


2,2'-Bipyridyl (32 mg, 203 µmol; bpy) was dissolved in THF (60 mL), neat 1,5-cyclooctadiene (20 mg, 185 µmol; COD) and $Ni(COD)_2$ (53 mg, 203 µmol) were added, and the mixture was stirred at room temperature for 15 min. Bromobenzene (29 mg, 185 µmol) was added to the deeply purple-colored mixture and stirred for 20 h; the reaction progress (to furnish biphenyl) was monitored by TLC. After the addition of solid **$B_2$-TBPA** (20 mg, 46 µmol), stirring was continued for 19 h at room temperature, the mixture was placed in an ice bath, and quenched by bubbling air through it. A yellow solution containing an off-white precipitate was obtained. All volatiles were removed under vacuum and the brownish solid residue was subjected to flash-column chromatography (*c*-hexane → *c*-hexane:$CH_2Cl_2$ = 1:1; large cartridge). Biphenyl (12 mg, 78 µmol, 85% yield) was obtained as a white solid, **ODBE** (10 mg, 23 µmol, 50% yield) as a bright yellow solid, and **$B_2$-TBPA** (3 mg, 7 µmol, 16% yield) recovered as a yellow solid ($^1$H NMR spectroscopic control).

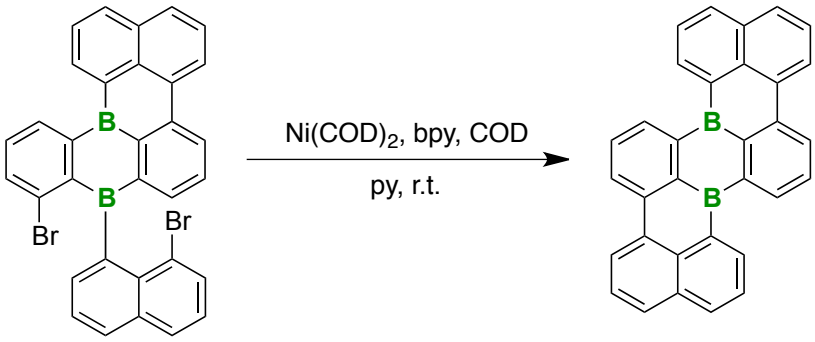


2,2'-Bipyridyl (10 mg, 64 µmol; bpy) was dissolved in pyridine (15 mL; py), neat 1,5-cyclooctadiene (6 mg, 58 µmol; COD) and $Ni(COD)_2$ (18 mg, 64 µmol) were added, and the mixture was stirred at room temperature for 1 h. The resulting dark-colored mixture was slowly added (over 4 h using a syringe pump) at room temperature to a pale yellow solution of **4** (17 mg, 29 µmol) in pyridine (40 mL). After complete addition, stirring was continued

for 24 h at room temperature, the mixture was placed in an ice bath, and quenched by bubbling air through it. A beige solution containing an off-white precipitate was obtained. All volatiles were removed under vacuum and the brownish solid residue was subjected to flash-column chromatography (*c*-hexane → *c*-hexane:$CH_2Cl_2$ = 1:1). The fraction containing the luminescent **$B_2$-TBPA** was evaporated to dryness under reduced pressure and the residue washed with ice-cold *n*-pentane (2 × 1 mL). **$B_2$-TBPA** was obtained as a yellow solid. Yield: 9 mg (21 µmol, 73%). The formation of **$B_2$-TBPA** was confirmed by $^1$H NMR.

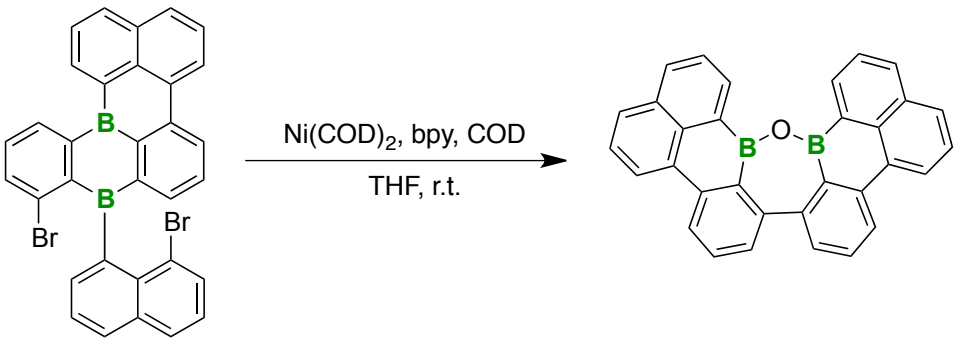


2,2'-Bipyridyl (9 mg, 56 µmol; bpy) was dissolved in THF (15 mL), neat 1,5-cyclooctadiene (5 mg, 51 µmol; COD) and $Ni(COD)_2$ (16 mg, 56 µmol) were added, and the mixture was stirred at room temperature for 1 h. The resulting deeply purple-colored mixture was slowly added (over 4 h using a syringe pump) at room temperature to a solution of **4** (15 mg, 26 µmol) in THF (40 mL). The initial pale yellow solution turned dark during the process. After complete addition, stirring was continued for 24 h at room temperature, the mixture was placed in an ice bath, and quenched by bubbling air through it. A yellow solution containing an off-white precipitate was obtained. All volatiles were removed under vacuum and the brownish solid residue was subjected to flash-column chromatography (*c*-hexane → *c*-hexane:$CH_2Cl_2$ = 1:1). The fraction containing the luminescent **ODBE** was evaporated to dryness under reduced pressure and the residue washed with ice-cold *n*-pentane (3 × 2 mL). **ODBE** was obtained as a bright yellow solid. Yield: 7 mg (16 µmol, 62%). The formation of **ODBE** was confirmed by $^1$H NMR.

## 3. Plots of $^{1}$H, $^{11}$B{$^{1}$H}, $^{13}$C{$^{1}$H}, $^{19}$F and $^{19}$F{$^{1}$H} NMR spectra of all new compounds

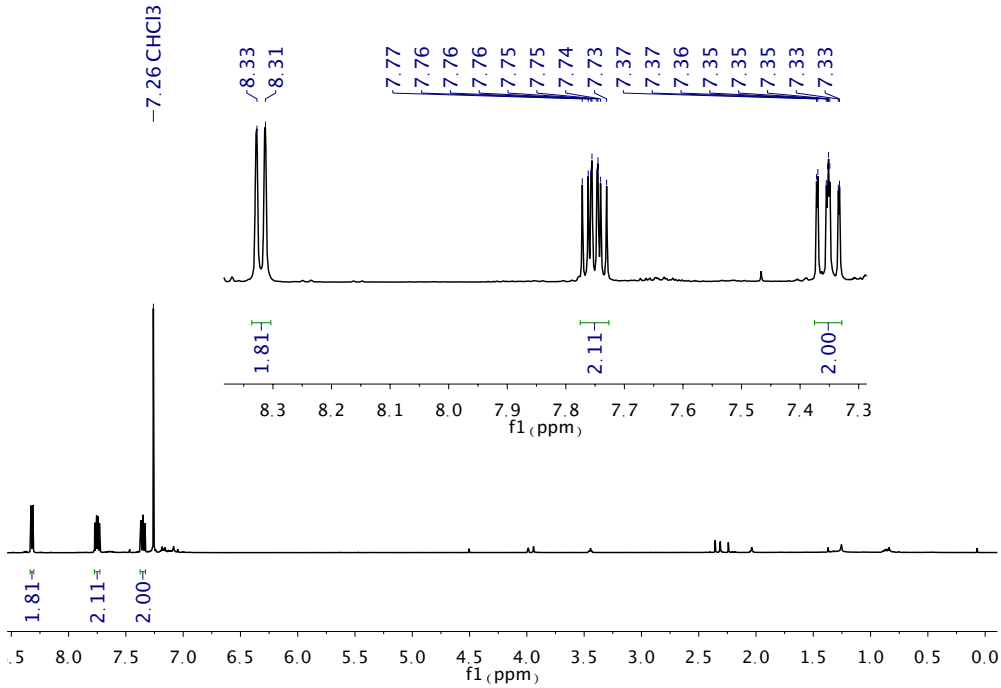


**Figure S3-1:** $^{1}$H NMR spectrum of **1,5-Difluoro-9,10-dibromo-9,10-dihydro-9,10-diboraanthracene (1$^{F}$)** ($CDCl_3$, 500.18 MHz).

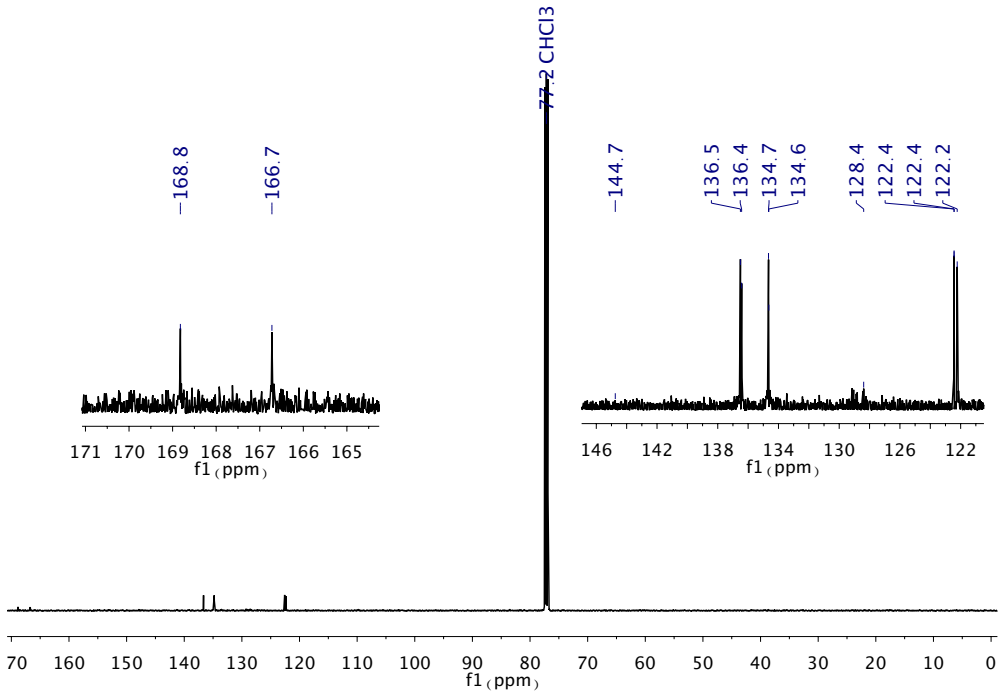


**Figure S3-2:** $^{13}$C{$^{1}$H} NMR spectrum of **1,5-difluoro-9,10-dibromo-9,10-dihydro-9,10-diboraanthracene (1$^{F}$)** ($CDCl_3$, 125.77 MHz).

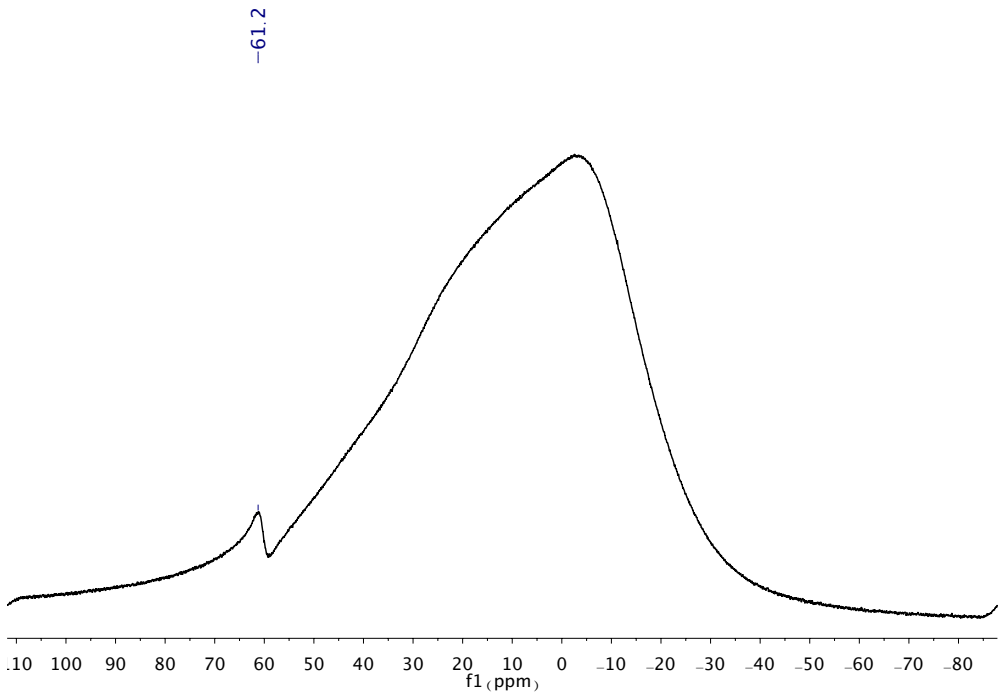


**Figure S3-3:** $^{11}B\{^{1}H\}$ NMR spectrum of **1,5-difluoro-9,10-dibromo-9,10-dihydro-9,10-diboraanthracene (1$^{F}$)** ($CDCl_3$, 160.48 MHz).

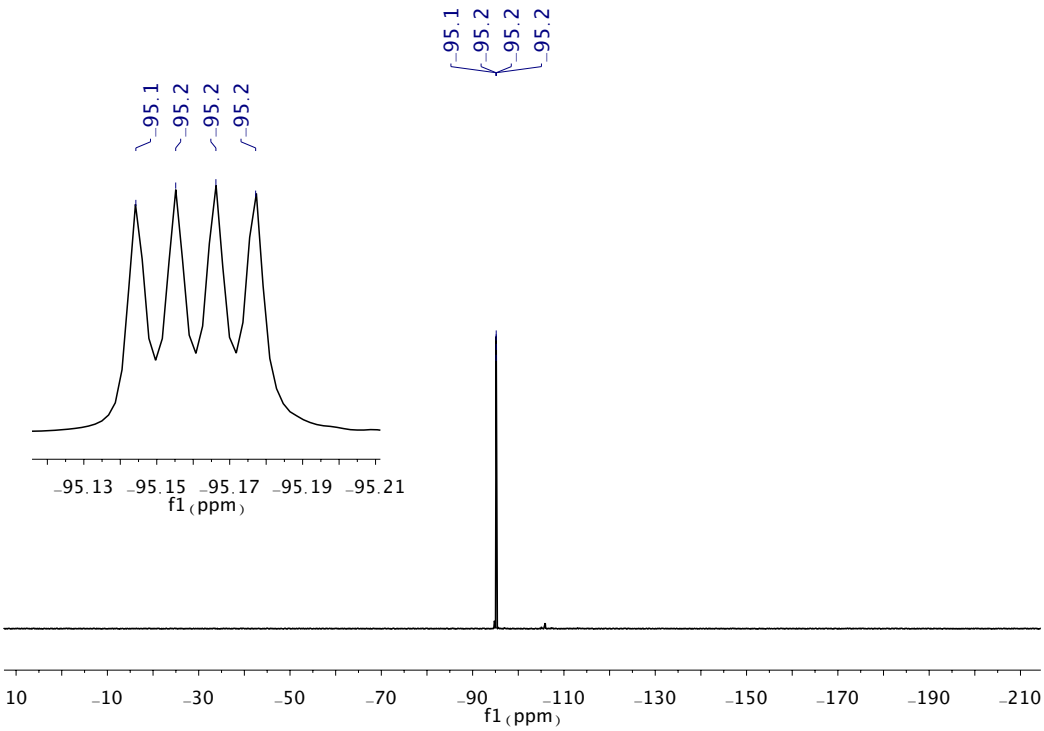


**Figure S3-4:** $^{19}F$ NMR spectrum of **1,5-difluoro-9,10-dibromo-9,10-dihydro-9,10-diboraanthracene (1$^{F}$)** ($CDCl_3$, 470.64 MHz).

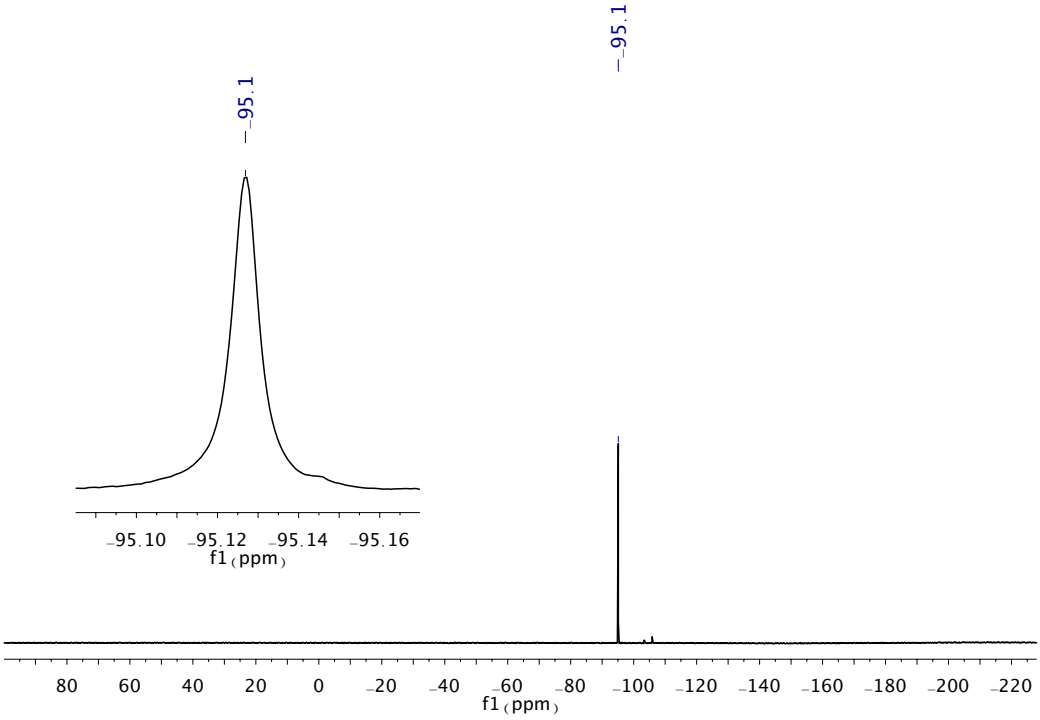


**Figure S3-5:** $^{19}F\{^{1}H\}$ NMR spectrum of **1,5-difluoro-9,10-dibromo-9,10-dihydro-9,10-diboraanthracene (1$^{F}$)** ($CDCl_3$, 282.29 MHz).

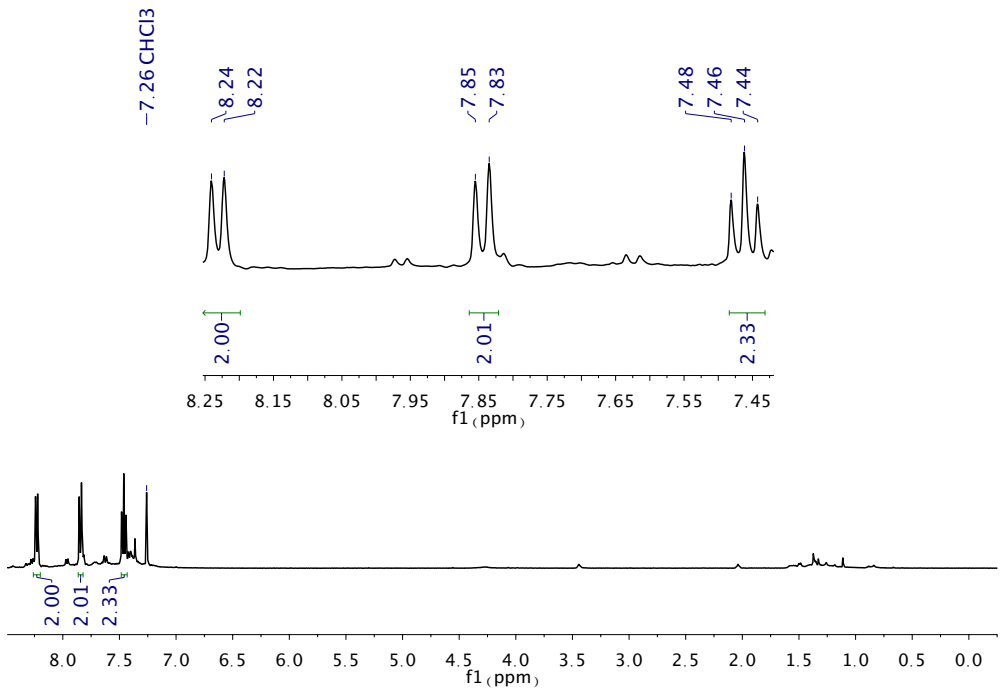


**Figure S3-6:** $^{1}$H NMR spectrum of **1,5,9,10-tetrabromo-9,10-dihydro-9,10-diboraanthracene (1$^{Br}$)** ($CDCl_3$, 400.13 MHz).

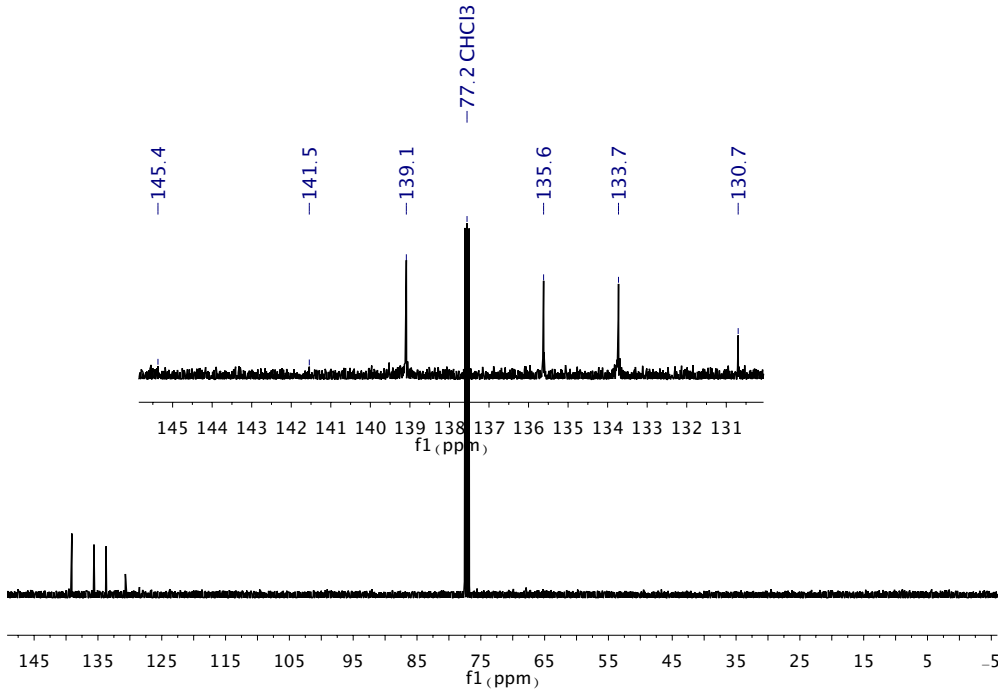


**Figure S3-7:** $^{13}$C{$^{1}$H} NMR spectrum of **1,5,9,10-tetrabromo-9,10-dihydro-9,10-diboraanthracene (1$^{Br}$)** ($CDCl_3$, 100.61 MHz).

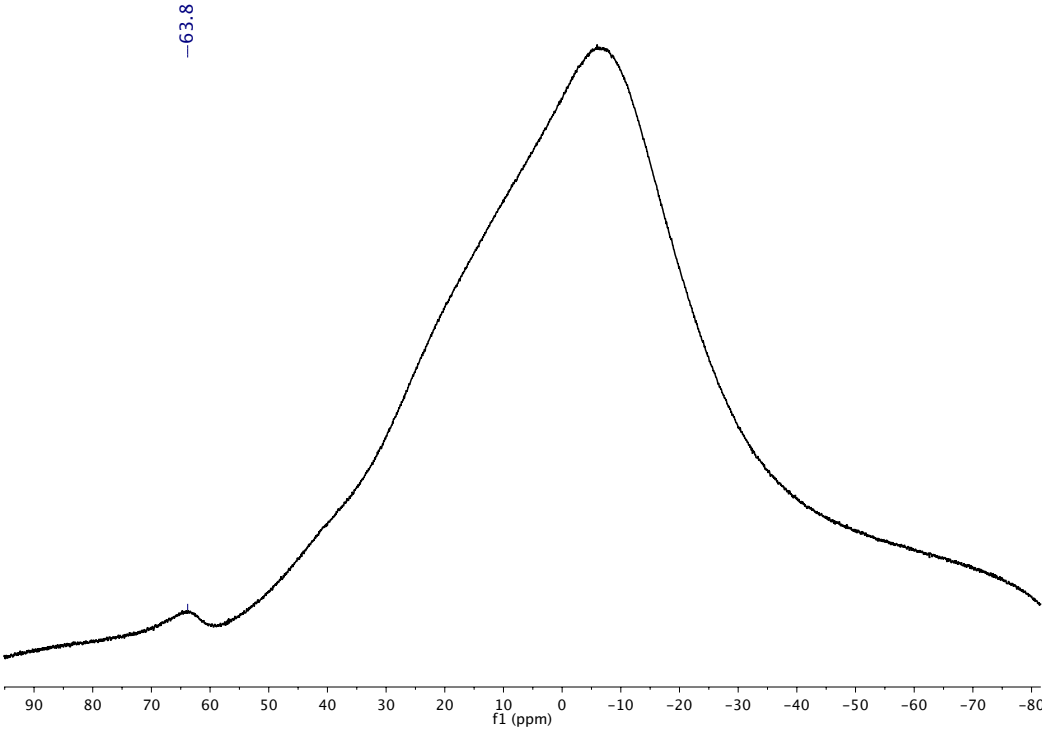


**Figure S3-8:** $^{11}B\{^{1}H\}$ NMR spectrum of **1,5,9,10-tetrabromo-9,10-dihydro-9,10-diboraanthracene (1$^{Br}$)** ($CDCl_3$, 128.38 MHz).

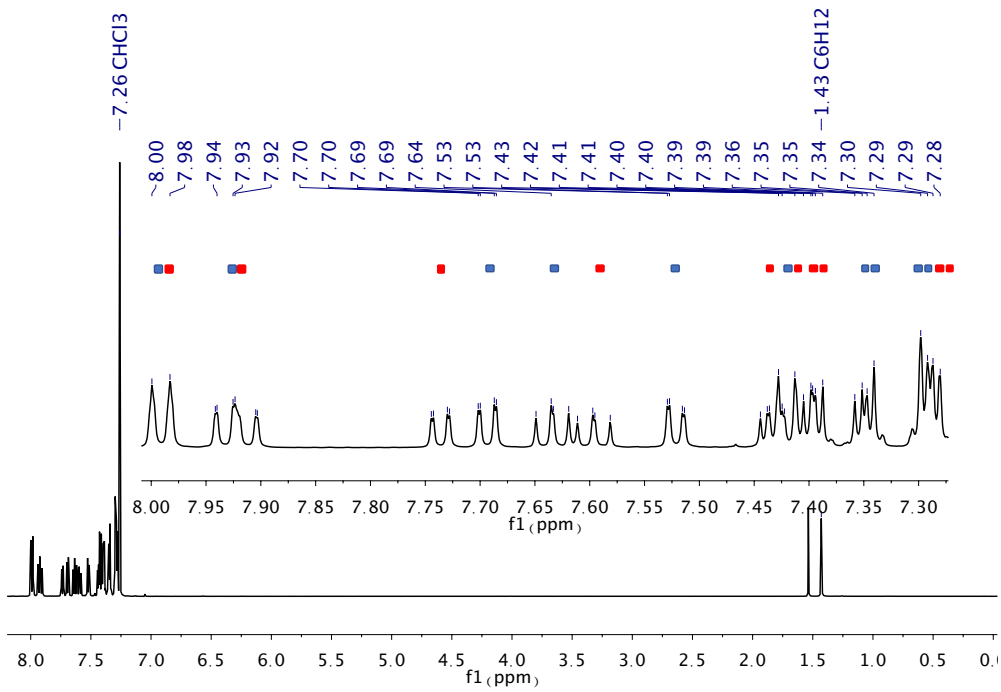


**Figure S3-9:** $^{1}$H NMR spectrum of **9,10-bis(8-bromonaphth-1-yl)-9,10-dihydro-9,10-diboraanthracene (2$^{H,Br}$)** ($CDCl_3$, 500.18 MHz).

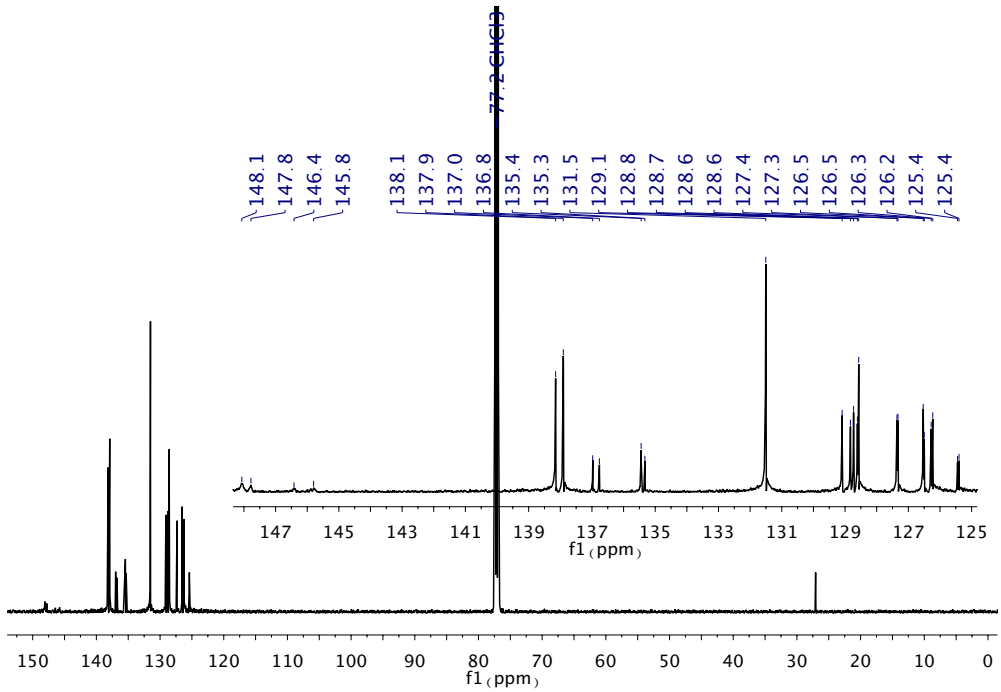


**Figure S3-10:** $^{13}$C{$^{1}$H} NMR spectrum of **9,10-bis(8-bromonaphth-1-yl)-9,10-dihydro-9,10-diboraanthracene (2$^{H,Br}$)** ($CDCl_3$, 125.77 MHz).

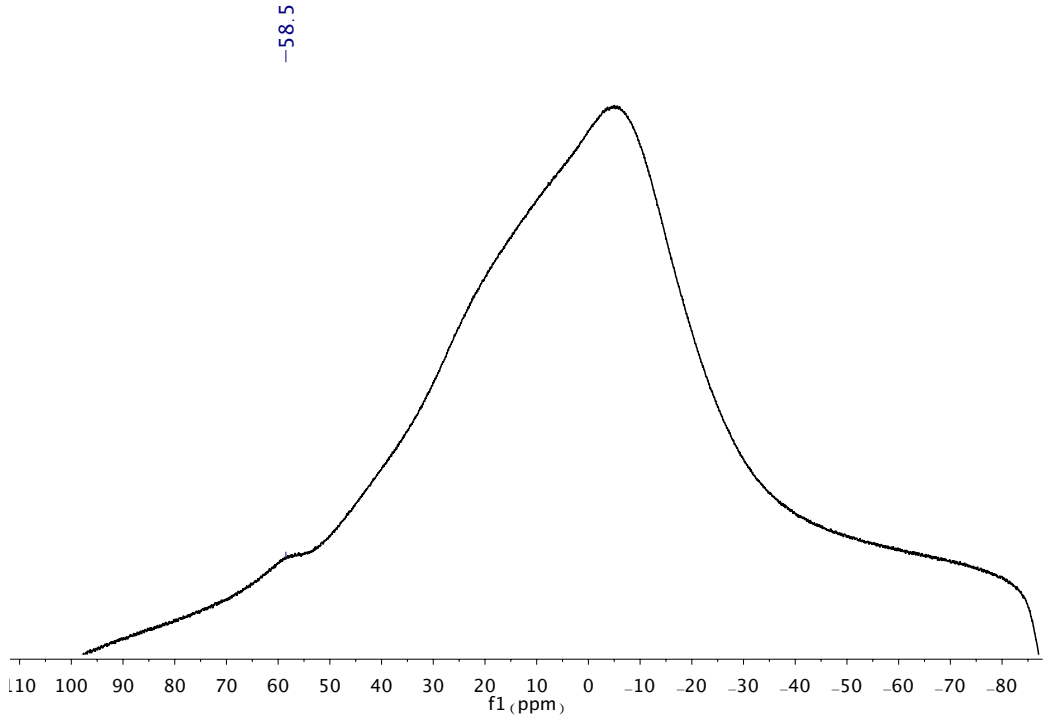


**Figure S3-11:** $^{11}B\{^{1}H\}$ NMR spectrum of **9,10-bis(8-bromonaphth-1-yl)-9,10-dihydro-9,10-diboraanthracene (2$^{H,Br}$)** ($CDCl_3$, 160.48 MHz).

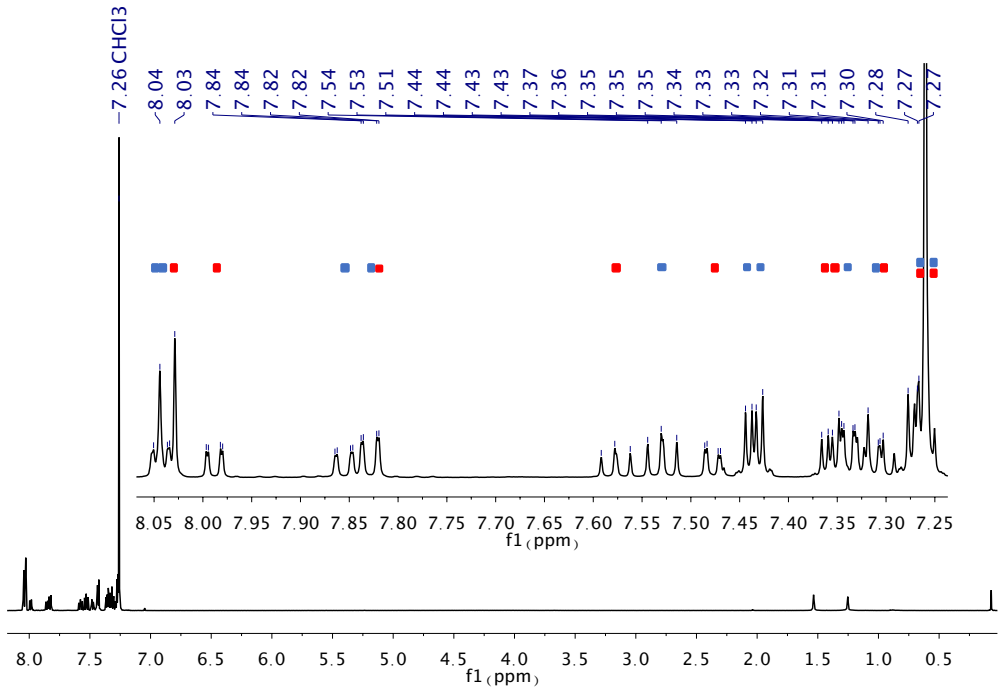


**Figure S3-12:** $^{1}$H NMR spectrum of **9,10-bis(8-iodonaphth-1-yl)-9,10-dihydro-9,10-diboraanthracene (2$^{H,I}$)** ($CDCl_3$, 500.18 MHz).

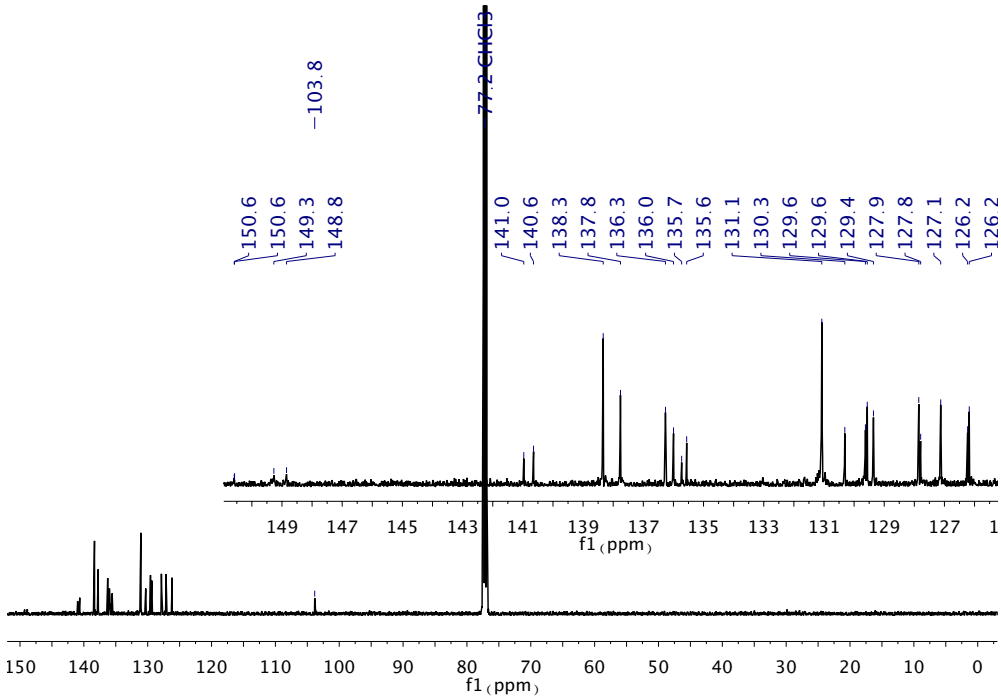


**Figure S3-13:** $^{13}$C{$^{1}$H} NMR spectrum of **9,10-bis(8-iodonaphth-1-yl)-9,10-dihydro-9,10-diboraanthracene (2$^{H,I}$)** ($CDCl_3$, 125.77 MHz).

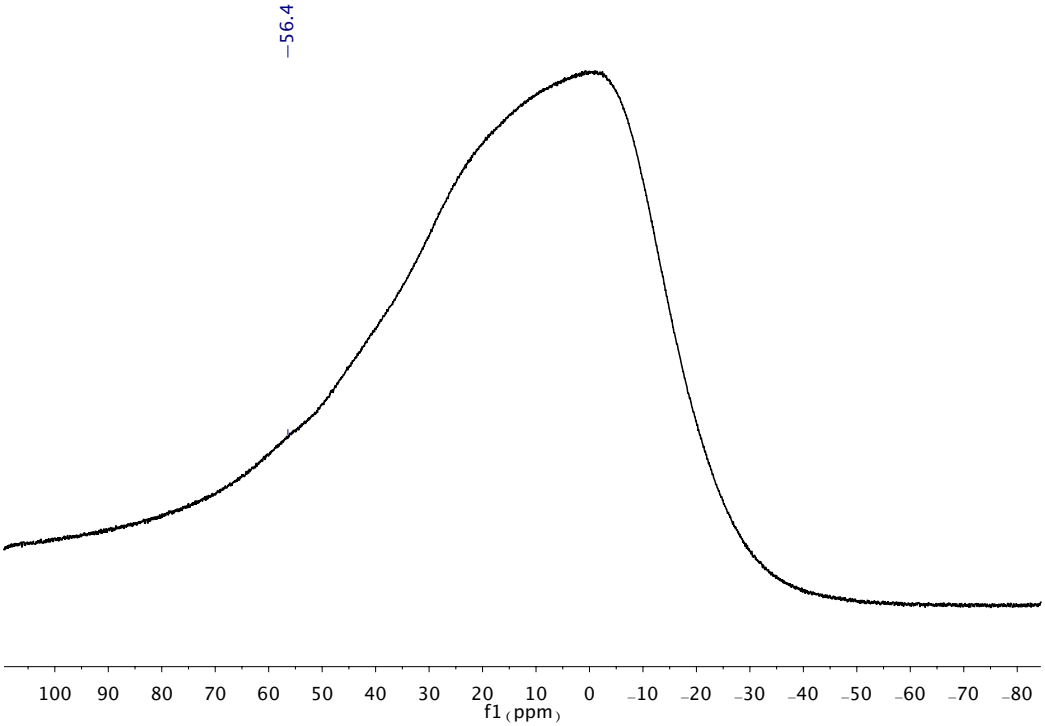


**Figure S3-14:** $^{11}B\{^{1}H\}$ NMR spectrum of **9,10-bis(8-iodonaphth-1-yl)-9,10-dihydro-9,10-diboraanthracene ($2^{H,I}$)** ($CDCl_3$, 160.48 MHz).

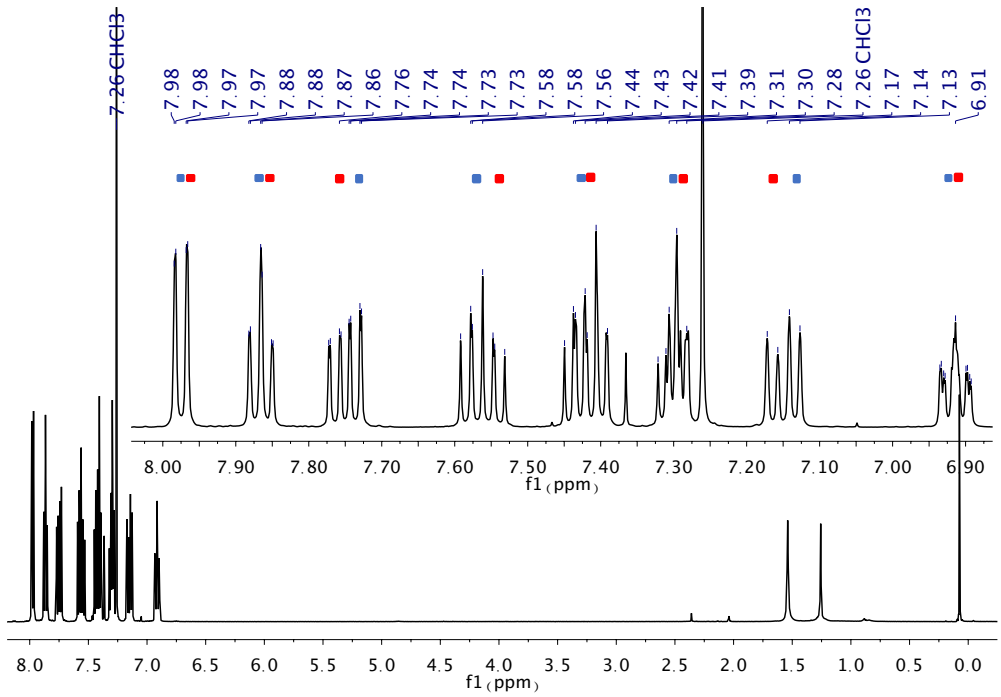


**Figure S3-15:** $^{1}$H NMR spectrum of **1,5-difluoro-9,10-bis(8-bromonaphth-1-yl)-9,10-dihydro-9,10-diboraanthracene (2$^{F,Br}$)** ($CDCl_3$, 500.18 MHz).

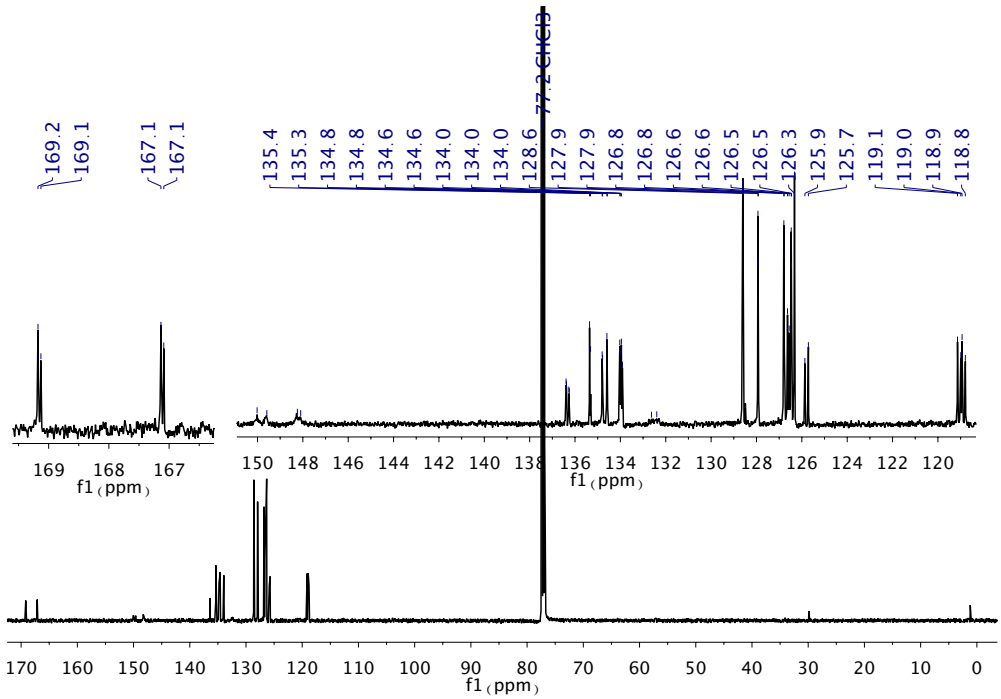


**Figure S3-16:** $^{13}$C{$^{1}$H} NMR spectrum of **1,5-difluoro-9,10-bis(8-bromonaphth-1-yl)-9,10-dihydro-9,10-diboraanthracene (2$^{F,Br}$)** ($CDCl_3$, 125.77 MHz).

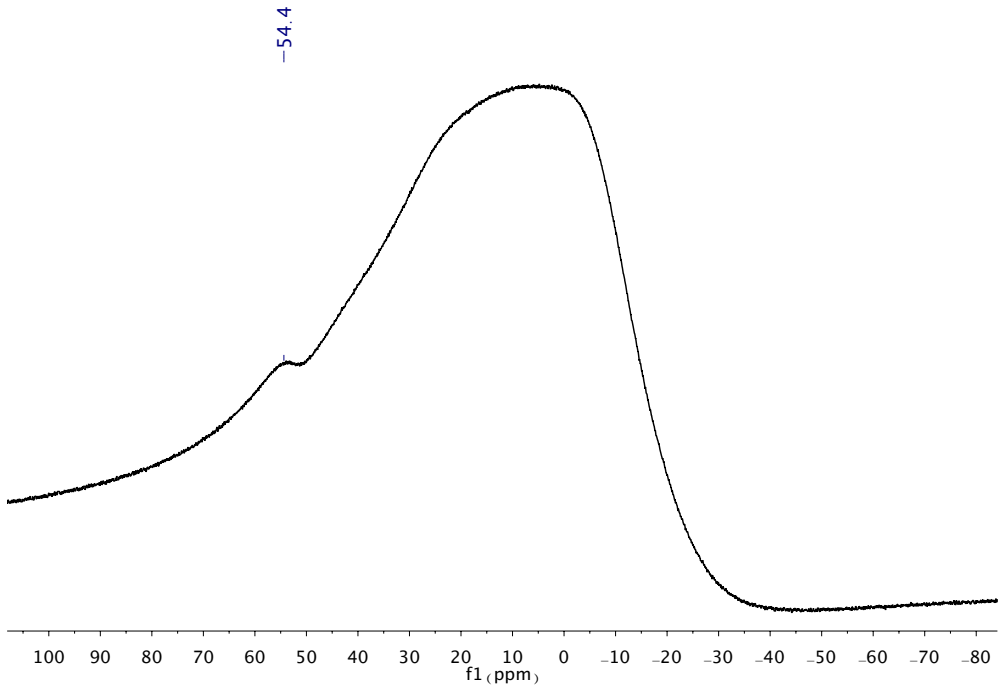


**Figure S3-17:** $^{11}B\{^{1}H\}$ NMR spectrum of **1,5-difluoro-9,10-bis(8-bromonaphth-1-yl)-9,10-dihydro-9,10-diboraanthracene (2$^{F,Br}$)** ($CDCl_3$, 160.48 MHz).

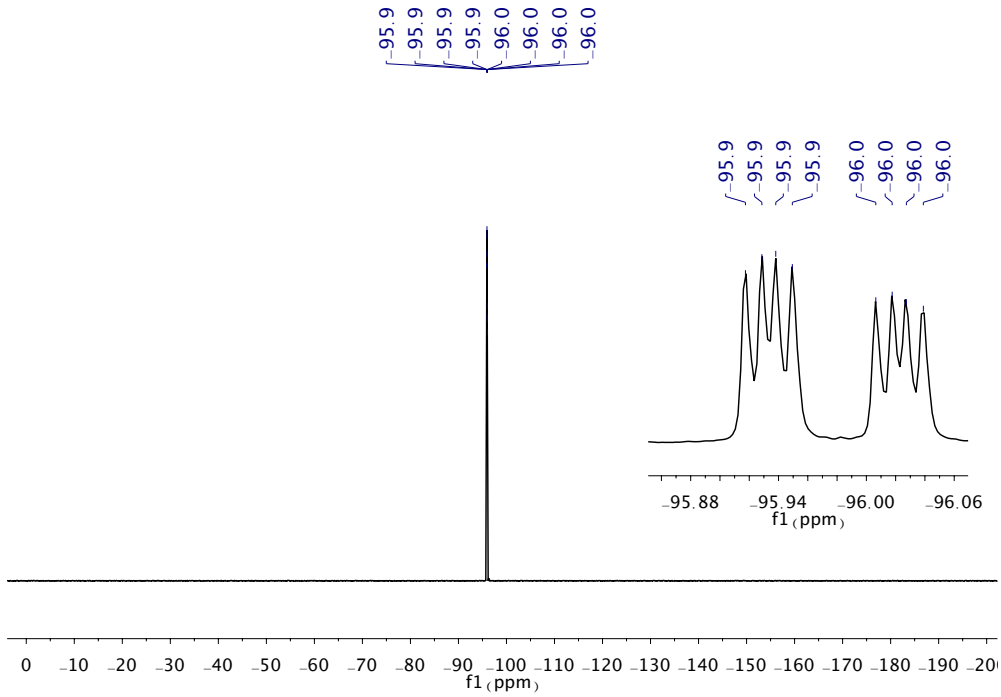


**Figure S3-18:** $^{19}F$ NMR spectrum of **1,5-difluoro-9,10-bis(8-bromonaphth-1-yl)-9,10-dihydro-9,10-diboraanthracene (2$^{F,Br}$)** ($CDCl_3$, 470.64 MHz).

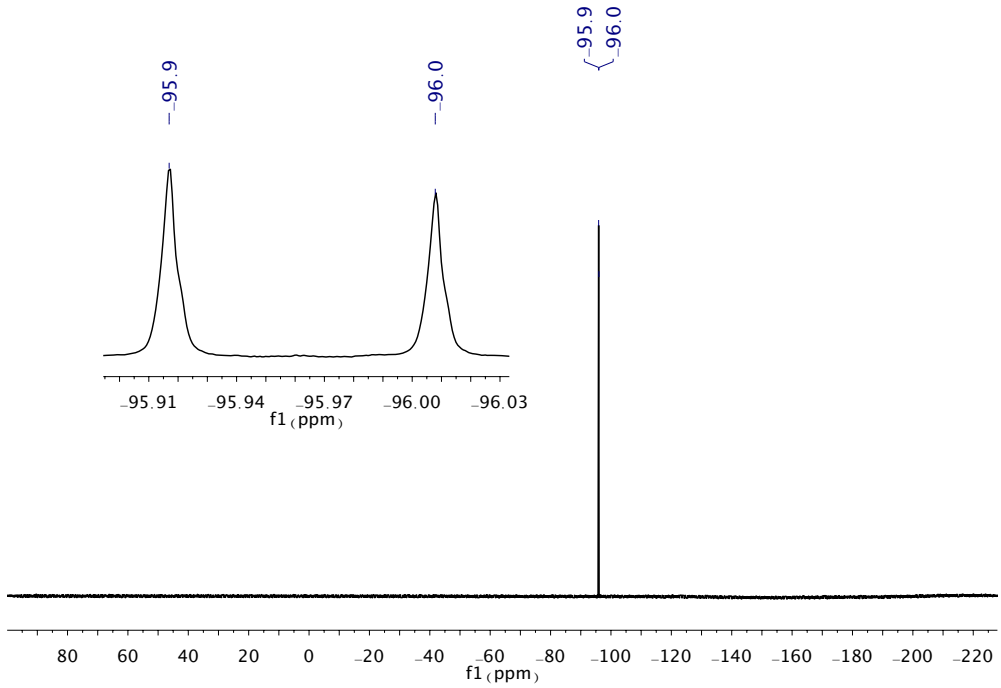


**Figure S3-19:** $^{19}F\{^{1}H\}$ NMR spectrum of **1,5-difluoro-9,10-bis(8-bromonaphth-1-yl)-9,10-dihydro-9,10-diboraanthracene ($2^{F,Br}$)** ($CDCl_3$, 282.29 MHz).

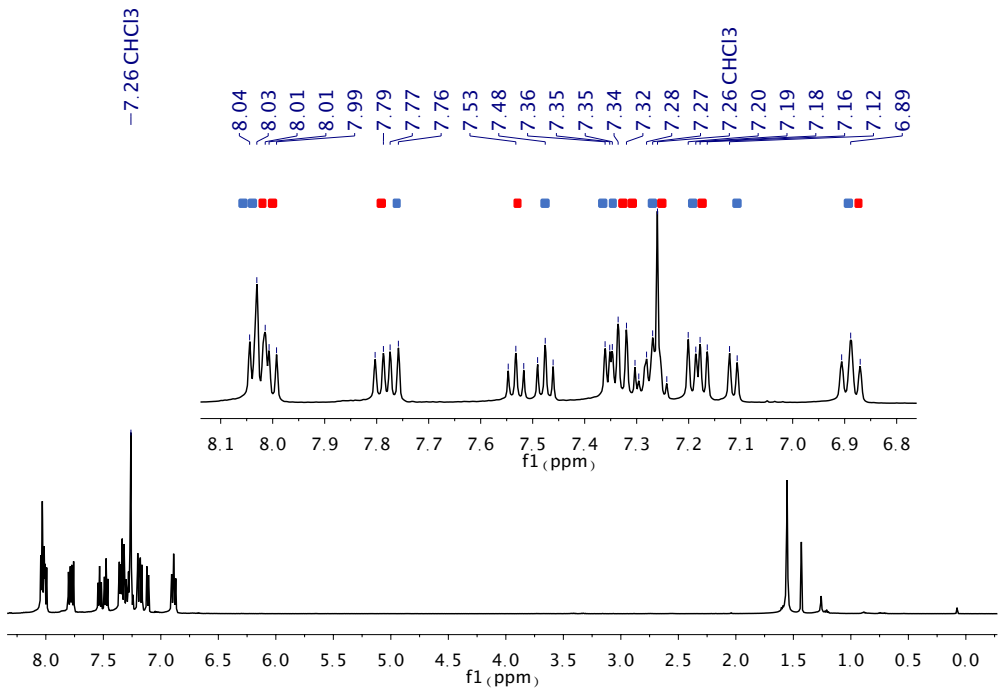


**Figure S3-20:** $^{1}$H NMR spectrum of **1,5-difluoro-9,10-bis(8-iodonaphth-1-yl)-9,10-dihydro-9,10-diboraanthracene (2$^{F,I}$)** ($CDCl_3$, 500.18 MHz).

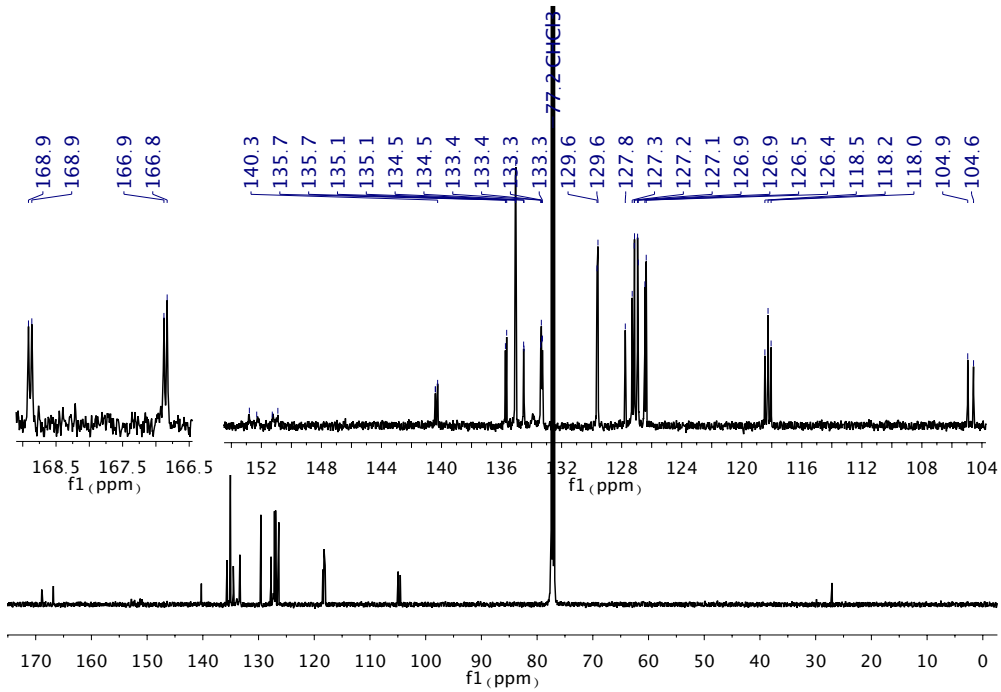


**Figure S3-21:** $^{13}$C{$^{1}$H} NMR spectrum of **1,5-difluoro-9,10-bis(8-iodonaphth-1-yl)-9,10-dihydro-9,10-diboraanthracene (2$^{F,I}$)** ($CDCl_3$, 125.77 MHz).

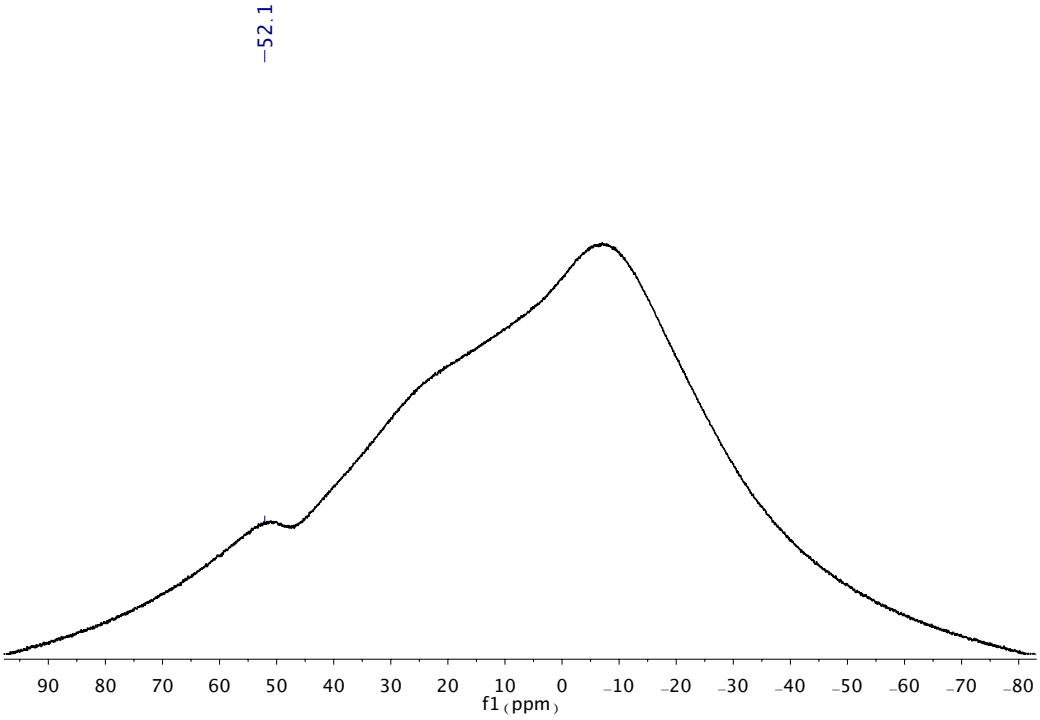


**Figure S3-22:** $^{11}B\{^{1}H\}$ NMR spectrum of **1,5-difluoro-9,10-bis(8-iodonaphth-1-yl)-9,10-dihydro-9,10-diboraanthracene (2$^{F,I}$)** ($CDCl_3$, 160.48 MHz).

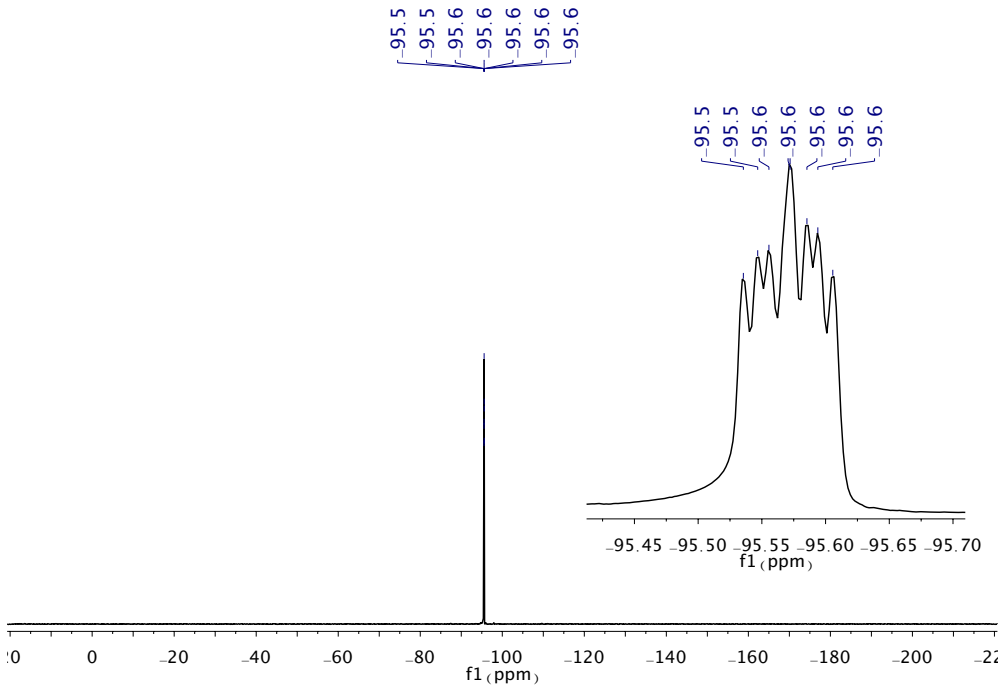


**Figure S3-23:** $^{19}F$ NMR spectrum of **1,5-difluoro-9,10-bis(8-iodonaphth-1-yl)-9,10-dihydro-9,10-diboraanthracene (2$^{F,I}$)** ($CDCl_3$, 470.64 MHz).

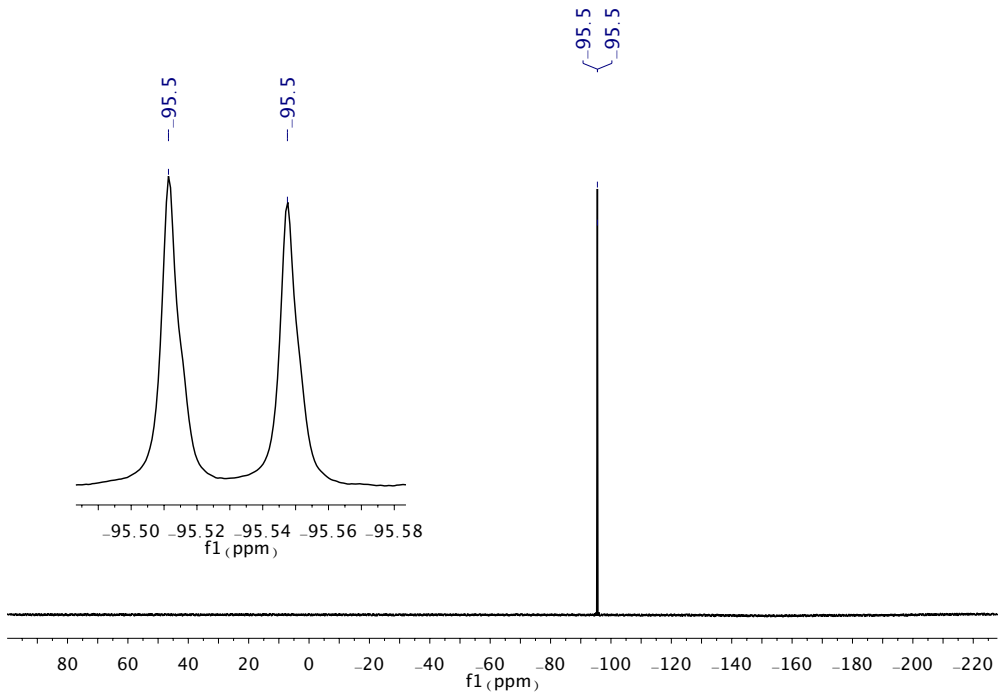


**Figure S3-24:** $^{19}F\{^{1}H\}$ NMR spectrum of **1,5-difluoro-9,10-bis(8-iodonaphth-1-yl)-9,10-dihydro-9,10-diboraanthracene ($2^{F,I}$)** ($CDCl_3$, 282.29 MHz).

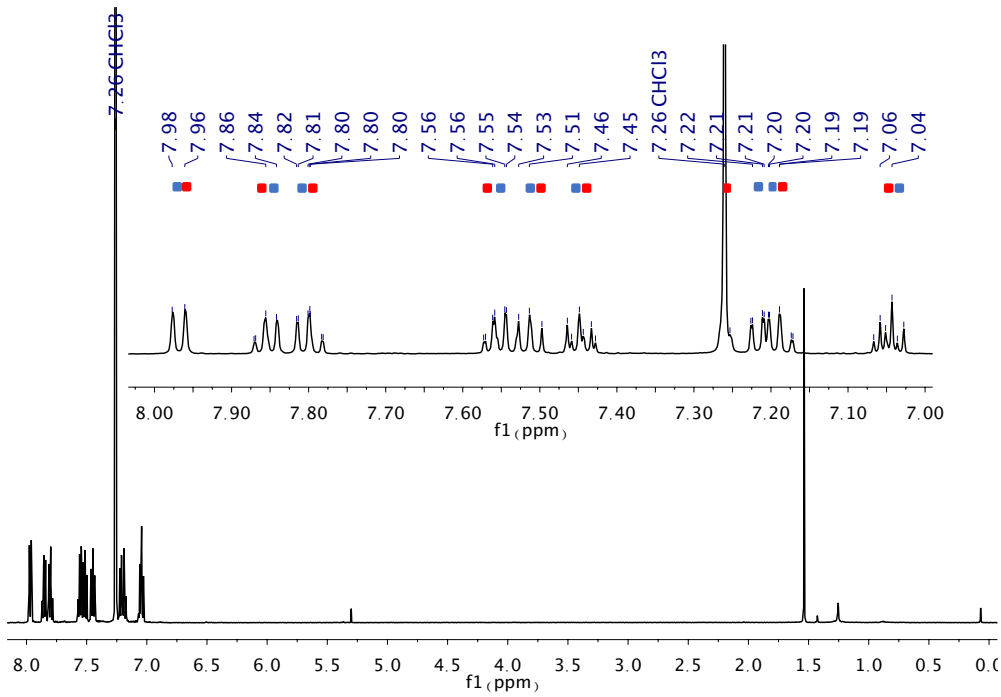


**Figure S3-25:** $^{1}$H NMR spectrum of **1,5-dibromo-9,10-bis(8-bromonaphth-1-yl)-9,10-dihydro-9,10-diboraanthracene (2$^{Br,Br}$)** ($CDCl_3$, 500.18 MHz).

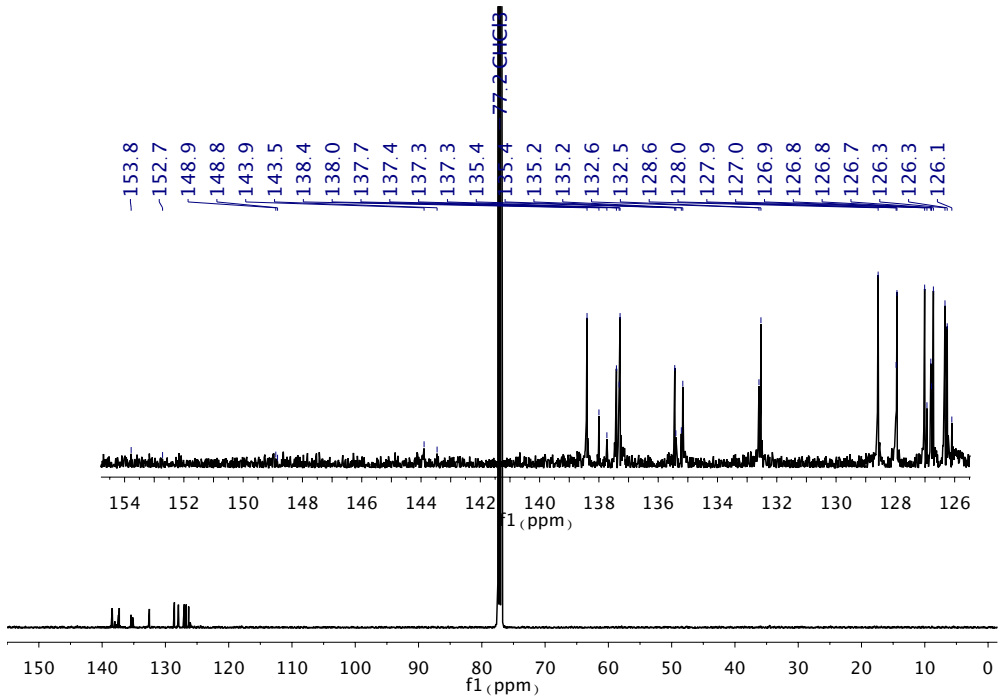


**Figure S3-26:** $^{13}$C{$^{1}$H} NMR spectrum of **1,5-dibromo-9,10-bis(8-bromonaphth-1-yl)-9,10-dihydro-9,10-diboraanthracene (2$^{Br,Br}$)** ($CDCl_3$, 125.77 MHz).

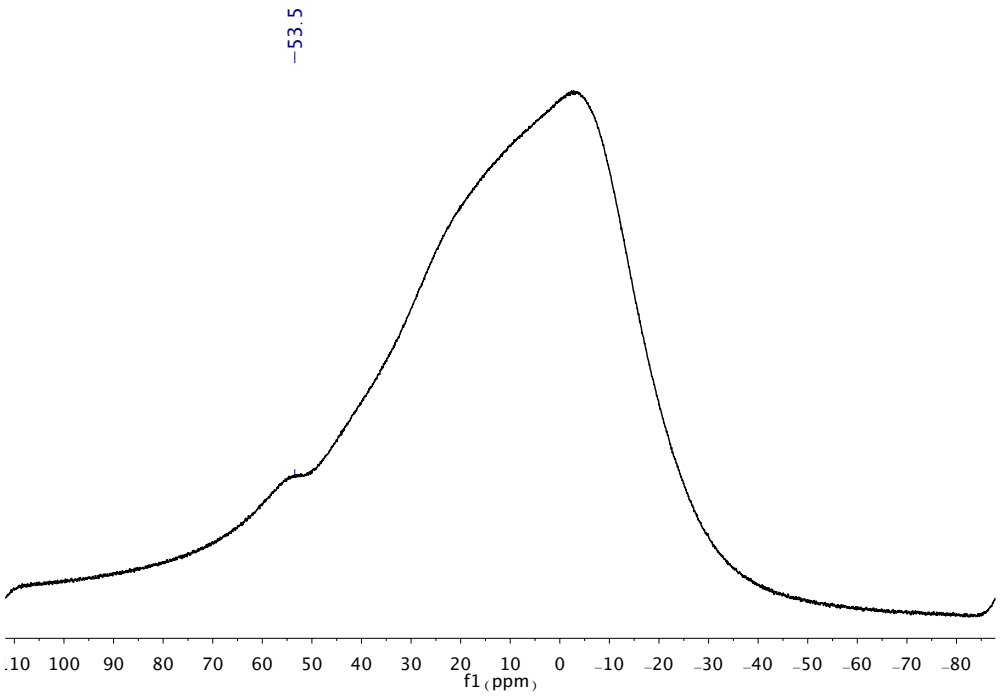


**Figure S3-27:** $^{11}B\{^{1}H\}$ NMR spectrum of **1,5-dibromo-9,10-bis(8-bromonaphth-1-yl)-9,10-dihydro-9,10-diboraanthracene ($2^{Br,Br}$)** ($CDCl_3$, 160.48 MHz).

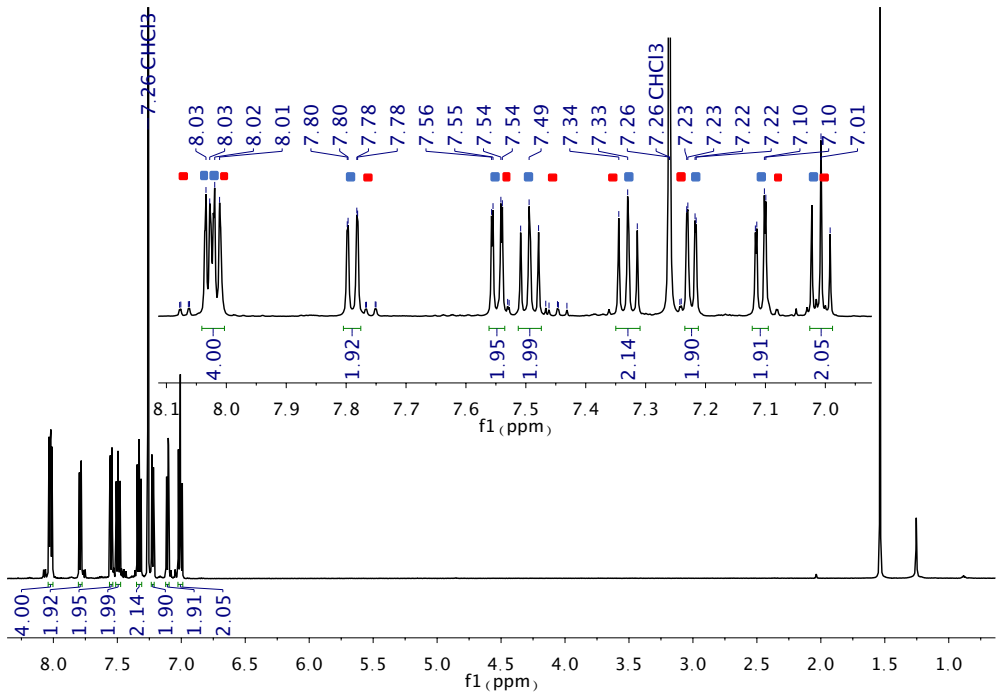


**Figure S3-28:** $^{1}$H NMR spectrum of **1,5-dibromo-9,10-bis(8-iodonaphth-1-yl)-9,10-dihydro-9,10-diboraanthracene (2$^{Br,I}$)** ($CDCl_3$, 500.18 MHz).

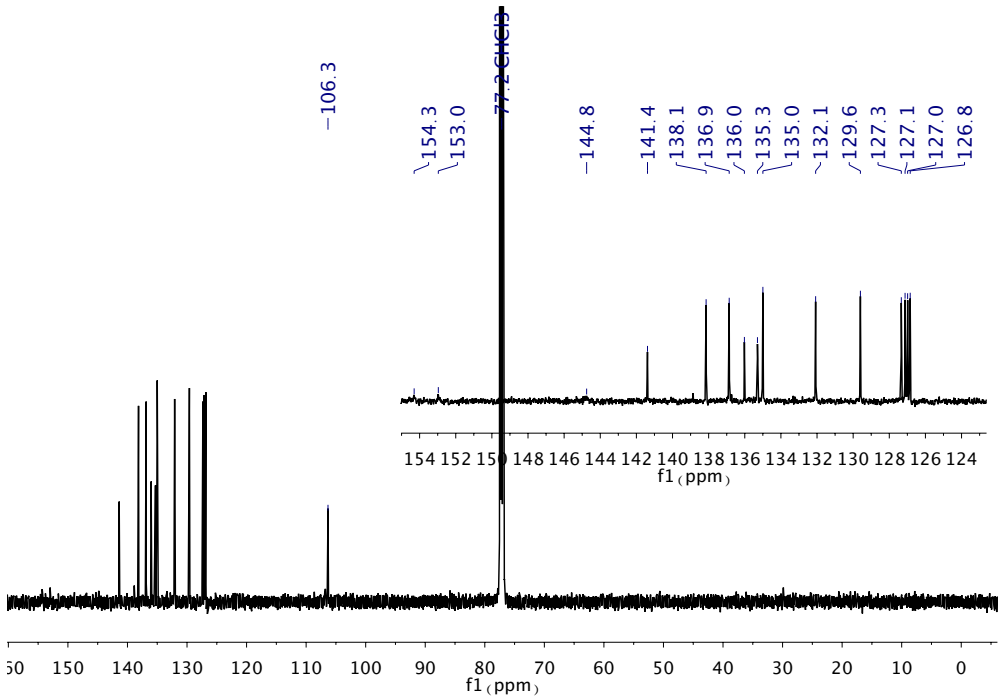


**Figure S3-29:** $^{13}$C{$^{1}$H} NMR spectrum of **1,5-dibromo-9,10-bis(8-iodonaphth-1-yl)-9,10-dihydro-9,10-diboraanthracene (2$^{Br,I}$)** ($CDCl_3$, 125.77 MHz).

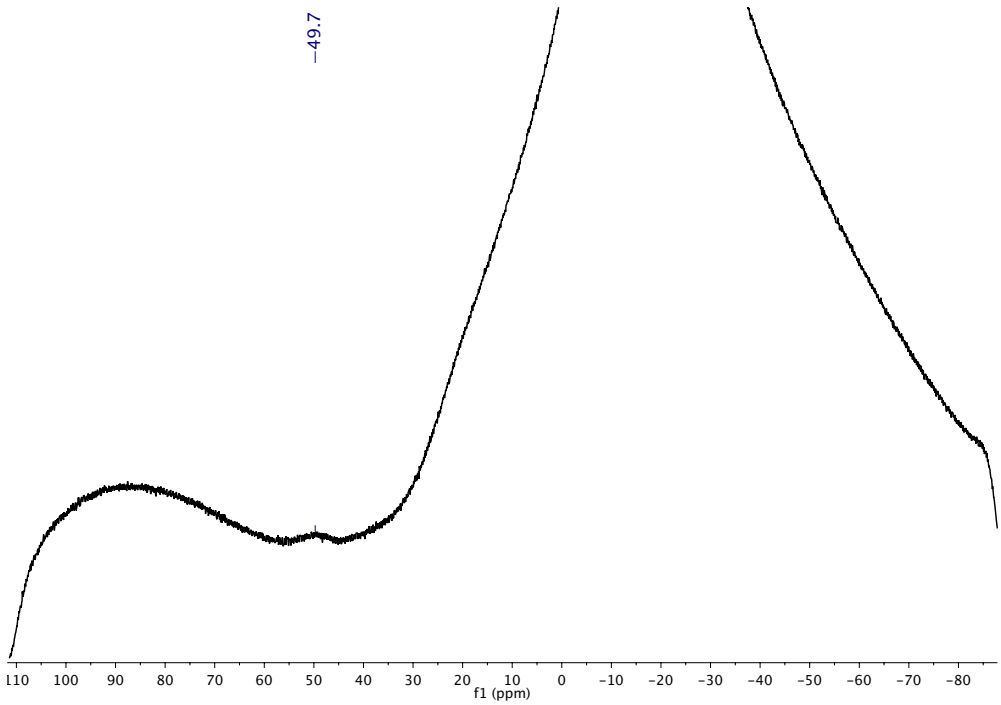


**Figure S3-30:** $^{11}B\{^{1}H\}$ NMR spectrum of **1,5-dibromo-9,10-bis(8-iodonaphth-1-yl)-9,10-dihydro-9,10-diboraanthracene (2$^{Br,I}$)** ($CDCl_3$, 160.48 MHz).

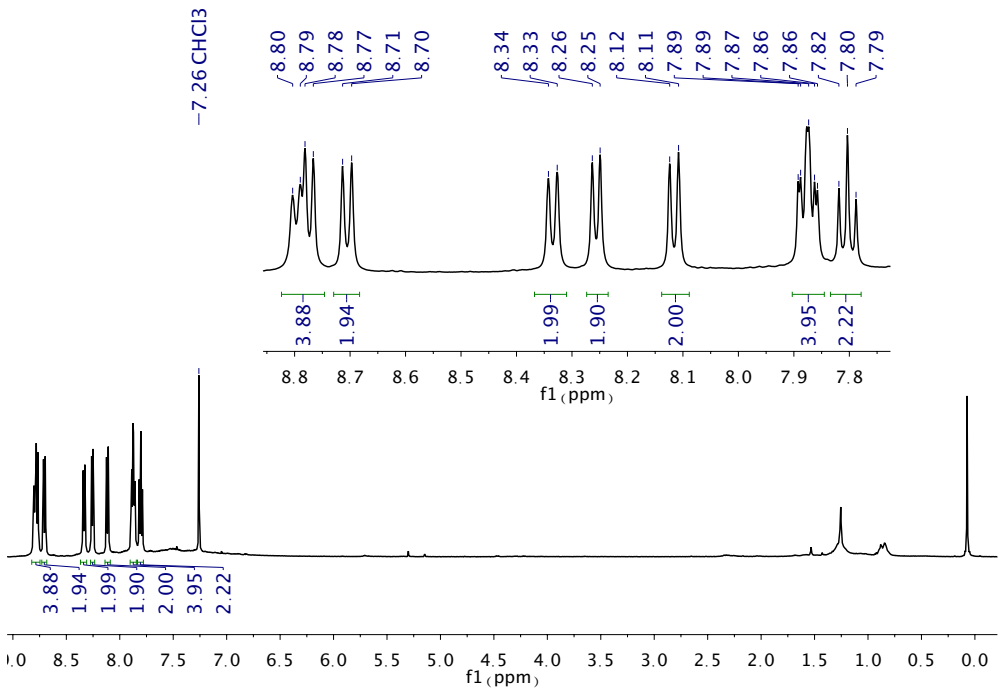


**Figure S3-31:** $^{1}$H NMR spectrum of **B$_2$-TBPA** ($CDCl_3$, 500.18 MHz).

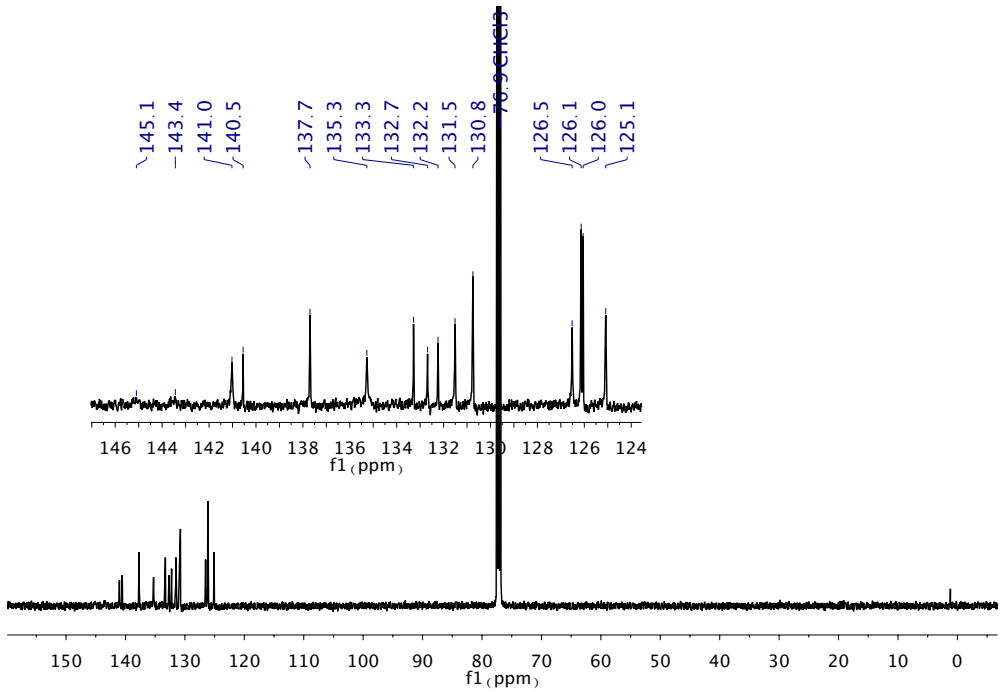


**Figure S3-32:** $^{13}$C{$^{1}$H} NMR spectrum of **B$_2$-TBPA** ($CDCl_3$, 125.77 MHz).

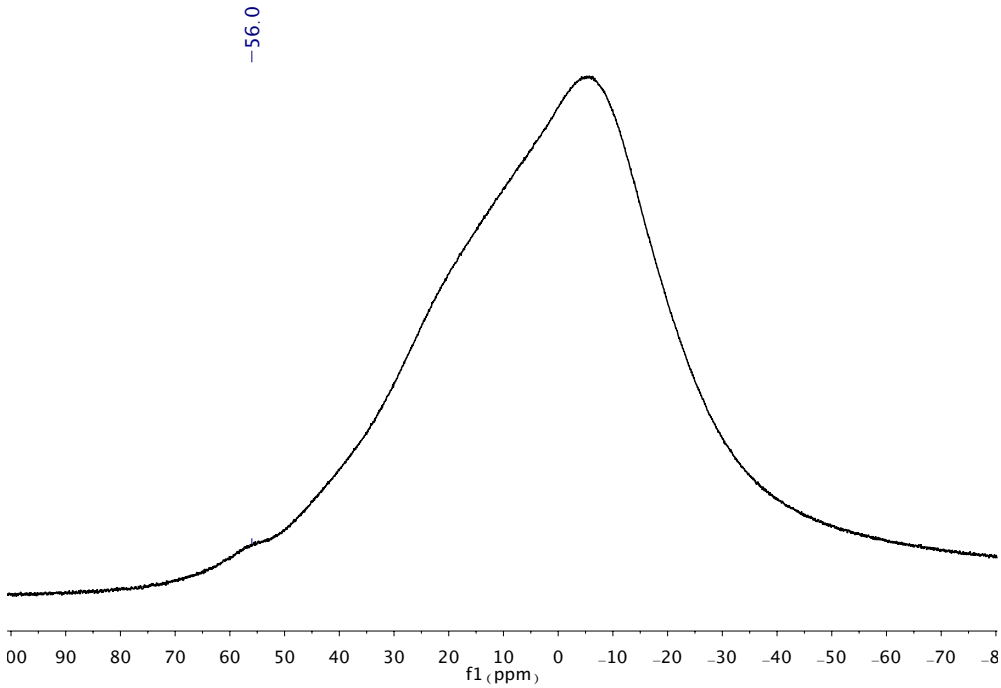


**Figure S3-33:** $^{11}B\{^{1}H\}$ NMR spectrum of **$B_2$-TBPA** ($CDCl_3$, 160.48 MHz).

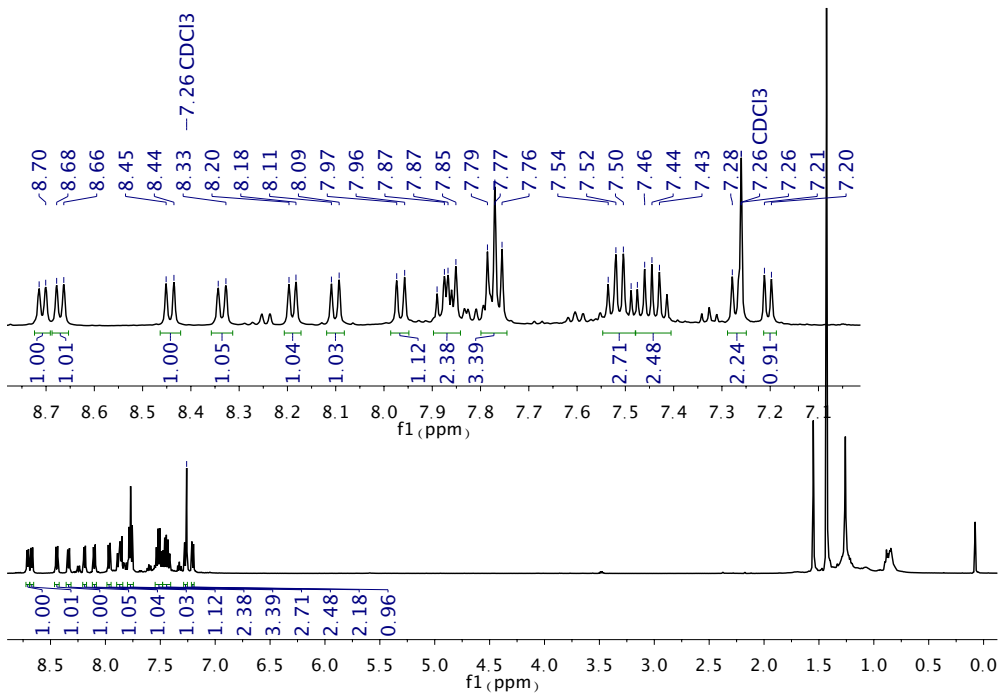


**Figure S3-34:** $^{1}$H NMR spectrum of **4** ($CDCl_3$, 500.18 MHz). *Note:* Only the $^{1}$H NMR shifts corresponding to the major compound were picked.

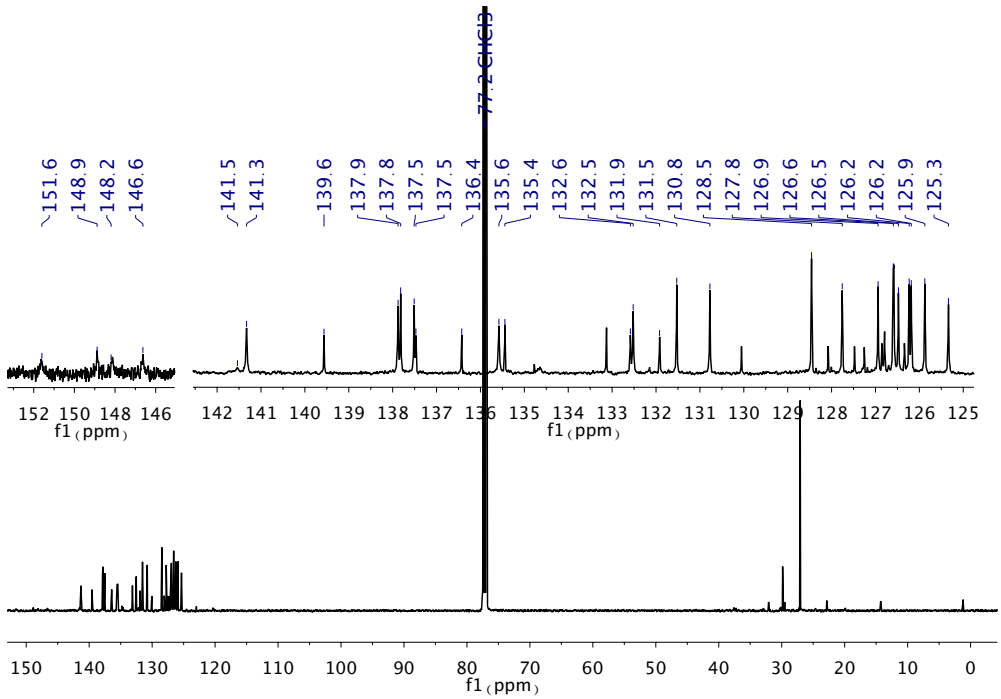


**Figure S3-35:** $^{13}$C{$^{1}$H} NMR spectrum of **4** ($CDCl_3$, 125.77 MHz). *Note:* Only the $^{13}$C NMR shifts corresponding to the major compound were picked.

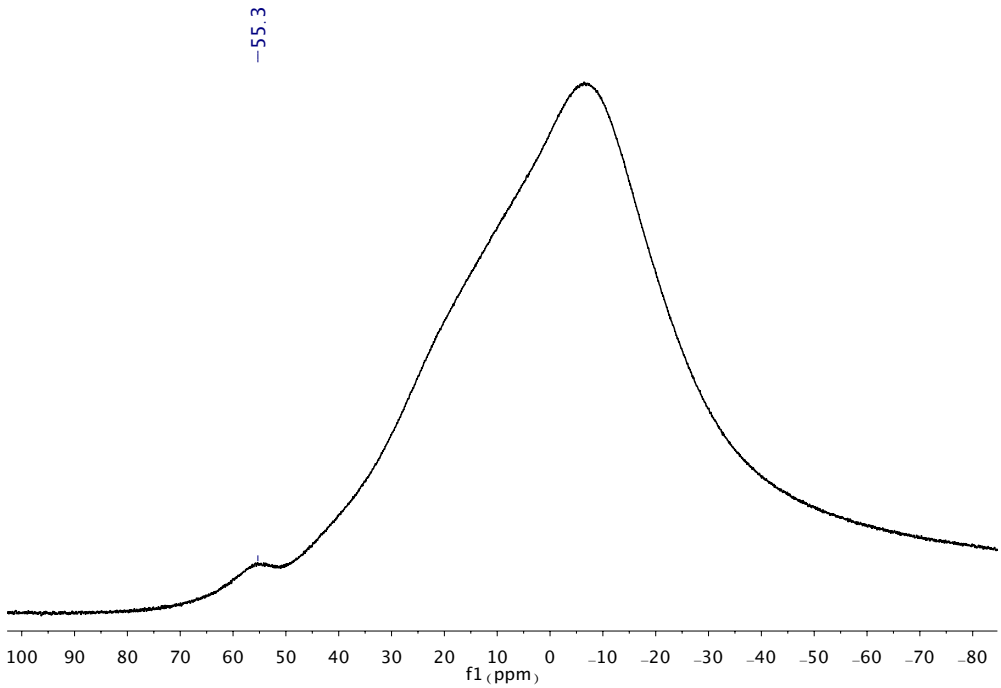


**Figure S3-36:** $^{11}B\{^{1}H\}$ NMR spectrum of **4** ($CDCl_3$, 160.48 MHz).

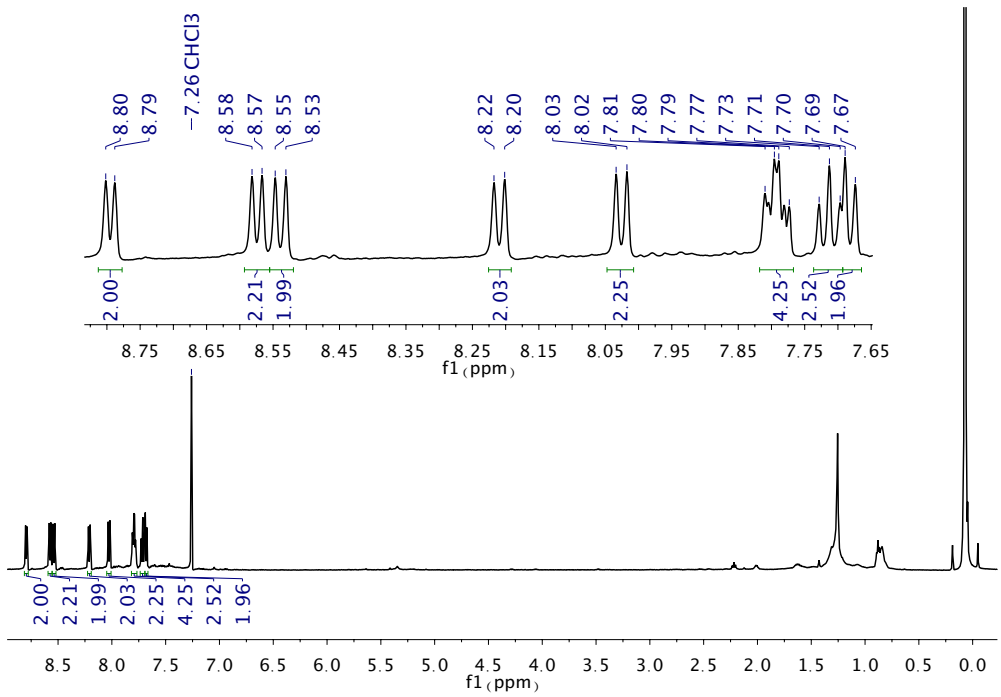


**Figure S3-37:** $^{1}$H NMR spectrum of **ODBE** ($CDCl_3$, 500.18 MHz).

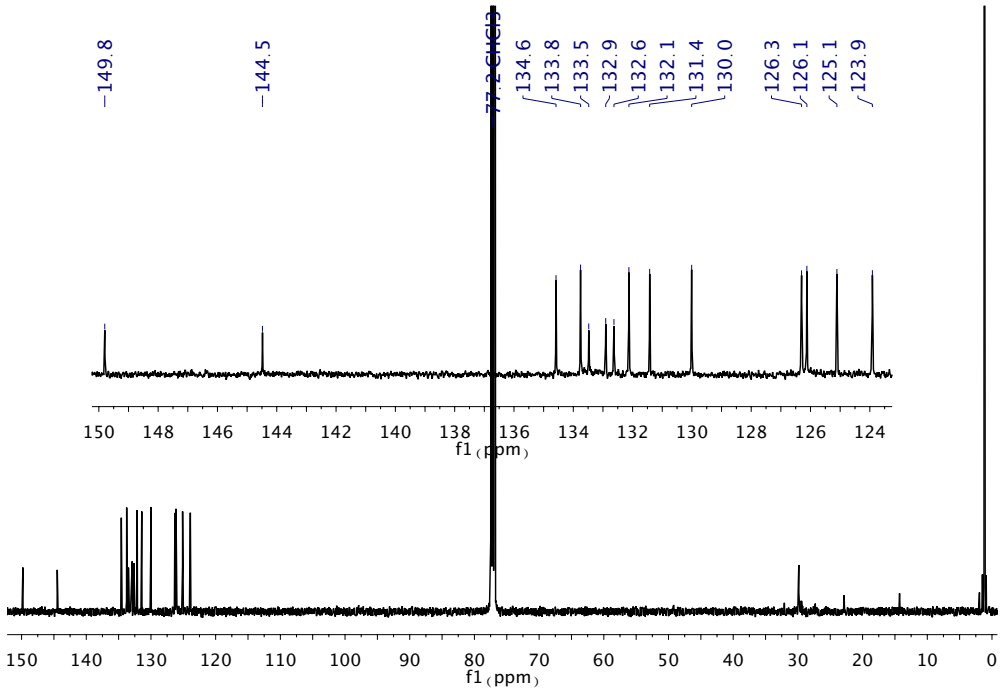


**Figure S3-38:** $^{13}$C{$^{1}$H} NMR spectrum of **ODBE** ($CDCl_3$, 125.77 MHz).

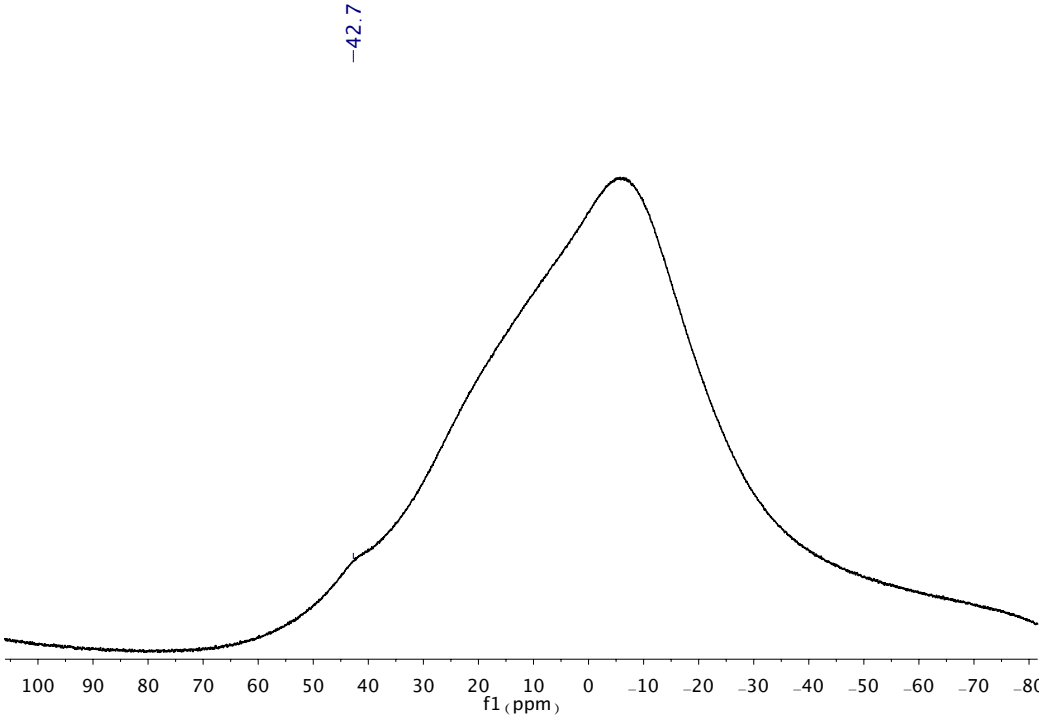


**Figure S3-39:** $^{11}B\{^{1}H\}$ NMR spectrum of **ODBE** ($CDCl_3$, 160.48 MHz).

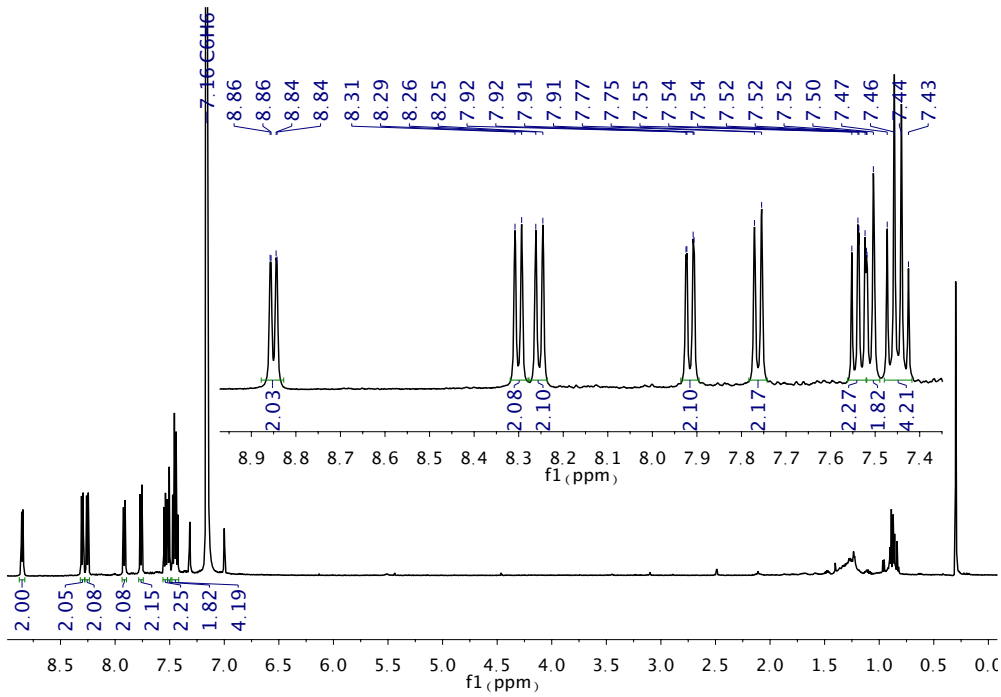


**Figure S3-40:** $^{1}$H NMR spectrum of **ODBE** ($C_6D_6$, 500.18 MHz).

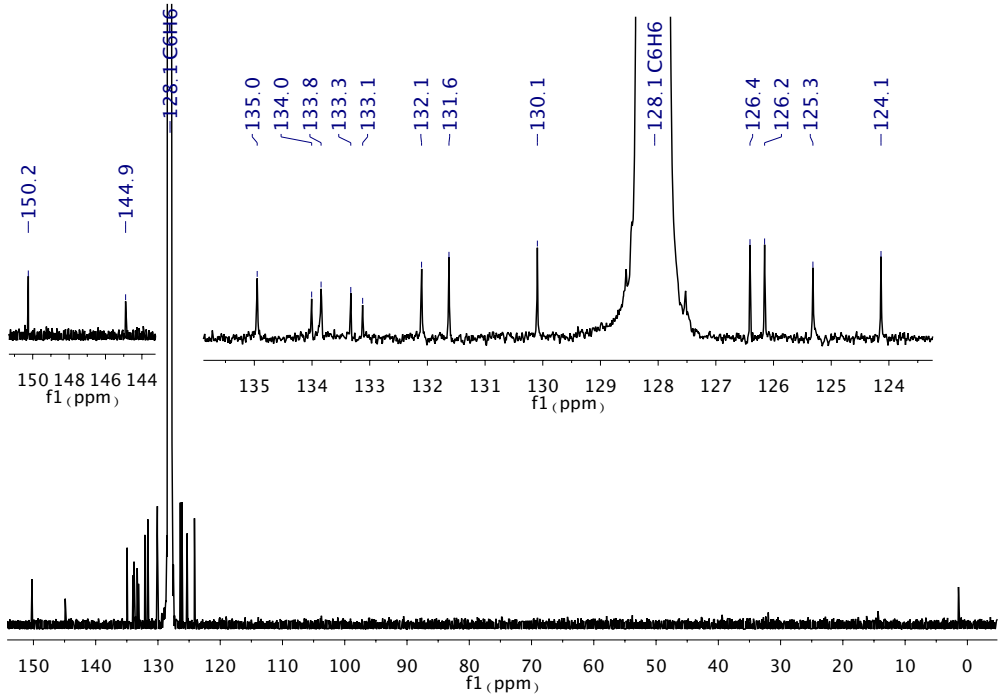


**Figure S3-41:** $^{13}$C{$^{1}$H} NMR spectrum of **ODBE** ($C_6D_6$, 125.77 MHz).

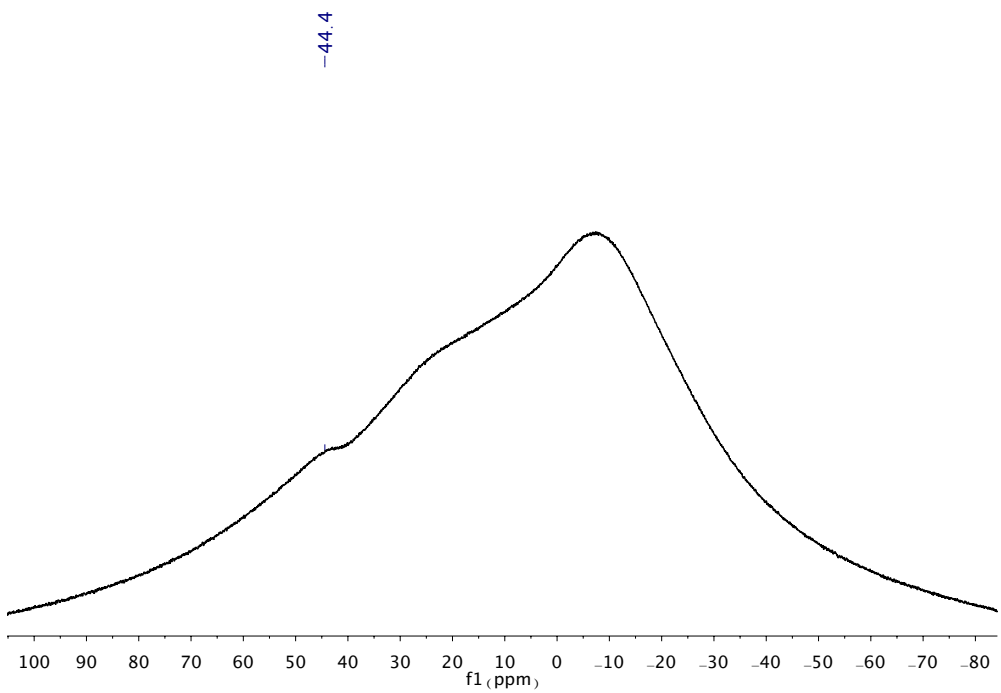


**Figure S3-42:** $^{11}B\{^{1}H\}$ NMR spectrum of **ODBE** ($C_6D_6$, 160.48 MHz).

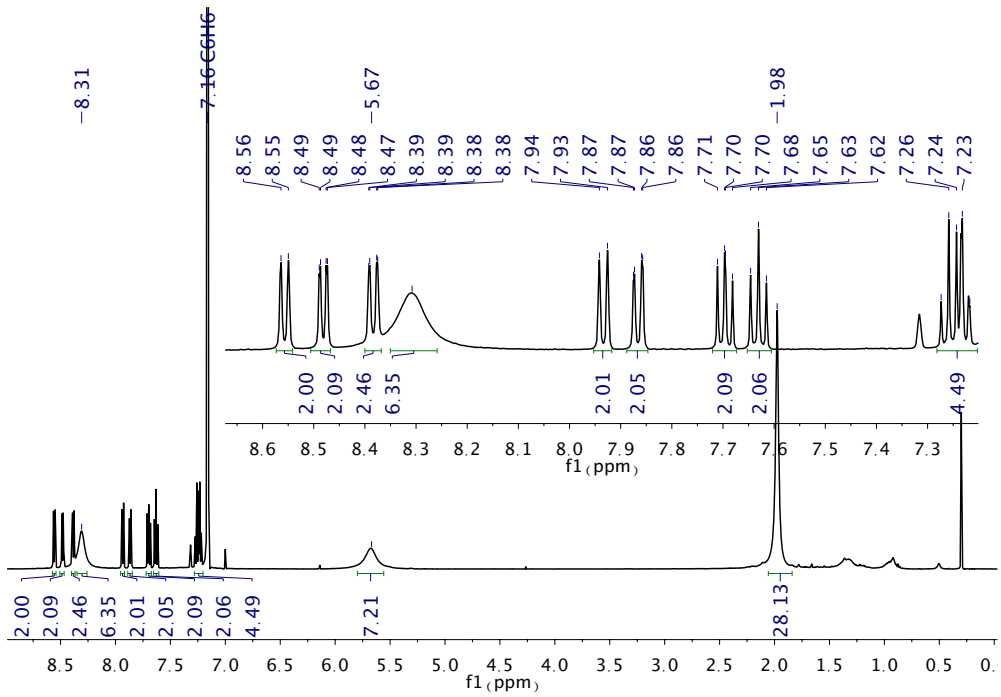


**Figure S3-43:** $^{1}$H NMR spectrum of **ODBE·DMAP** ($C_6D_6$, 500.18 MHz).

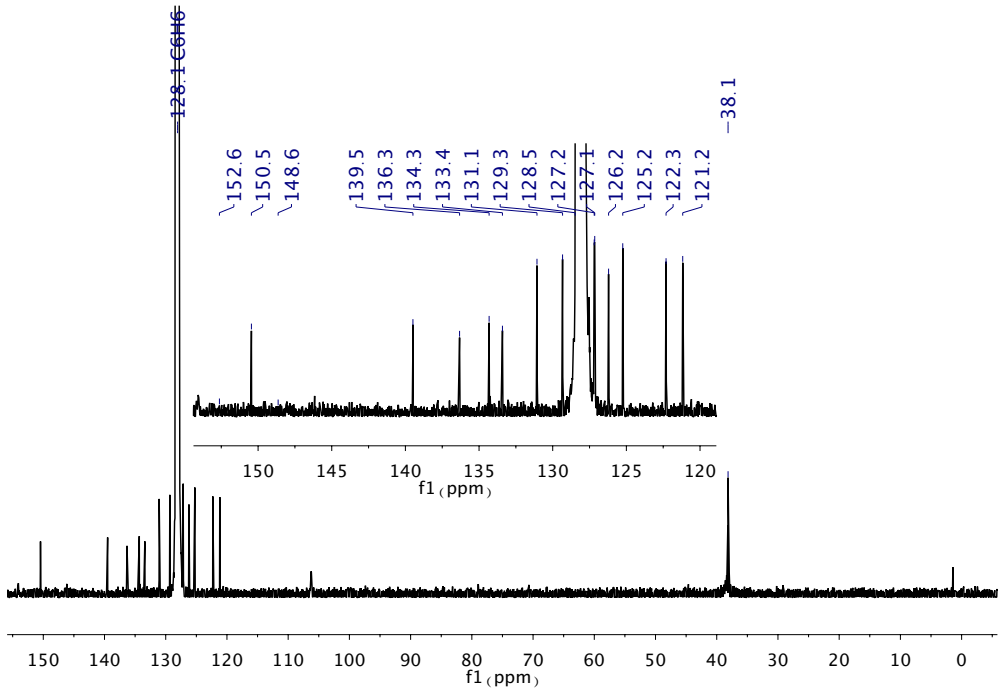


**Figure S3-44:** $^{13}$C{$^{1}$H} NMR spectrum of **ODBE·DMAP** ($C_6D_6$, 125.77 MHz).

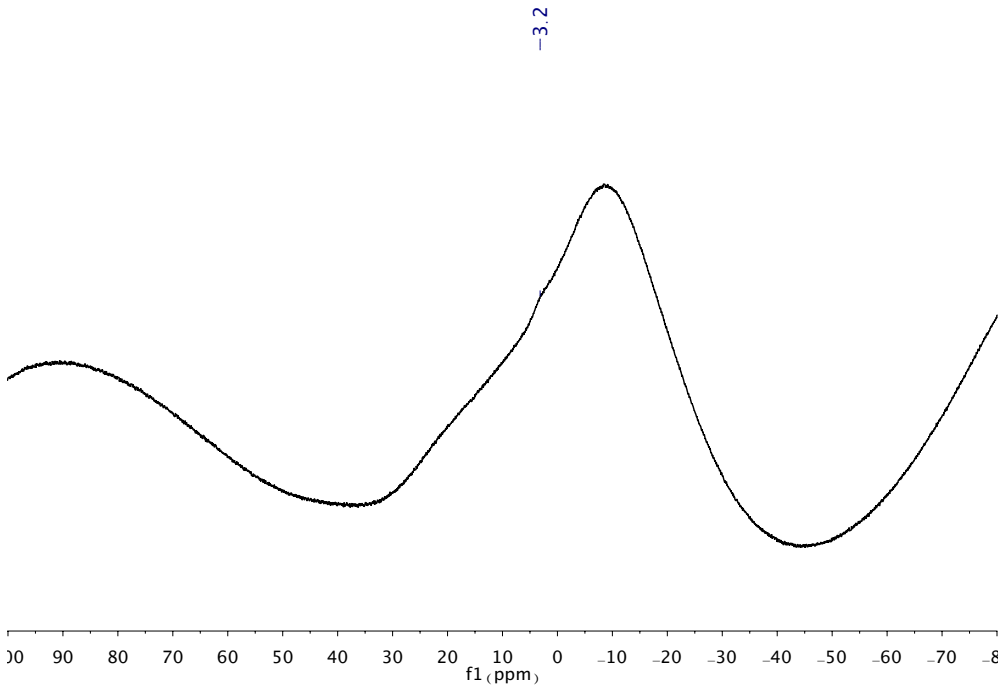


**Figure S3-45:** $^{11}B\{^{1}H\}$ NMR spectrum of **ODBE·DMAP** ($C_6D_6$, 160.48 MHz).

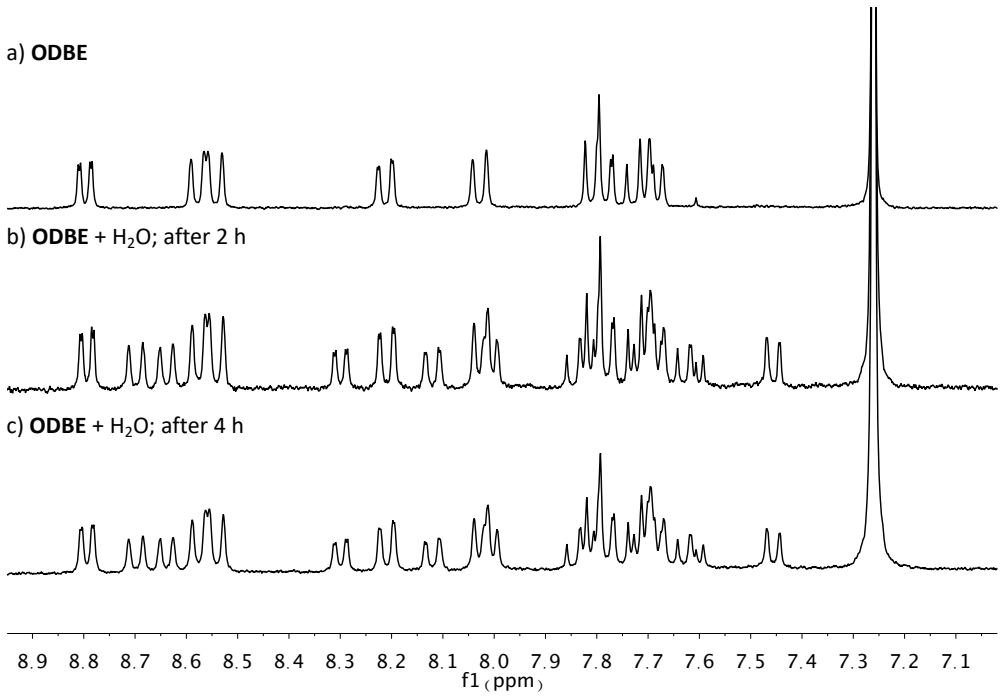


**Figure S3-46:** Blow-up of the $^{1}H$ NMR spectra ($CDCl_3$, 300.03 MHz) showing the partial hydrolysis of the B–O–B bond in **ODBE** (a) and two drops of added $H_2O$ over the course of 2 h (b) and after 4 h (c).

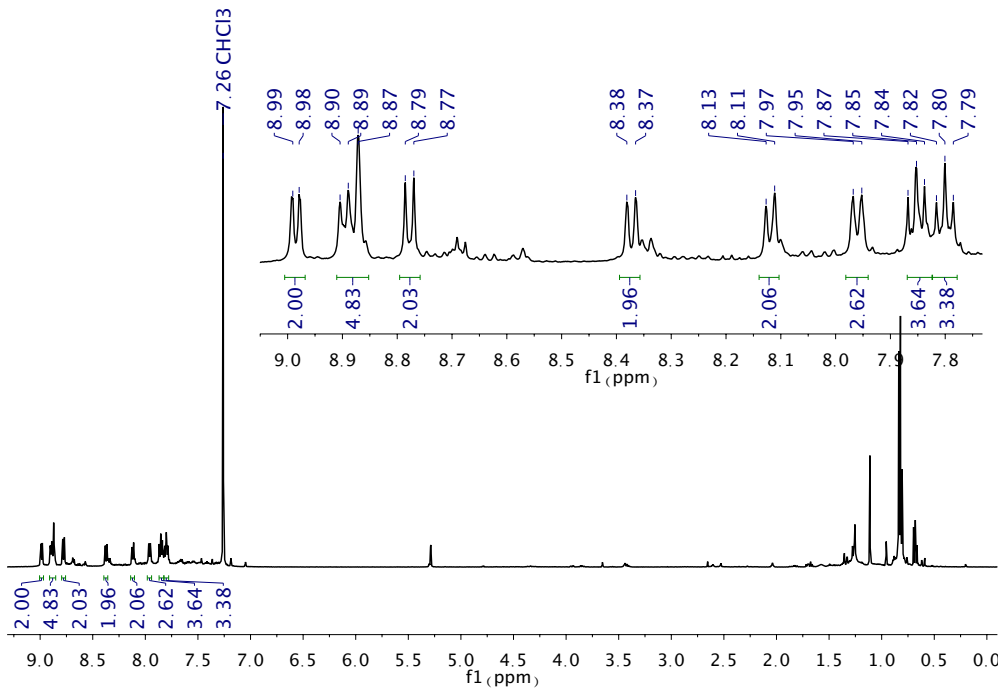


**Figure S3-47:** $^{1}$H NMR spectrum of **3** ($CDCl_3$, 500.18 MHz).

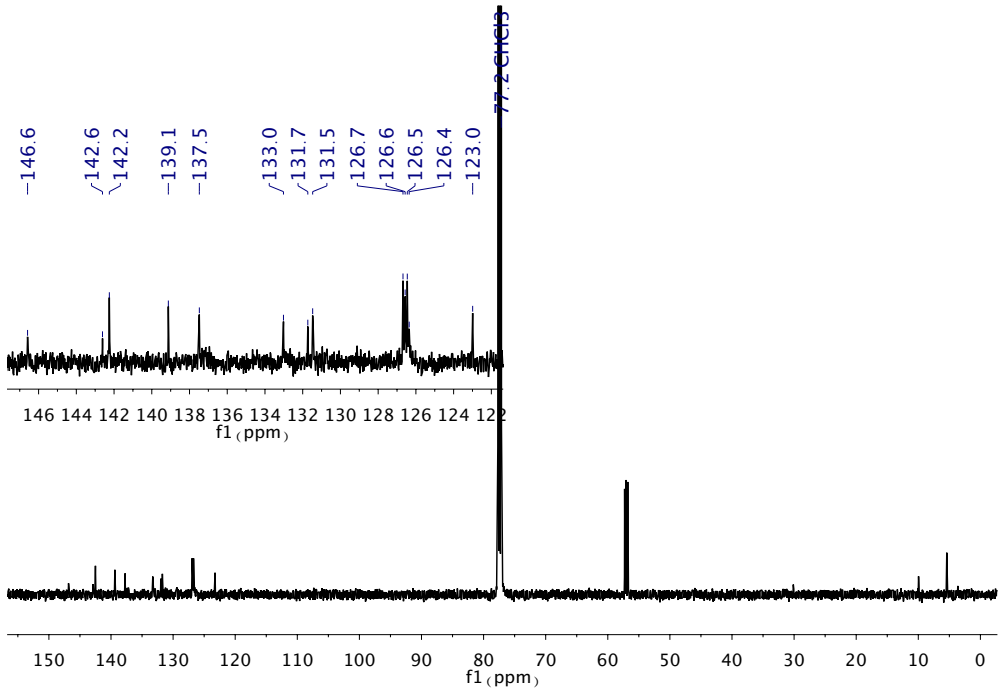


**Figure S3-48:** $^{13}$C{$^{1}$H} NMR spectrum of **3** ($CDCl_3$, 125.77 MHz).

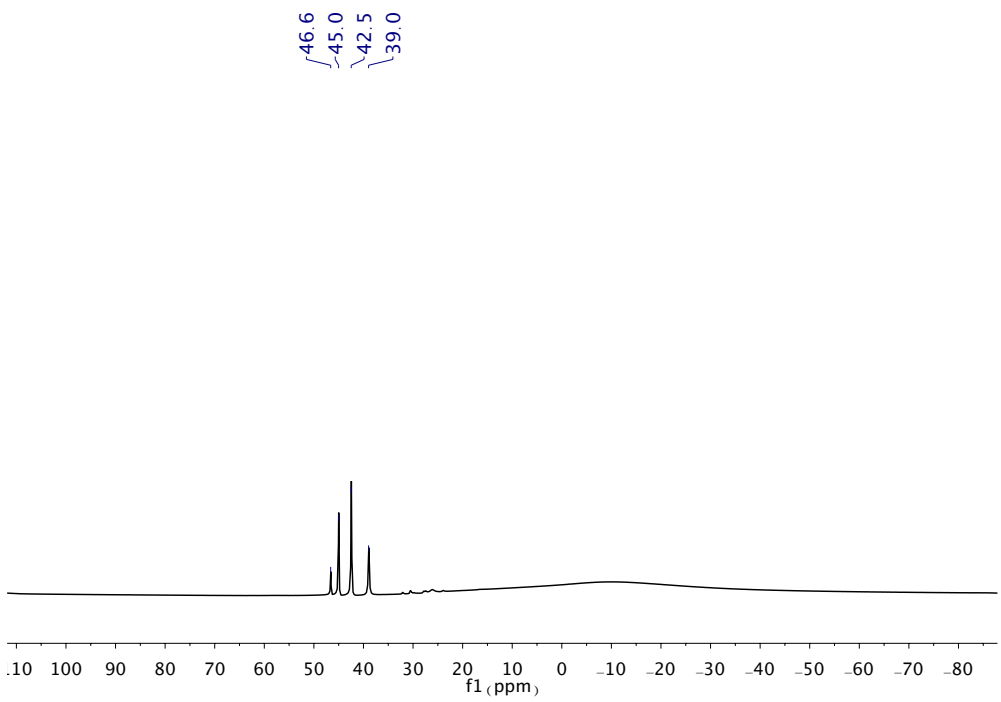


**Figure S3-49:** $^{11}B\{^{1}H\}$ NMR spectrum of **3** ($CDCl_3$, 160.48 MHz). *Note*: Due to halogen scrambling between $BBr_3$ and $CDCl_3$ the following species are observed in the $^{11}B\{^{1}H\}$ NMR spectrum: $BCl_3$, $BBrCl_2$, $BBr_2Cl$, and $BBr_3$.

## 4. Photophysical and electrochemical properties of $B_2$-TBPA and ODBE

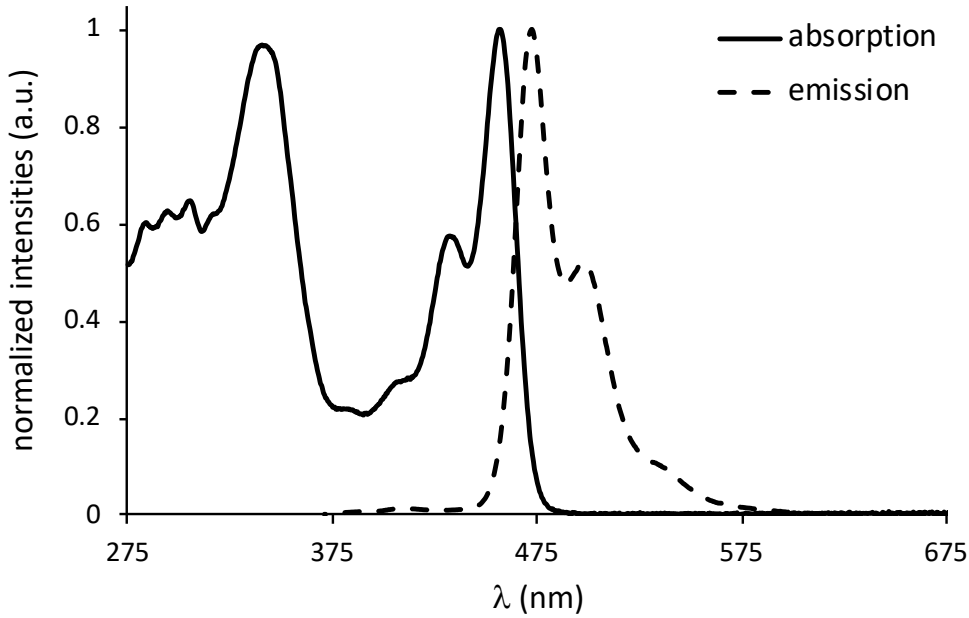


**Figure S4-1:** Normalized UV-vis absorption and emission spectra of **$B_2$-TBPA**, measured in *c*-hexane ($\lambda_{ex}$ = 340 nm).

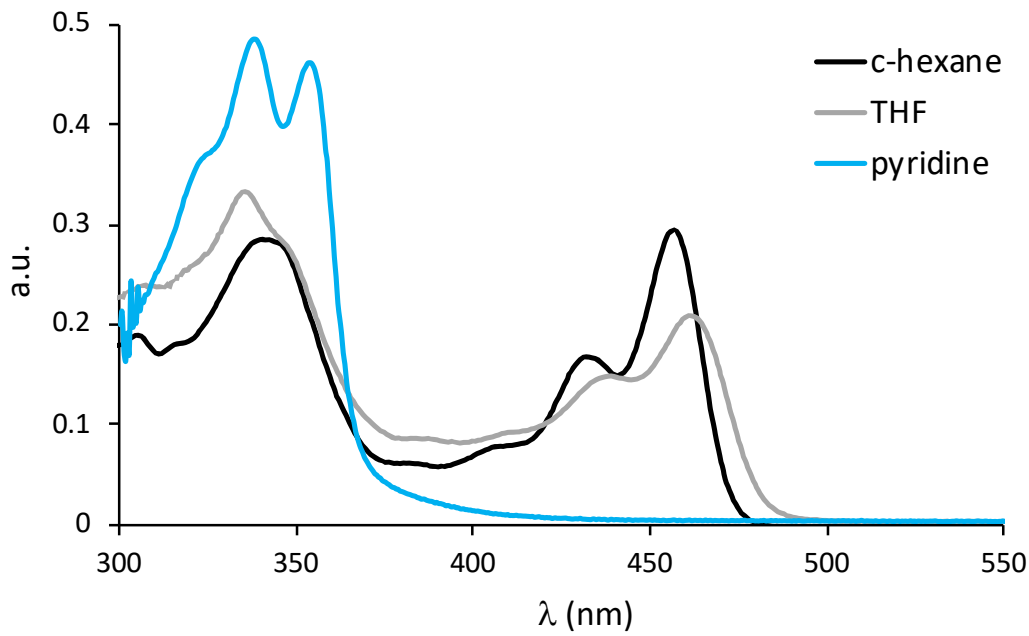


**Figure S4-2:** UV-vis absorption spectra of **$B_2$-TBPA** measured in *c*-hexane, THF, and pyridine at a concentration of $10^{-4}$ M.

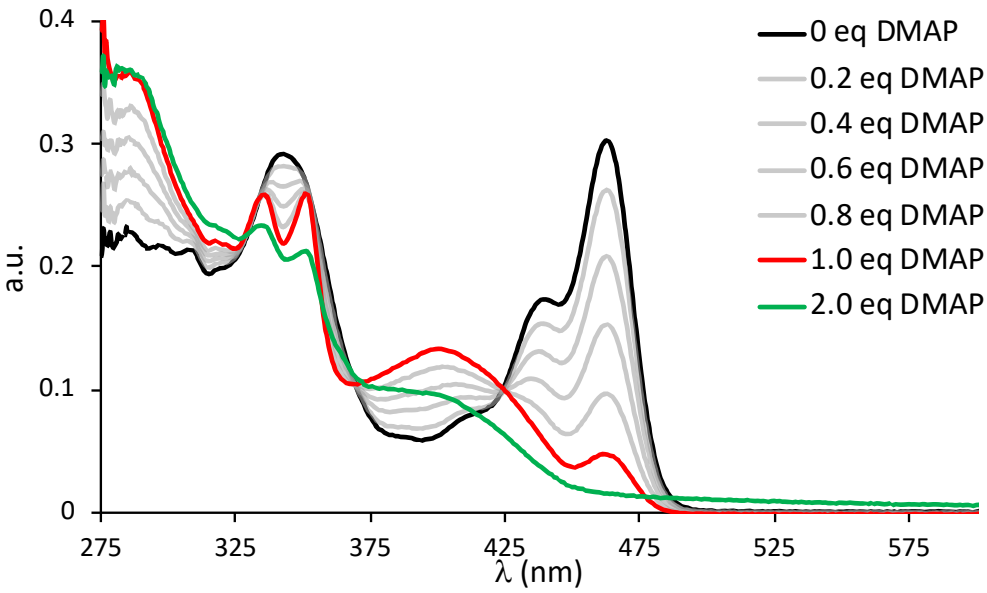


**Figure S4-3:** UV-vis absorption spectra of **$B_2$-TBPA** in the presence of various amounts of 4-dimethylaminopyridine (DMAP), measured in $C_6H_6$ at a concentration of $10^{-4}$ M.

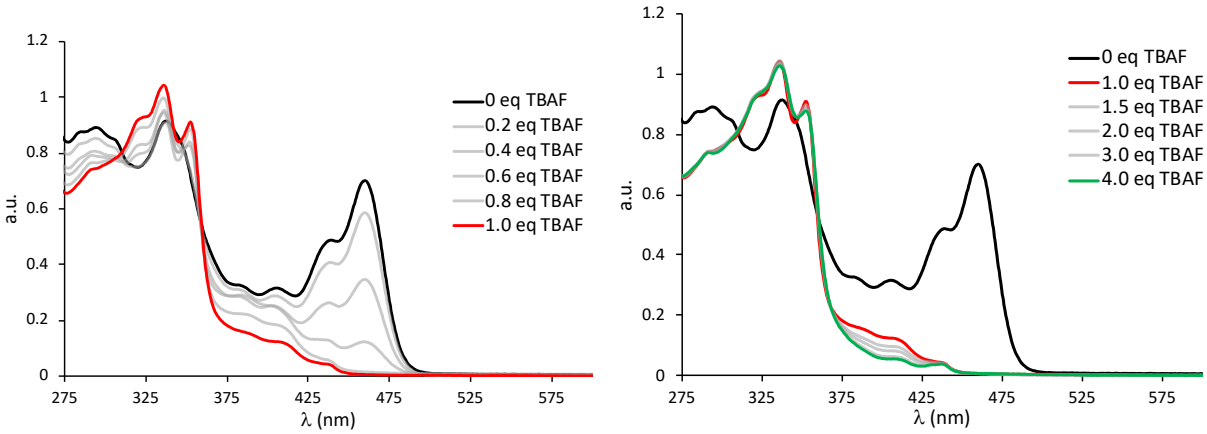


**Figure S4-4:** UV-vis absorption spectra of **$B_2$-TBPA** in the presence of various amounts of [*n*-$Bu_4N$]F (TBAF), measured in $CH_2Cl_2$ at a concentration of $10^{-4}$ M.

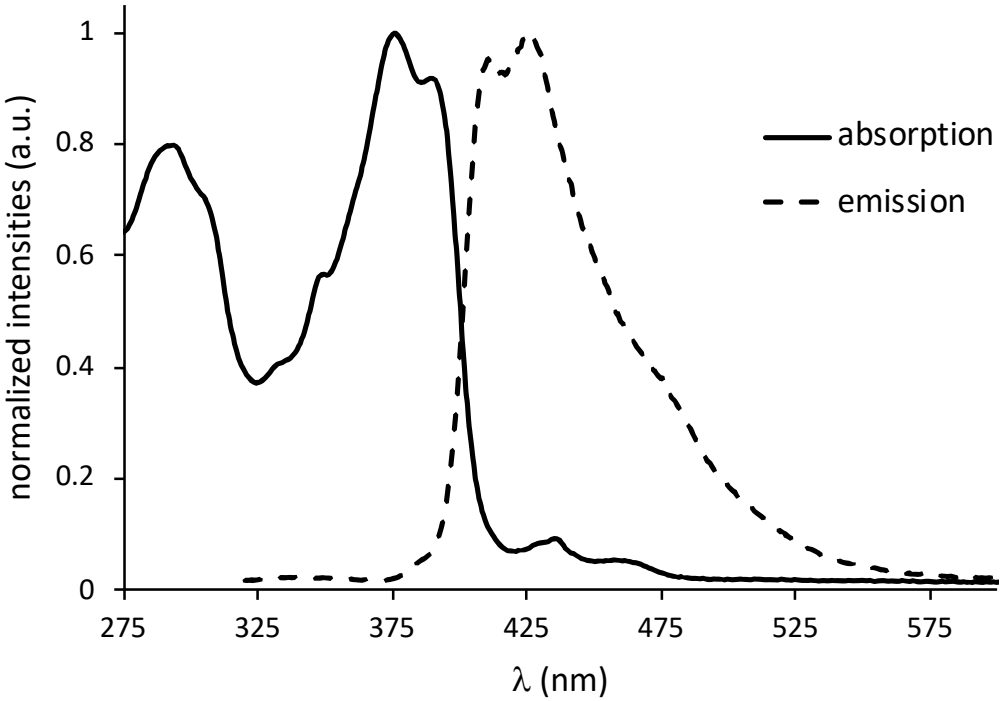


**Figure S4-5:** Normalized UV-vis absorption and emission spectra of **ODBE**, measured in *c*-hexane ($\lambda_{ex}$ = 300 nm).

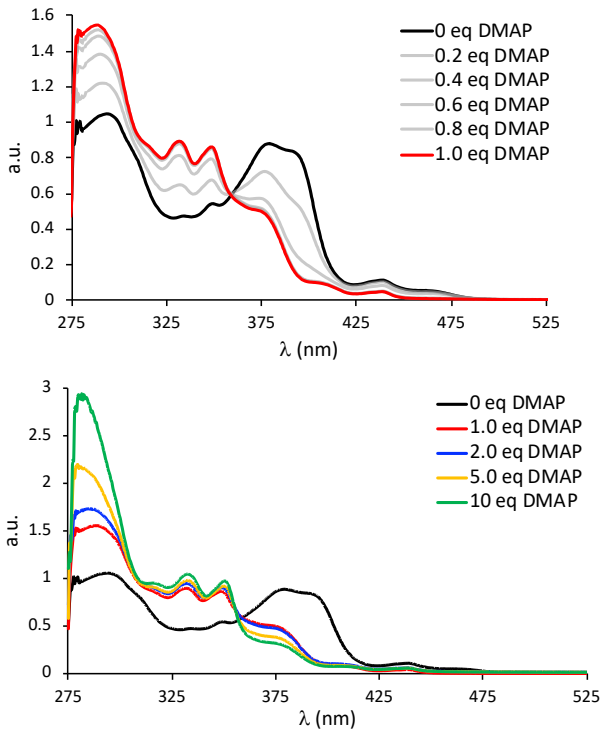


**Figure S4-6:** UV-vis absorption spectra of **ODBE** in the presence of various amounts of 4-dimethylaminopyridine (DMAP), measured in $C_6H_6$ at a concentration of $10^{-4}$ M.

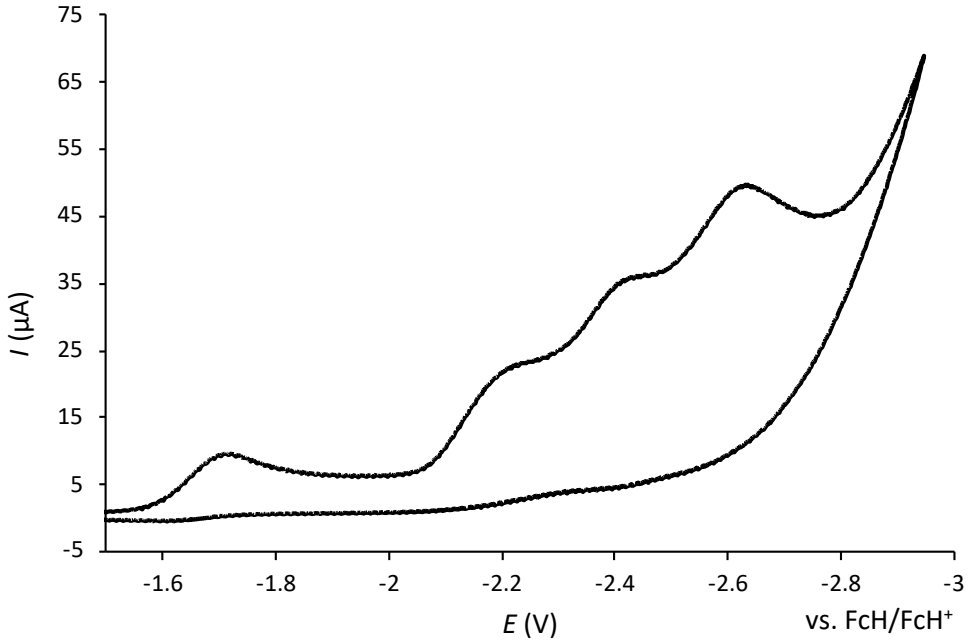


**Figure S4-7:** Cyclic voltammogram of the **$B_2$-TBPA** in $CH_2Cl_2$ (room temperature, supporting electrolyte: [*n*-$Bu_4N$][$PF_6$] (0.1 M), scan rate 200 mV $s^{-1}$).

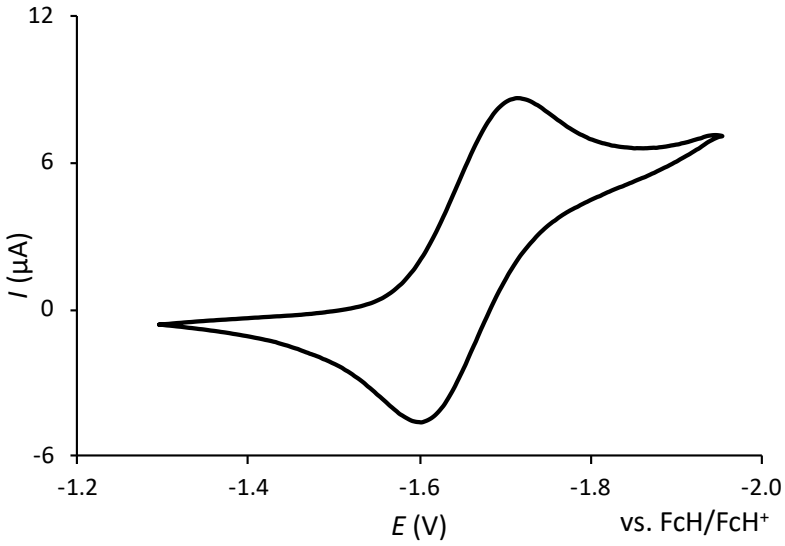


**Figure S4-8:** Cyclic voltammogram of the first reduction event of the **$B_2$-TBPA** in $CH_2Cl_2$ (room temperature, supporting electrolyte: [*n*-$Bu_4N$][$PF_6$] (0.1 M), scan rate 200 mV $s^{-1}$).

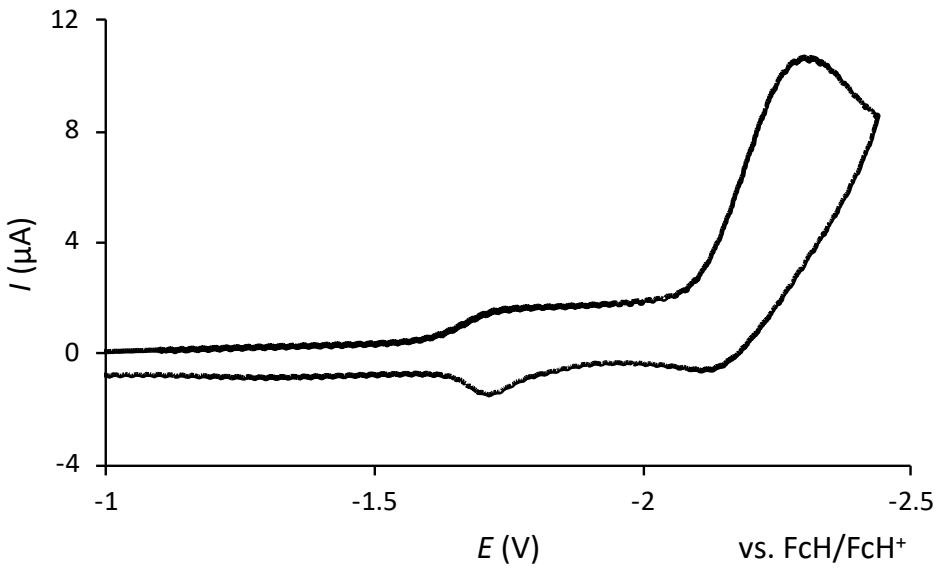


**Figure S4-9:** Cyclic voltammogram of the **$B_2$-TBPA** in THF (room temperature, supporting electrolyte: [*n*-$Bu_4N$][$PF_6$] (0.1 M), scan rate 200 mV $s^{-1}$).

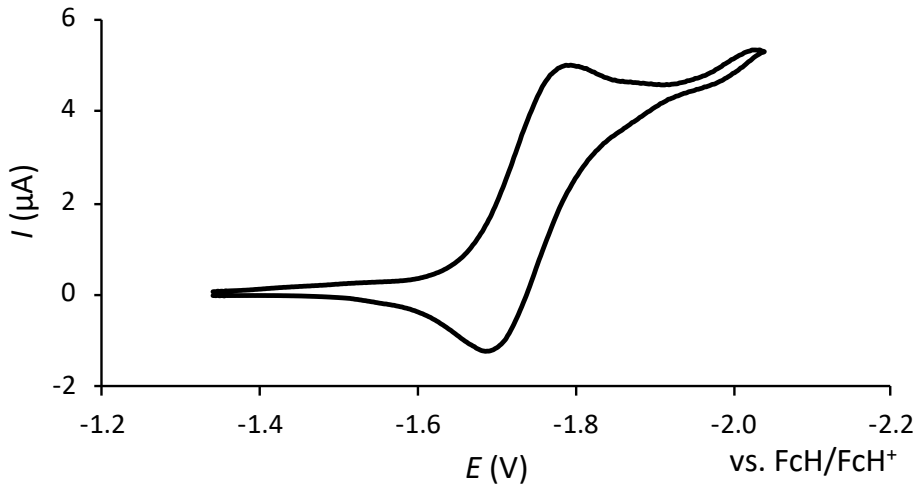


**Figure S4-10:** Cyclic voltammogram of the first reduction event of the **$B_2$-TBPA** in THF (room temperature, supporting electrolyte: [*n*-$Bu_4N$][$PF_6$] (0.1 M), scan rate 200 mV $s^{-1}$).

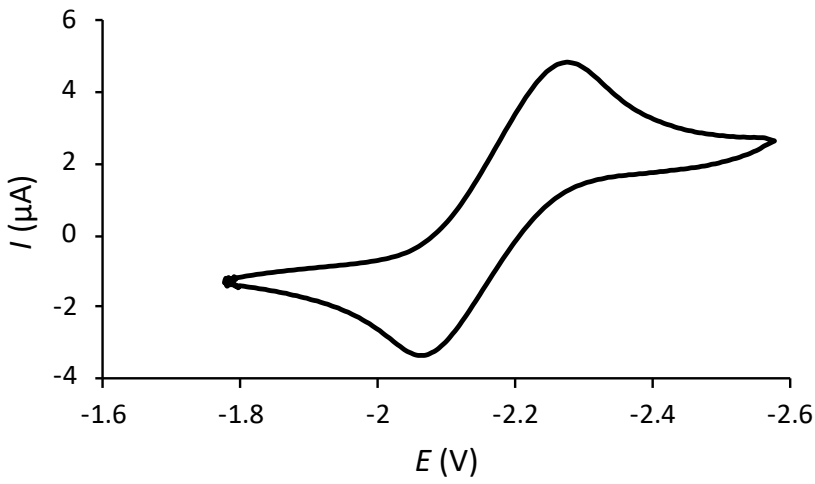


**Figure S4-11:** Cyclic voltammogram of the first reduction event of the **$B_2$-TBPA** in pyridine (room temperature, supporting electrolyte: [*n*-$Bu_4N$][$PF_6$] (0.1 M), scan rate 200 mV $s^{-1}$).

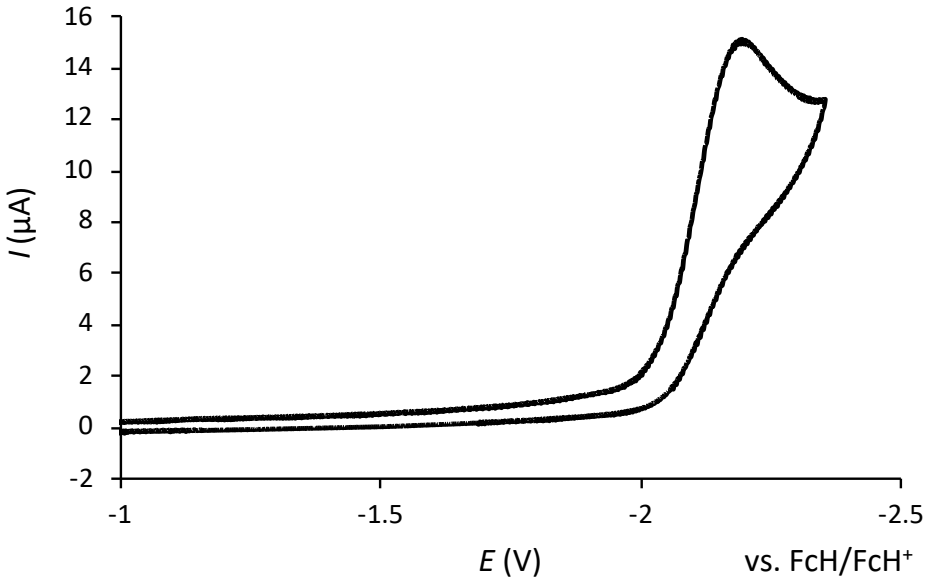


**Figure S4-12:** Cyclic voltammogram of the **ODBE** in $CH_2Cl_2$ (room temperature, supporting electrolyte: [*n*-$Bu_4N$][$PF_6$] (0.1 M), scan rate 200 mV $s^{-1}$).

**Table S4-1:** Photophysical and electrochemical data of **$B_2$-TBPA** and **ODBE**. Optical measurements were performed in *c*-hexane.

| | $\lambda_{abs}$ [nm][a] (ε [$M^{-1}cm^{-1}$]) | $\lambda_{onset}$[nm][b] | $\lambda_{em}$ [nm][a] | $\Phi_{PL}$ [%][c] | Stokes shift [$cm^{-1}$][d] | $E_{LUMO}$ [eV][e] | $E_{1/2}$ [V] | $E_G^{opt}$ [eV][f] |
|---|---|---|---|---|---|---|---|---|
| **$B_2$-TBPA** | 340 (14100)<br>*432* (8300)<br>456 (14600) | 472 | 472<br>*496* | 69 | 719 | –3.15[g]<br>–3.07[h]<br>–2.64[i] | –1.65[g]<br>–1.73[h]<br>–2.16[i] | 2.63 |
| **ODBE** | 295 (15600)<br>307 (13900)<br>*350* (11100)<br>*379* (18900)<br>392 (17200)<br>441 (1841)<br>467 (1353) | 486 | 411<br>*426* | 45 | 1179 | –/– | –2.19[g,k] | 2.55 |

[a] Resolved vibrational fine structure (italicized values). [b] Each onset wavelength ($\lambda_{onset}$) was determined by constructing a tangent on the point of inflection of the bathochromic slope of the most red-shifted absorption maximum. [c] Quantum yields were determined by using a calibrated integrating sphere. [d] Stokes shifts represent the difference between each longest wavelength absorption maximum and the corresponding shortest wavelength emission maximum. [e] $E_{LUMO} = -4.8\ eV - E_{1/2}^{Red1}$ ($FcH/FcH^+ = -4.8$ eV vs vacuum level). [f] Optical band gap $E_G^{opt} = 1240/\lambda_{onset}$. [g] Measurements were performed in $CH_2Cl_2$. [h] Measurements were performed in THF. [i] Measurements were performed in pyridine. [k] Only an irreversible reduction event was observed for compound **ODBE**.

# 5. X-Ray crystal structure analyses

Data for **ODBE** were collected on a STOE IPDS II-T two-circle diffractometer with an Incoatec Microfocus tube with mirror optics using Cu$K_\alpha$ radiation ($\lambda$ = 1.54186 Å). Data for the remaining structures were collected on a STOE IPDS II two-circle diffractometer with a Genix Microfocus tube with mirror optics using Mo$K_\alpha$ radiation ($\lambda$ = 0.71073 Å). The data were scaled using the frame scaling procedure in the *X-AREA* program system.[S23] The structures were solved by direct methods using the program *SHELXS* and refined against $F^2$ with full-matrix least-squares techniques using the program *SHELXL*.[S24]

CCDC 1922188 crystallizes together with 1 equiv of $C_6H_6$ (**$2^{H,Br}$·$C_6H_6$**). The bromonaphthyl residue at B(1) is disordered over two positions with a site occupation factor of 0.8550(11) for the major occupied sites. The minor occupied atoms were isotropically refined.

CCDC 1922189 (*syn*-**$2^{Br,I}$**) crystallizes with two symmetry-independent molecules, *syn*-**$2^{Br,I}$** and *syn*-**$2^{Br,I}$(A)**, in the asymmetric unit. In *syn*-**$2^{Br,I}$(A)**, the iodonaphthyl residue at B(2A) is disordered over two positions with a site occupation factor of 0.914(2) for the major occupied sites. The minor occupied atoms were isotropically refined with a common displacement parameter for the C atoms. The geometric parameters of the minor occupied atoms were restrained to those of a non-disordered iodonaphthyl moiety.

The molecule of CCDC 1922190 (**$B_2$-TBPA**) is located on a two-fold rotation axis. Due to the absence of anomalous scatterers, the absolute structure could not be determined.

CCDC 1922191 (**ODBE**) was non-merohedrally twinned with a fractional contribution of 0.485(4) for the minor domain.

CCDC 1922192 crystallizes with 0.5 equiv of $C_6H_6$ (**ODBE·pthz·0.5$C_6H_6$**), the displacement parameters of all non-H atoms were treated with a rigid bond restraint (RIGU in *SHELXL*). There are two symmetry-independent molecules, **ODBE·pthz** and **ODBE·pthz**(A), in the asymmetric unit.

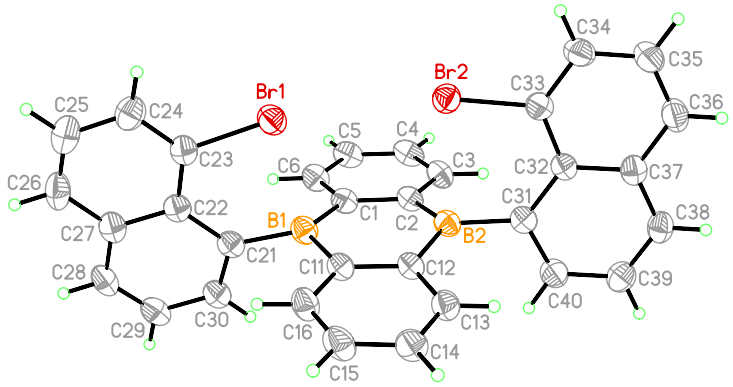


**Figure S5-1:** Molecular structure of $\mathbf{2^{H,Br}}\cdot C_6H_6$ in the solid state; *syn*/*anti* ratio in the crystal = 0.855/0.145, only the *syn*-conformer is shown. Displacement ellipsoids are drawn at the 50% probability level. Selected bond lengths [Å], atom···atom distances [Å], and bond angles [°]: C(1)−B(1) = 1.569(4), C(11)−B(1) = 1.569(4), C(21)−B(1) = 1.591(4), C(2)−B(2) = 1.570(4), C(12)−B(2) = 1.559(4), C(31)−B(2) = 1.583(4); B(1)···Br(1) = 2.690(3), B(2)···Br(2) = 2.801(3); C(1)−B(1)−C(11) = 118.6(2), C(1)−B(1)−C(21) = 119.0(2), C(11)−B(1)−C(21) = 119.3(2), C(2)−B(2)−C(12) = 119.1(2), C(2)−B(2)−C(31) = 120.4(2), C(12)−B(2)−C(31) = 119.3(2).

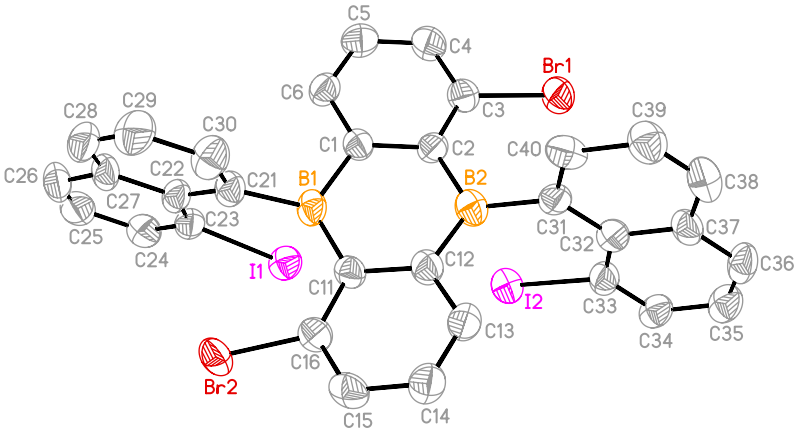


**Figure S5-2:** Molecular structure of *syn*-**2**$^{\mathbf{Br,I}}$ in the solid state. The compound crystallizes with two symmetry-independent molecules, *syn*-**2**$^{\mathbf{Br,I}}$ and *syn*-**2**$^{\mathbf{Br,I}}$**(A)**, in the asymmetric unit. In *syn*-**2**$^{\mathbf{Br,I}}$**(A)**, the iodonaphthyl residue at B(2A) is disordered over two positions with a site occupation factor of 0.914(2) for the major occupied sites. Shown and discussed here is only the non-disordered *syn*-**2**$^{\mathbf{Br,I}}$. Displacement ellipsoids are drawn at the 50% probability level; hydrogen atoms are omitted for clarity. Selected bond lengths [Å], atom···atom distances [Å], and bond angles [°]: C(1)−B(1) = 1.589(12), C(11)−B(1) = 1.587(13), C(21)−B(1) = 1.583(10), C(2)−B(2) = 1.565(13), C(12)−B(2) = 1.570(12), C(31)−B(2) = 1.606(12); B(1)···I(1) = 2.775(9), B(2)···I(2) = 2.822(10); C(1)−B(1)−C(11) = 118.8(6), C(1)−B(1)−C(21) = 114.7(7), C(11)−B(1)−C(21) = 121.2(7), C(2)−B(2)−C(12) = 120.5(7), C(2)−B(2)−C(31) = 120.8(7), C(12)−B(2)−C(31) = 115.4(7).

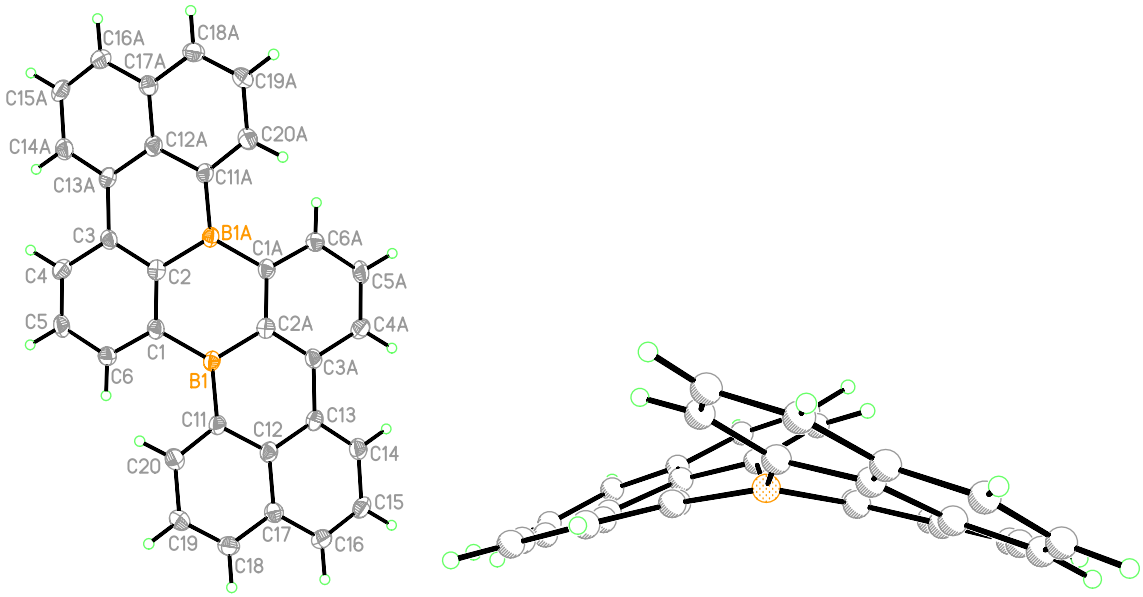


**Figure S5-3:** Molecular structure of **$B_2$-TBPA** in the solid state. Displacement ellipsoids are drawn at the 50% probability level. Selected bond lengths [Å], bond angles [°], torsion angles [°], and dihedral angle [°]: B(1)−C(1) = 1.572(7), B(1)−C(11) = 1.548(6), B(1)−C(2A) = 1.540(6), C(3A)−C(13) = 1.486(5); C(2A)–B(1)–C(1) = 118.3(4), C(2A)–B(1)–C(11) = 116.5(4), C(11)–B(1)–C(1) = 125.2(4); C(11)–B(1)–C(1)–C(6) = –21.1(6), C(1)–B(1)–C(11)–C(20) = –20.7(7), Ph(1)–Naph(11)//Ph(1A)–Naph(11A) = 42.20(4). Ph(X)–Naph(X): phenylene and naphthylene ring containing the carbon atom C(X). Symmetry operation used to generate equivalent atoms: –x+1, y, –z+1.

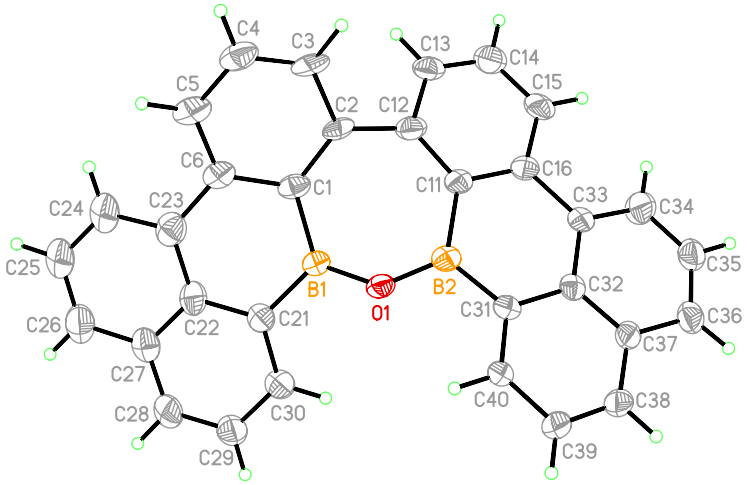


**Figure S5-4:** Molecular structure of **ODBE** in the solid state. Displacement ellipsoids are drawn at the 50% probability level. Selected bond lengths [Å], bond angles [°], torsion angles [°], and dihedral angle [°]: B(1)–C(1) = 1.567(13), B(1)–C(21) = 1.458(16), B(1)–O(1) = 1.418(13), B(2)–C(11) = 1.496(15), B(2)–C(31) = 1.564(14), B(2)–O(1) = 1.382(14), C(1)−C(2) = 1.392(14), C(2)−C(12) = 1.470(14), C(6)−C(23) = 1.451(15), C(11)−C(12) = 1.464(12), C(16)−C(33) = 1.508(13); B(1)–O(1)–B(2) = 134.8(10), O(1)–B(1)–C(1) = 119.6(11), O(1)–B(1)–C(21) = 118.3(10), C(1)–B(1)–C(21) = 121.2(10), O(1)–B(2)–C(11) = 126.6(11), O(1)–B(2)–C(31) = 113.9(10), C(11)–B(2)–C(31) = 119.1(11); O(1)–B(1)–C(21)–C(30) = –14.3(19), O(1)–B(2)–C(31)–C(40) = –13.0(17), C(3)–C(2)–C(12)–C(13) = –37.4(16); Ph(1)//Ph(11)= 41.8(3). Ph(X): phenylene ring containing the carbon atom C(X).

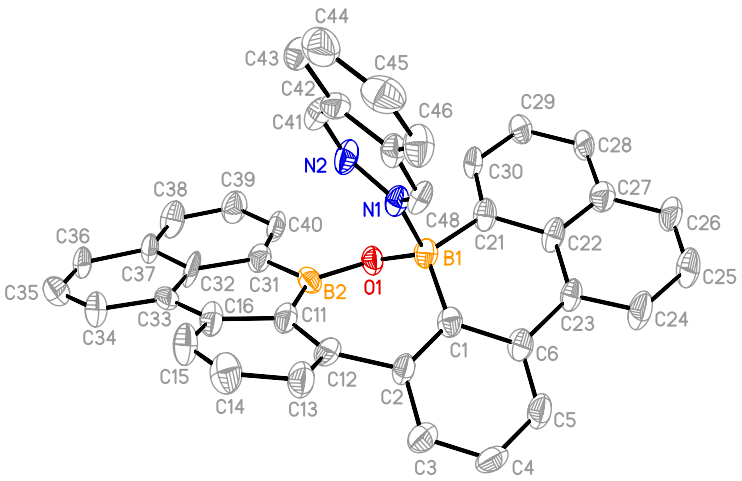


**Figure S5-5:** Molecular structure of **ODBE·pthz**·0.5$C_6H_6$ in the solid state. There are two symmetry-independent molecules, **ODBE·pthz** and **ODBE·pthz**(A), and one $C_6H_6$ molecule in the asymmetric unit. Bond lengths and angles of both molecules are equal within the experimental error margins. Shown and discussed here is therefore only molecule **ODBE·pthz**. Displacement ellipsoids are drawn at the 50% probability level; hydrogen atoms are omitted for clarity. Selected bond lengths [Å], bond angles [°], torsion angles [°], and dihedral angles [°]: B(1)–C(1) = 1.599(15), B(1)–C(21) = 1.617(14), B(1)–N(1) = 1.686(14), B(1)–O(1) =1.426(13), B(2)–C(11) = 1.538(15), B(2)–C(31) = 1.575(16), B(2)–O(1) = 1.370(12), C(1)−C(2) = 1.404(13), C(2)−C(12) = 1.540(12), C(6)−C(23) = 1.492(14), C(11)−C(12) = 1.425(14), C(16)−C(33) = 1.489(15); B(1)–O(1)–B(2) = 128.4(8), O(1)–B(1)–C(1) = 114.2(9), O(1)–B(1)–C(21) = 110.2(8), C(1)–B(1)–C(21) = 113.0(8), O(1)–B(1)–N(1) = 104.9(7), C(1)–B(1)–N(1) = 107.6(8), C(21)–B(1)–N(1) = 106.2(8), O(1)–B(2)–C(11) = 123.6(10), O(1)–B(2)–C(31) = 116.4(9), C(11)–B(2)–C(31) = 119.8(8); O(1)–B(1)–C(21)–C(30) = 42.5(14), O(1A)–B(1A)–C(21A)–C(30A) = 51.2(12), O(1)–B(2)–C(31)–C(40) = 3.0(16), O(1A)–B(2A)–C(31A)–C(40A) = 26.0(15), C(3)–C(2)–C(12)–C(13) = 42.8(15), C(3A)–C(2A)–C(12A)–C(13A) = 40.0(14); Ph(1)//Ph(11) = 47.9(4), Ph(1A)//Ph(11A) = 44.4(4), Ph(1)//Ph(23) = 18.0(5), Ph(1A)//Ph(23A) = 13.2(6). Ph(X): phenylene ring containing the carbon atom C(X).

**Table S5-1.** Selected crystallographic data for $\mathbf{2^{H,Br}\cdot C_6H_6}$, $\mathbf{2^{Br,I}}$, and $\mathbf{B_2}$**-TBPA**.

| **compound** | $\mathbf{2^{H,Br}\cdot C_6H_6}$ | $\mathbf{2^{Br,I}}$ | $\mathbf{B_2}$**-TBPA** |
|---|---|---|---|
| CCDC | 1922188 | 1922189 | 1922190 |
| formula | $C_{32}H_{20}B_2Br_2$ x $C_6H_6$ | $C_{32}H_{18}B_2Br_2I_2$ | $C_{32}H_{18}B_2$ |
| *M*r | 664.03 | 837.70 | 424.08 |
| *T* (K) | 173(2) | 173(2) | 173(2) |
| radiation, $\lambda$ (Å) | 0.71073 | 0.71073 | 0.71073 |
| crystal system | monoclinic | triclinic | monoclinic |
| space group | $P2_1/c$ | $P$–1 | $C2$ |
| *a* (Å) | 9.4242(3) | 10.1254(6) | 24.030(5) |
| *b* (Å) | 23.7038(9) | 11.9749(7) | 3.8493(6) |
| *c* (Å) | 13.4085(4) | 23.3063(15) | 10.627(3) |
| α (°) | 90 | 89.356(5) | 90 |
| β (°) | 100.468(3) | 89.874(5) | 92.763(19) |
| γ (°) | 90 | 84.455(5) | 90 |
| *V* (Å$^3$) | 2945.46(17) | 2812.5(3) | 981.8(4) |
| *Z* | 4 | 4 | 2 |
| $D_{calcd}$ (g cm$^{-3}$) | 1.497 | 1.978 | 1.434 |
| *F*(000) | 1336 | 1584 | 440 |
| μ (mm−1) | 2.779 | 5.099 | 0.080 |
| crystal size (mm) | 0.450 x 0.170 x 0.070 | 0.170 x 0.110 x 0.040 | 0.110 x 0.030 x 0.010 |
| crystal form, color | yellow needle | colorless plate | light brown plate |
| reflections collected | 49497 | 35871 | 7193 |
| independent reflections | 6477 | 12391 | 1976 |
| $R_{int}$ | 0.0803 | 0.0611 | 0.0808 |
| data/restraints/parameters | 6477/0/430 | 12391/140/721 | 1976/1/154 |
| $R_1$, $wR_2$ ($I > 2\sigma(I)$) | 0.0427, 0.0939 | 0.0567, 0.1259 | 0.0611, 0.1262 |
| $R_1$, $wR_2$ (all data) | 0.0509, 0.0976 | 0.0988, 0.1424 | 0.0855, 0.1358 |
| Goodness-of-fit on $F^2$ | 1.146 | 0.935 | 1.036 |
| largest diff peak and hole (e Å$^{-3}$) | 0.510, –0.411 | 1.282, –1.137 | 0.281, –0.263 |

**Table S5-2.** Selected crystallographic data for **ODBE** and **ODBE·pthz·0.5$C_6H_6$**.

| **compound** | **ODBE** | **ODBE·pthz·0.5$C_6H_6$** |
|---|---|---|
| CCDC | 1922191 | 1922192 |
| formula | $C_{32}H_{18}B_2O$ | $C_{40}H_{24}B_2N_2O$ x 0.5 $C_6H_6$ |
| *M*r | 440.08 | 609.28 |
| *T* (K) | 173(2) | 173(2) |
| radiation, $\lambda$ (Å) | 1.54186 | 0.71073 |
| crystal system | monoclinic | triclinic |
| space group | $P2_1/c$ | $P$–1 |
| *a* (Å) | 3.8376(6) | 14.113(4) |
| *b* (Å) | 13.5325(14) | 14.980(5) |
| *c* (Å) | 38.521(6) | 16.668(5) |
| α (°) | 90 | 103.27(3) |
| β (°) | 93.020(12) | 101.80(2) |
| γ (°) | 90 | 108.84(2) |
| *V* (Å$^3$) | 1997.7(5) | 3093.9(17) |
| *Z* | 4 | 4 |
| $D_{calcd}$ (g cm$^{-3}$) | 1.463 | 1.308 |
| *F*(000) | 912 | 1268 |
| μ (mm−1) | 0.656 | 0.077 |
| crystal size (mm) | 0.350 x 0.040 x 0.020 | 0.190 x 0.030 x 0.020 |
| crystal form, color | light brown needle | colorless needle |
| reflections collected | 10326 | 35886 |
| independent reflections | 3544 | 10890 |
| $R_{int}$ | 0.1008 | 0.2623 |
| data/restraints/parameters | 3544/0/318 | 10890/882/865 |
| $R_1$, $wR_2$ ($I > 2\sigma(I)$) | 0.1307, 0.2252 | 0.1174, 0.2009 |
| $R_1$, $wR_2$ (all data) | 0.2342, 0.2720 | 0.3199, 0.2919 |
| Goodness-of-fit on $F^2$ | 1.780 | 0.881 |
| largest diff peak and hole (e Å$^{-3}$) | 0.396, –0.428 | 0.309, –0.318 |

## 6. TD-DFT calculation data of $B_2$-TBPA and ODBE

**Table S6-1.** TD-DFT calculated electronic transitions for **$B_2$-TBPA** along with their corresponding excitation energies and oscillator strengths.

| Compound | Spin State | Transition Configuration | Excitation Energy (nm, eV) | Oscillator Strength |
|---|---|---|---|---|
| **$B_2$-TBPA** | $S_1$ | HOMO → LUMO (98%) | 462.83 (2.68) | 0.3321 |
| | $S_2$ | HOMO–1 → LUMO (90%) | 417.82 (2.97) | 0.0004 |
| | | HOMO–2 → LUMO (6%) | | |
| | $S_3$ | HOMO–2 → LUMO (70%) | 392.65 (3.16) | 0.0002 |
| | | HOMO → LUMO+1 (24%) | | |
| | | HOMO–1 → LUMO (4%) | | |
| | $S_4$ | HOMO → LUMO+1 (66%) | 379.78 (3.26) | 0.0061 |
| | | HOMO–2 → LUMO (19%) | | |
| | | HOMO–4 → LUMO (11%) | | |
| | $S_5$ | HOMO–3 → LUMO (55%) | 368.57 (3.36) | 0.0003 |
| | | HOMO–1 → LUMO+1 (34%) | | |
| | | HOMO–5 → LUMO (3%) | | |
| | | HOMO–4 → LUMO+1 (3%) | | |
| | $S_6$ | HOMO–1 → LUMO+1 (57%) | 353.20 (3.51) | 0.3293 |
| | | HOMO–3 → LUMO (35%) | | |
| | | HOMO–2 → LUMO+1 (4%) | | |

**Table S6-2.** TD-DFT calculated electronic transitions for **ODBE** along with their corresponding excitation energies and oscillator strengths.

| Compound | Spin State | Transition Configuration | Excitation Energy (nm, eV) | Oscillator Strength |
|---|---|---|---|---|
| **ODBE** | $S_1$ | HOMO → LUMO (96%) | 397.18 (3.12) | 0.0719 |
| | $S_2$ | HOMO–1 → LUMO (98%) | 394.73 (3.14) | 0.274 |
| | $S_3$ | HOMO → LUMO+1 (96%) | 367.98 (3.37) | 0.1493 |
| | $S_4$ | HOMO–1 → LUMO+1 (93%) | 352.29 (3.52) | 0.0674 |
| | $S_5$ | HOMO–2 → LUMO (81%) | 334.82 (3.70) | 0.0009 |
| | | HOMO–1 → LUMO+2 (8%) | | |
| | | HOMO–3 → LUMO+1 (5%) | | |
| | | HOMO–6 → LUMO (4%) | | |
| | $S_6$ | HOMO–3 → LUMO (68%) | 324.22 (3.82) | 0.0534 |
| | | HOMO–2 → LUMO+1 (13%) | | |
| | | HOMO → LUMO+2 (10%) | | |
| | | HOMO–6 → LUMO+1 (4%) | | |
| | $S_7$ | HOMO–1 → LUMO+2 (45%) | 308.88 (4.01) | 0.0651 |
| | | HOMO–4 → LUMO (24%) | | |
| | | HOMO–2 → LUMO (8%) | | |
| | | HOMO–6 → LUMO (6%) | | |
| | | HOMO→ LUMO+4 (4%) | | |
| | | HOMO–3 → LUMO+1 (3%) | | |
| | | HOMO–1 → LUMO+5 (3%) | | |

**Table S6-3.** Primary orbitals which contribute to the calculated transitions of **$B_2$-TBPA**. H-atoms have been omitted for clarity.

| | | | |
|---|---|---|---|
| 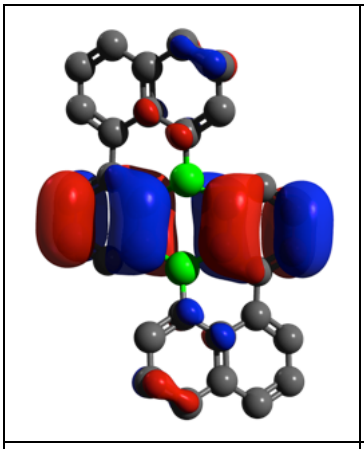 | 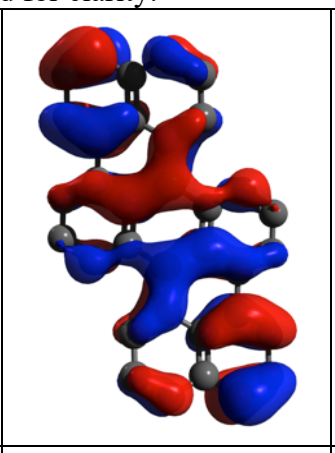 | 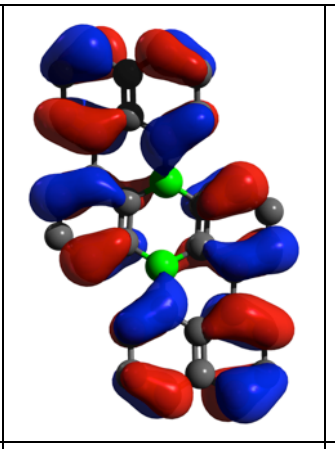 | 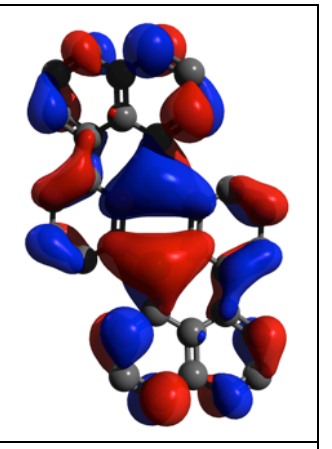 |
| HOMO-2 | HOMO-1 | HOMO | LUMO |

**Table S6-4.** Primary orbitals which contribute to the calculated transitions of **ODBE**. H-atoms have been omitted for clarity.

| | | | |
|---|---|---|---|
| 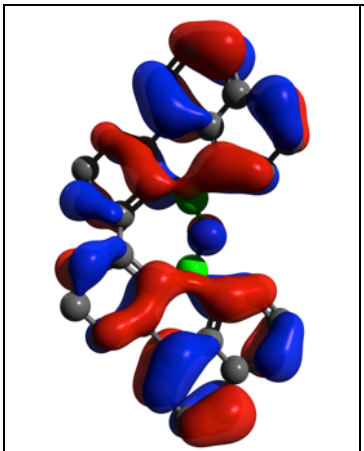 | 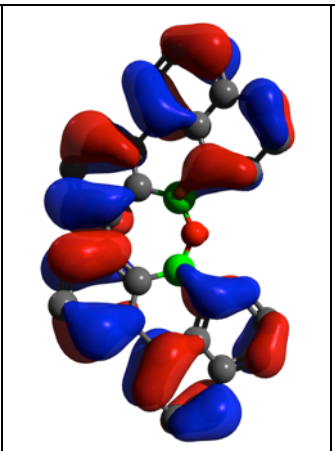 | 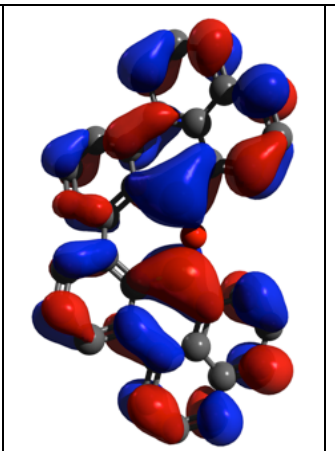 | 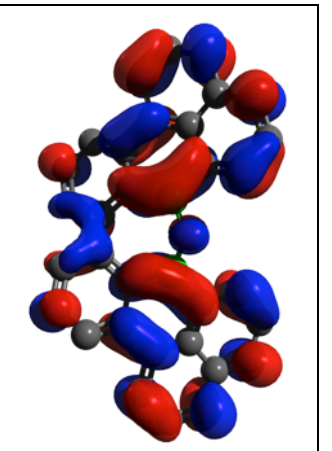 |
| HOMO-1 | HOMO | LUMO | LUMO+1 |

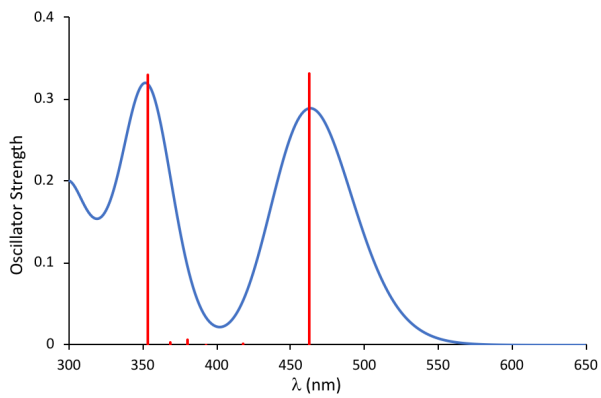


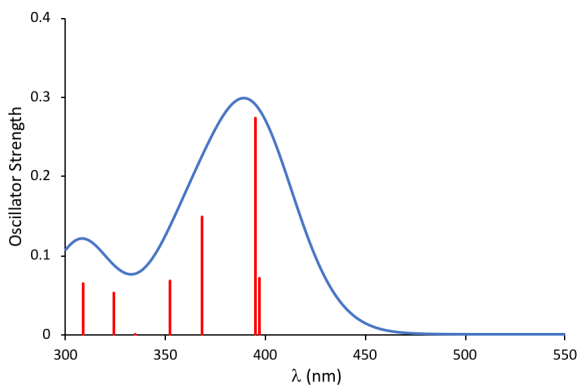


**Figure S6-1:** Predicted UV-vis spectra of **$B_2$-TBPA** for its first seven excited states (left) and **ODBE** for its first six excited states (right).

**Table S6-5.** HOMO/LUMO energies of **$B_2$-TBPA** and **ODBE**.

| ***Compound*** | **HOMO** (eV) | **LUMO** (eV) | $E_{gap}$ (eV) |
|---|---|---|---|
| **$B_2$-TBPA** | –5.52 | –2.41 | 3.11 |
| **ODBE** | –5.57 | –2.05 | 3.52 |

**Table S6-6.** Atomic coordinates for the optimized geometry of **$B_2$-TBPA**

| Center Number | Atomic Number | Atomic Type | Coordinates (Angstroms) X | Y | Z |
|---|---|---|---|---|---|
| 1 | 5 | 0 | 1.342659 | -0.591081 | -0.048865 |
| 2 | 6 | 0 | 0.109909 | -1.514797 | -0.339535 |
| 3 | 6 | 0 | -1.190999 | -0.933502 | -0.274849 |
| 4 | 5 | 0 | -1.342658 | 0.591091 | -0.048854 |
| 5 | 6 | 0 | -0.109913 | 1.514804 | -0.339561 |
| 6 | 6 | 0 | 1.190997 | 0.933515 | -0.27485 |
| 7 | 6 | 0 | 2.350528 | 1.725158 | -0.471975 |
| 8 | 6 | 0 | 2.17958 | 3.084072 | -0.812735 |
| 9 | 6 | 0 | 0.912909 | 3.637815 | -0.93834 |
| 10 | 6 | 0 | -0.226295 | 2.866382 | -0.68885 |
| 11 | 1 | 0 | 3.035384 | 3.72809 | -0.982793 |
| 12 | 1 | 0 | 0.811707 | 4.682781 | -1.221672 |
| 13 | 1 | 0 | -1.206133 | 3.322214 | -0.794566 |
| 14 | 6 | 0 | -2.35053 | -1.725146 | -0.471962 |
| 15 | 6 | 0 | -2.179591 | -3.084089 | -0.812607 |
| 16 | 6 | 0 | -0.912921 | -3.637847 | -0.938167 |
| 17 | 6 | 0 | 0.226286 | -2.866397 | -0.688738 |
| 18 | 1 | 0 | 1.206124 | -3.322238 | -0.794426 |
| 19 | 1 | 0 | -3.035401 | -3.728124 | -0.982574 |
| 20 | 1 | 0 | -0.811721 | -4.682838 | -1.221407 |
| 21 | 6 | 0 | -2.746834 | 1.079779 | 0.389131 |
| 22 | 6 | 0 | 2.746839 | -1.079783 | 0.389076 |
| 23 | 6 | 0 | 2.973615 | -2.324084 | 0.97817 |
| 24 | 6 | 0 | 3.868871 | -0.203895 | 0.191216 |
| 25 | 6 | 0 | 5.188598 | -0.678174 | 0.493224 |
| 26 | 6 | 0 | 5.351222 | -1.967127 | 1.064558 |
| 27 | 6 | 0 | 4.262974 | -2.768341 | 1.329671 |
| 28 | 1 | 0 | 4.396347 | -3.742663 | 1.792033 |
| 29 | 1 | 0 | 2.126872 | -2.971078 | 1.185459 |
| 30 | 1 | 0 | 6.35745 | -2.305909 | 1.301666 |
| 31 | 6 | 0 | 3.704721 | 1.138367 | -0.300767 |
| 32 | 6 | 0 | 4.851847 | 1.886942 | -0.548346 |
| 33 | 6 | 0 | 6.147878 | 1.393708 | -0.302627 |
| 34 | 6 | 0 | 6.318072 | 0.136974 | 0.228019 |
| 35 | 1 | 0 | 7.006861 | 2.022563 | -0.519796 |
| 36 | 1 | 0 | 7.311089 | -0.248299 | 0.446585 |
| 37 | 1 | 0 | 4.769389 | 2.894311 | -0.939802 |
| 38 | 6 | 0 | -2.973606 | 2.324039 | 0.978314 |
| 39 | 6 | 0 | -4.262966 | 2.768278 | 1.329835 |
| 40 | 6 | 0 | -5.351217 | 1.967092 | 1.064652 |
| 41 | 6 | 0 | -5.188596 | 0.678175 | 0.493236 |
| 42 | 6 | 0 | -3.868868 | 0.203905 | 0.191223 |
| 43 | 6 | 0 | -6.318071 | -0.136947 | 0.227953 |
| 44 | 6 | 0 | -6.147876 | -1.393645 | -0.30278 |
| 45 | 6 | 0 | -4.851843 | -1.886879 | -0.548489 |
| 46 | 6 | 0 | -3.704719 | -1.138336 | -0.300815 |
| 47 | 1 | 0 | -7.006861 | -2.022474 | -0.520018 |
| 48 | 1 | 0 | -4.769381 | -2.894218 | -0.940025 |
| 49 | 1 | 0 | -7.31109 | 0.248316 | 0.446529 |
| 50 | 1 | 0 | -4.396338 | 3.742566 | 1.792268 |
| 51 | 1 | 0 | -6.357446 | 2.305864 | 1.301777 |
| 52 | 1 | 0 | -2.126863 | 2.971013 | 1.185657 |

**Table S6-7.** Atomic coordinates for the optimized geometry of **ODBE**

| Center Number | Atomic Number | Atomic Type | Coordinates (Angstroms) X | Y | Z |
|---|---|---|---|---|---|
| 1 | 5 | 0 | 1.269725 | -0.296975 | 0.108528 |
| 2 | 6 | 0 | 1.638144 | 1.173792 | -0.200766 |
| 3 | 6 | 0 | 0.69139 | 2.234853 | -0.294054 |
| 4 | 6 | 0 | -0.691309 | 2.234893 | 0.293826 |
| 5 | 6 | 0 | -1.638086 | 1.173834 | 0.200784 |
| 6 | 5 | 0 | -1.269731 | -0.296883 | -0.108782 |
| 7 | 8 | 0 | -0.000014 | -0.80665 | -0.000271 |
| 8 | 6 | 0 | -1.078246 | 3.433029 | 0.916676 |
| 9 | 6 | 0 | -2.373661 | 3.610258 | 1.392829 |
| 10 | 6 | 0 | -3.332263 | 2.628791 | 1.19213 |
| 11 | 6 | 0 | -2.99979 | 1.414413 | 0.565039 |
| 12 | 6 | 0 | 2.999873 | 1.414321 | -0.564975 |
| 13 | 6 | 0 | 3.332377 | 2.628524 | -1.19237 |
| 14 | 6 | 0 | 2.37378 | 3.60995 | -1.393338 |
| 15 | 6 | 0 | 1.078359 | 3.432849 | -0.917151 |
| 16 | 6 | 0 | -4.070693 | 0.415128 | 0.282247 |
| 17 | 6 | 0 | -3.759165 | -0.901959 | -0.19672 |
| 18 | 6 | 0 | -2.405926 | -1.310378 | -0.389603 |
| 19 | 6 | 0 | -5.414942 | 0.748527 | 0.420803 |
| 20 | 6 | 0 | -6.453921 | -0.16289 | 0.143638 |
| 21 | 6 | 0 | -6.166152 | -1.434927 | -0.291921 |
| 22 | 6 | 0 | -4.816858 | -1.828287 | -0.476146 |
| 23 | 6 | 0 | -4.489104 | -3.130959 | -0.935325 |
| 24 | 6 | 0 | -3.177184 | -3.514471 | -1.113084 |
| 25 | 6 | 0 | -2.14136 | -2.60052 | -0.835008 |
| 26 | 6 | 0 | 2.40585 | -1.310568 | 0.389217 |
| 27 | 6 | 0 | 3.759136 | -0.902057 | 0.196803 |
| 28 | 6 | 0 | 4.07074 | 0.415107 | -0.281835 |
| 29 | 6 | 0 | 2.141213 | -2.600814 | 0.834261 |
| 30 | 6 | 0 | 3.177004 | -3.514781 | 1.112453 |
| 31 | 6 | 0 | 4.488961 | -3.131152 | 0.935216 |
| 32 | 6 | 0 | 4.81679 | -1.828362 | 0.47641 |
| 33 | 6 | 0 | 6.166122 | -1.434867 | 0.292744 |
| 34 | 6 | 0 | 6.453963 | -0.16271 | -0.142437 |
| 35 | 6 | 0 | 5.41501 | 0.748672 | -0.419807 |
| 36 | 1 | 0 | -0.348402 | 4.223111 | 1.058249 |
| 37 | 1 | 0 | -2.638917 | 4.528515 | 1.910506 |
| 38 | 1 | 0 | -4.33677 | 2.807992 | 1.556481 |
| 39 | 1 | 0 | 4.336877 | 2.80758 | -1.556823 |
| 40 | 1 | 0 | 2.639039 | 4.528051 | -1.911289 |
| 41 | 1 | 0 | 0.348529 | 4.222912 | -1.058904 |
| 42 | 1 | 0 | -5.701804 | 1.746184 | 0.73158 |
| 43 | 1 | 0 | -7.48487 | 0.154395 | 0.27421 |
| 44 | 1 | 0 | -6.96055 | -2.146096 | -0.50522 |
| 45 | 1 | 0 | -5.299583 | -3.825759 | -1.144762 |
| 46 | 1 | 0 | -2.941883 | -4.515147 | -1.465786 |
| 47 | 1 | 0 | -1.107068 | -2.902963 | -0.975992 |
| 48 | 1 | 0 | 1.106893 | -2.903336 | 0.974877 |
| 49 | 1 | 0 | 2.941635 | -4.515535 | 1.464884 |
| 50 | 1 | 0 | 5.299409 | -3.825944 | 1.144795 |
| 51 | 1 | 0 | 6.960487 | -2.146029 | 0.506187 |
| 52 | 1 | 0 | 7.484935 | 0.15468 | -0.272558 |
| 53 | 1 | 0 | 5.701871 | 1.746443 | -0.730222 |

## 7. References


[S1] E. Januszewski, A. Lorbach, R. Grewal, M. Bolte, J. W. Bats, H. Lerner and M. Wagner, *Chem. Eur. J.*, 2011, **17**, 12696–12705.

[S2] S. Brend'amour, J. Gilmer, M. Bolte, H.-W. Lerner and M. Wagner, *Chem. Eur. J.*, 2018, **24**, 16910–16918.

[S3] A. M. Brouwer, *Pure Appl. Chem.*, 2011, **83**, 2213–2228.

[S4] T.-S. Ahn, R. O. Al-Kaysi, A. M. Müller, K. M. Wentz and C. J. Bardeen, *Rev. Sci. Instrum.*, 2007, **78**, 086105.

[S5] M. J. Frisch, G. W. Trucks, H. B. Schlegel, G. E. Scuseria, M. A. Robb, J. R. Cheeseman, G. Scalmani, V. Barone, B. Mennucci, G. A. H. Petersson, M. Nakatsuji, X. Caricato, H. P. F. Li, A. Hratchian, J. Izmaylov, G. Bloino, J. L. Zheng, M. Sonnenberg, M. Hada, K. Ehara, R. Toyota, J. Fukuda, M. Hasegawa, T. Ishida, Y. Nakajima, O. Honda, H. Kitao, T. Nakai, J. A. Vreven, J. E. Montgomery Jr., F. Peralta, M. Ogliaro, J. J. Bearpark, E. Heyd, K. N. Brothers, V. N. Kudin, T. Staroverov, R. Keith, J. Kobayashi, K. Normand, A. Raghavachari, J. C. Rendell, S. S. Burant, J. Iyengar, M. Tomasi, N. Cossi, J. M. Rega, M. Millam, J. E. Klene, J. B. Knox, V. Cross, C. Bakken, J. Adamo, R. Jaramillo, R. E. Gomperts, O. Stratmann, A. J. Yazyev, R. Austin, C. Cammi, J. W. Pomelli, R. L. Ochterski, K. Martin, V. G. Morokuma, G. A. Zakrzewski, P. Voth, J. J. Salvador, S. Dannenberg, A. D. Dapprich, O. Daniels, J. B. Farkas, J. V. Foresman, J. Ortiz, J. Cioslowski, D. J. Fox, Gaussian 09 Revision C.01, 2010.

[S6] M. D. Hanwell, D. E. Curtis, D. C. Lonie, T. Vandermeersch, E. Zurek and G. R. Hutchison, *J. Cheminform.*, 2012, **4**, 17.

[S7] T. Yanai, D. P. Tew and N. C. Handy, *Chem. Phys. Lett.*, 2004, **393**, 51–57.

[S8] R. Ditchfield, W. J. Hehre and J. A. Pople, *J. Chem. Phys.*, 1971, **54**, 724–728.

[S9] A. D. McLean and G. S. Chandler, *J. Chem. Phys.*, 1980, **72**, 5639–5648.

[S10] Persistence of Vision Pty. Ltd. (2004). Persistence of Vision (TM) Raytracer. Persistence of Vision Pty. Ltd., Williamstown, Victoria, Australia. Http://Www.Povray.Org/.

[S11] N. M. O'Boyle, A. L. Tenderholt and K. M. Langner, *J. Comput. Chem.*, 2008, **29**, 839–845.

[S12] M. Weimar, G. Dürner, J. W. Bats and M. W. Göbel, *J. Org. Chem.*, 2010, **75**, 2718–2721.

[S13] P. A. A. Klusener, J. C. Hanekamp, L. Brandsma and P. von R. Schleyer, *J. Org.*

*Chem.*, 1990, **55**, 1311–1321.

[S14] K. Schickedanz, T. Trageser, M. Bolte, H.-W. Lerner and M. Wagner, *Chem. Commun.*, 2015, **51**, 15808–15810.

[S15] W. Nakanishi, T. Matsuno, J. Ichikawa and H. Isobe, *Angew. Chem. Int. Ed.*, 2011, **50**, 6048–6051.

[S16] W. Nakanishi, T. Yoshioka, H. Taka, J. Y. Xue, H. Kita and H. Isobe, *Angew. Chem. Int. Ed.*, 2011, **50**, 5323–5326.

[S17] K. Ikemoto, R. Kobayashi, S. Sato and H. Isobe, *Angew. Chem. Int. Ed.*, 2017, **56**, 6511–6514.

[S18] K. Ikemoto, J. Lin, R. Kobayashi, S. Sato and H. Isobe, *Angew. Chem. Int. Ed.*, 2018, **57**, 8555–8559.

[S19] K. Senthilkumar, M. Kondratowicz, T. Lis, P. J. Chmielewski, J. Cybińska, J. L. Zafra, J. Casado, T. Vives, J. Crassous, L. Favereau and M. Stępień, *J. Am. Chem. Soc.*, 2019, **141**, 7421–7427.

[S20] D. Myśliwiec and M. Stępień, *Angew. Chem. Int. Ed.*, 2013, **52**, 1713–1717.

[S21] G. Povie, Y. Segawa, T. Nishihara, Y. Miyauchi and K. Itami, *Science*, 2017, **356**, 172–175.

[S22] G. Povie, Y. Segawa, T. Nishihara, Y. Miyauchi and K. Itami, *J. Am. Chem. Soc.*, 2018, **140**, 10054–10059.

[S23] Stoe & Cie, X-AREA. Diffractometer Control Program System. Stoe & Cie, Darmstadt, Germany, 2002.

[S24] G. M. Sheldrick, *Acta Crystallogr. Sect. A Found. Crystallogr.*, 2008, **64**, 112–122.